AD_____

Award Number: DAMD17-99-C-9090

TITLE: Comparison of Novel and Known Neuroprotectants for Treating Exposure to Different Types of Toxins

PRINCIPAL INVESTIGATOR: Ben A. Bahr, Ph.D.

CONTRACTING ORGANIZATION: University of Connecticut
Storrs, Connecticut 06269-1133

REPORT DATE: September 2004

TYPE OF REPORT: Final

PREPARED FOR: U.S. Army Medical Research and Materiel Command
Fort Detrick, Maryland 21702-5012

DISTRIBUTION STATEMENT: Approved for Public Release;
Distribution Unlimited

The views, opinions and/or findings contained in this report are those of the author(s) and should not be construed as an official Department of the Army position, policy or decision unless so designated by other documentation.

20040917 060

REPORT DOCUMENTATION PAGE

Form Approved
OMB No. 074-0188

Public reporting burden for this collection of information is estimated to average 1 hour per response, including the time for reviewing instructions, searching existing data sources, gathering and maintaining the data needed, and completing and reviewing this collection of information. Send comments regarding this burden estimate or any other aspect of this collection of information, including suggestions for reducing this burden to Washington Headquarters Services, Directorate for Information Operations and Reports, 1215 Jefferson Davis Highway, Suite 1204, Arlington, VA 22202-4302, and to the Office of Management and Budget, Paperwork Reduction Project (0704-0188), Washington, DC 20503

1. AGENCY USE ONLY (Leave blank)

2. REPORT DATE
September 2004

3. REPORT TYPE AND DATES COVERED
Final (16 Aug 99-15 Aug 04)

4. TITLE AND SUBTITLE
Comparison of Novel and Known Neuroprotectants for Treating Exposure to Different Types of Toxins

5. FUNDING NUMBERS
DAMD17-99-C-9090

6. AUTHOR(S)
Ben A. Bahr, Ph.D.

7. PERFORMING ORGANIZATION NAME(S) AND ADDRESS(ES)
University of Connecticut
Storrs, Connecticut 06269-1133

E-Mail: Bahr@uconn.edu

8. PERFORMING ORGANIZATION REPORT NUMBER

9. SPONSORING / MONITORING AGENCY NAME(S) AND ADDRESS(ES)
U.S. Army Medical Research and Materiel Command
Fort Detrick, Maryland 21702-5012

10. SPONSORING / MONITORING AGENCY REPORT NUMBER

11. SUPPLEMENTARY NOTES

12a. DISTRIBUTION / AVAILABILITY STATEMENT
Approved for Public Release; Distribution Unlimited

12b. DISTRIBUTION CODE

13. ABSTRACT (Maximum 200 Words)

Studies using cultured brain slices have found that compensatory signals are activated in response to different types of excitotoxicity/seizures related to environmental toxin or military threat agent exposure. Soman, an irreversible anticholinesterase and devastating weapon of mass destruction, produces convulsions, memory impairment, and cell loss in the brain, especially in the hippocampus. Soman-induced accumulation of acetylcholine initiates mechanisms responsible for the development of incapacitating seizures. However, another excitatory neurotransmitter, glutamate, also has been linked to the toxic action of the chemical agent. We found that after repeated exposures to sub-toxic levels of soman, long-term hippocampal slice cultures from rat exhibit enhanced vulnerability to brief excitotoxic episodes of glutamate receptor over-stimulation. In particular, the hippocampal tissue became sensitive to cytoskeletal damage and synaptic decline in response to secondary pathogenic events. Thus, seemingly innocuous soman exposures leave the brain vulnerable to excitotoxic insults that are implicated in traumatic brain injury and stroke. The findings also suggest that asymptomatic exposures to soman can lead to hippocampal damage and that early indicators of low-level soman contact are critical for the prevention of subsequent brain injury. Studies with receptor modulators are helping to identify key signal transduction pathways that lead to neuroprotection vs. those that enhance neuronal vulnerability. Accordingly, a neuroprotectant that acts against excitotoxicity through the MAP kinase pathway eliminates soman-induced neuronal vulnerability.

14. SUBJECT TERMS
No subject terms provided.

15. NUMBER OF PAGES
61

16. PRICE CODE

17. SECURITY CLASSIFICATION OF REPORT	18. SECURITY CLASSIFICATION OF THIS PAGE	19. SECURITY CLASSIFICATION OF ABSTRACT	20. LIMITATION OF ABSTRACT
Unclassified	Unclassified	Unclassified	Unlimited

3. TABLE OF CONTENTS

Cover..... 1

SF 298..... 2

Table of Contents..... 3

Introduction..... 4

Body..... 4

Key Research Accomplishments..... 8

Reportable Outcomes..... 10

Conclusions..... 18

References..... 19

Appendices..... 23

4. INTRODUCTION

Acute exposure to soman, a military-threat agent that is three times more potent than sarin, causes seizure activity and long-term damage in the central nervous system (Lemercier et al., 1983; Pazdernik et al., 1985; Taylor, 2001). Soman is a serious concern to soldiers as well as civilians during the threat of a chemical attack and the unpredictable movement of the airborne toxin. While an irreversible inhibitor of acetylcholinesterase, the nerve agent also promotes the release of excitatory amino acids such as glutamate that participate in the neurodegeneration (Wade et al., 1987; Lallement et al., 1991, 1992, 1993; Raveh et al., 2003). Evidence suggests that septo-hippocampal areas of the glutamatergic system are recruited early after soman exposure and the resultant accumulation of extracellular acetylcholine. Excess glutamatergic stimulation in turn causes distinct damage to brain tissue, and blocking specific glutamate receptors reduces neuropathogenic responses including soman toxicity (Choi, 1988; Sheardown et al., 1990; Sparenborg et al., 1992; Lallement et al., 1993; de Groot et al., 2001).

Excitotoxic levels of glutamate may be involved in the dendritic and synaptic damage following acute soman exposure that leads to neuronal dysfunction and memory impairment (Carpentier et al., 1991; Filliat et al., 1999; de Groot et al., 2001; Munirathinam and Bahr, 2002; Raveh et al., 2002, 2003). Over-stimulation of glutamate receptors indeed causes marked deterioration in the hippocampus (Siman et al., 1989; Bahr et al., 1995b, 2002), a brain region involved in information processing and one that exhibits early degeneration following ischemia and related brain trauma. The synaptic integrity required for stable neuronal connections is particularly vulnerable to damage. Hence, hippocampal circuitries that are important for memory encoding express a high susceptibility to both nerve agents and excitotoxicity.

Events of excitotoxicity in hippocampal neurons enhance the vulnerability to other types of neuropathogenesis (e.g., see Mattson, 1990; Bahr et al., 1994). The hippocampus is a brain region that has been extensively utilized to study the action of neurotoxins. Organotypic hippocampal slice cultures provide a sensitive model system that exhibits toxic responses comparable to those expected from *in vivo* studies (Bahr et al., 1994, 1995b, 2002; Munirathinam et al., 2002). The three-dimensional slice cultures possess features that are characteristic of the adult hippocampus in vivo, including circuitry, cellular interactions, morphological integrity, and organization of neuronal subfields (Bahr, 1995; Bahr et al., 1995a). Using this model, we report that the hippocampus becomes susceptible to injury after sub-toxic soman exposure. Selective deterioration of synapses is linked to the enhanced vulnerability, associated with proteolytic activation and resultant cytoskeletal damage.

5. BODY

Chemicals and antibodies. Soman (pinacolyl methylphosphonofluoridate) was synthesized and supplied by the U.S. Army. The glutamate receptor agonist AMPA and antagonists MK801 and CNQX were from TOCRIS (Ballwin, MO). Trimethyltin (TMT) was from Aldrich Chemicals (Milwaukee, WI). The monoclonal antibody against synaptophysin was obtained from Boehringer Mannheim (Indianapolis, IN), and anti-actin was from Sigma (St. Louis, MO). Affinity-purified antibodies to the AMPA receptor subunit GluR1 were prepared as described (Bahr et al., 1996). The spectrin breakdown product BDP_N was measured using affinity-purified antibodies against end residues (Gln-Gln-Glu-Val-Tyr) of the aminoterminal fragment produced by calpain I (Bahr et al.,

1995b). Cell culture supplies and protease inhibitors were obtained from Sigma and Boehringer Mannheim. Nitrocellulose paper was from Osmonics, Inc. (Westborough, MA). Alkaline phosphatase-conjugated and horseradish peroxidase-conjugated antibodies and substrate kits were from Bio-Rad Laboratories (Richmond, CA) and Vector Laboratories Inc. (Burlingame, CA).

Organotypic hippocampal slice cultures. Conventional methods were used to prepare hippocampal slices from rat pups (Bahr et al., 1995a). Sprague-Dawley rat litters (Charles River Laboratories, Wilmington, MA) were housed in accordance with guidelines from the National Institutes of Health. The brains from 11- to 12-day postnatal rats were rapidly removed and cooled in ice-cold buffer containing 124 mM NaCl, 3 mM KCl, 2 mM $CaCl_2$, 4 mM $MgSO_4$, 1.25 mM KH_2PO_4, 26 mM $NaHCO_3$, 10 mM D-glucose, 2 mM ascorbic acid and 75 μM adenosine (pH 7.2). Hippocampi were quickly dissected and cooled, and transverse slices of 400 μm were collected from the septal to the temporal end. Groups of 8-10 slices were distributed on Millicell-CM culture inserts (Millipore; Bedford, MA). The Biopore insert membrane was maintained in contact with culture media consisting of 50% Basal Medium Eagle, 25% Earl's salt solution, 25% horse serum, and supplemented to the following final concentrations: 136 mM NaCl, 2 mM $CaCl_2$, 2.5 mM $MgSO_4$, 4 mM $NaHCO_3$, 3 mM glutamine, 40 mM glucose, 0.4 mM ascorbic acid, 20 mM HEPES buffer (pH 7.3 at 23°C), 1 mg/L insulin (24 I.U. per mg), 5 units/ml penicillin, and 5 mg/l streptomycin. The slices were maintained for 14-18 days in culture before used, at 37°C in a humid incubator supplied with 5% CO_2, with the media being changed every 2-3 days.

For transient exposure to soman (nerve agent GD), a single treatment of freshly prepared agent was applied to both surfaces of the cultured slices, and this was repeated daily for up to one week. For induction of excitotoxic pathology, slices were subjected to a 3-min AMPA (100 μM) or 1-h TMT (100 μM) exposure. After removal of the excitotoxins, the cultures were subsequently quenched with media containing 40 μM CNQX and 20 μM MK-801 for 20 min to stop further glutamate receptor stimulation. Treatment groups (n=4-6 per time point) were staggered so that all slices were harvested on the same day, at which time they were washed thoroughly in serum-free media and prepared for subsequent analyses.

Immunoblot analysis. Cultured slices were gently removed with a soft brush and homogenized by sonication in groups of 6-8 slices each using ice-cold buffer containing 8 mM HEPES buffer (pH 7.4), 1 mM EDTA, 1 mM EGTA, 0.02% NaN_3, 10 μg/l antipain, and 2 μg/l each of leupeptin, aprotinin, and pepstatin. Samples were assessed for protein content with a BSA standard, and equal protein aliquots (85 μg) were denatured in SDS and β-mercaptoethanol for 5 min at 100°C then separated by 4-16% SDS-PAGE and blotted to nitrocellulose. The nitrocellulose membrane was incubated with primary antibodies at 4°C overnight with gentle agitation. Secondary antibody incubation utilized anti-IgG-alkaline phosphatase conjugates, and color development used the 5-bromo-4-chloro-3-indolyl phosphate and nitroblue tetrazolium substrate system. Development of immunoreactive bands was terminated before maximal intensity was reached in order to avoid saturation and to ensure a linear relationship with increasing amount of sample protein. Single blots were used for comparative studies between different antigens. Bands were scanned at high resolution and assessed for integrated density within single immunoblots with BIOQUANT software (R & M Biometrics, Nashville, TN).

Histology. Slices were rinsed with 0.1 M phosphate buffer, pH 7.4 (PB) and fixed for 2 h in PB plus 4% paraformaldehyde. Slices were then cryoprotected in 20% sucrose for 1 h and carefully removed

from the insert, and serial sections were prepared at 20-μm thickness and mounted on Superfrost plus coated slides (Fisher Scientific, Pittsburgh, PA). Sections were immunolabeled with anti-synaptophysin using the avidin-biotin-peroxidase technique and 3,3'-diaminobenzidine as the chromogen. Alternatively, separate sections were stained with cresyl violet. BIOQUANT image analysis included the use of a computerized deconvolution system with motorized Z focus drive.

Statistics. Immunoreactivity levels were expressed as means ± SEM and statistical significance was determined by unpaired t-tests and by one-way analyses of variance followed by the Tukey-Kramer multiple range tests. Differences were considered significant at $p<0.05$.

Results

As described in Munirathinam and Bahr (2004; PDF attached), different concentrations of soman were administered to cultured hippocampal slices in order to determine levels that do not cause synaptic degeneration after an extended exposure period. Single daily applications produced transient exposure of the chemical agent before rapid hydrolysis in the culture medium, and this was repeated over a 7-day schedule. Slice cultures treated with up to 150 nM soman for 7 days of exposure exhibited no appreciable change in the synaptic vesicle component synaptophysin or in the AMPA receptor subunit GluR1. Similar concentrations of soman have been shown to inhibit acetylcholinesterase by >90% while having no effect on cell viability in cultured hippocampal neurons (Deshpande et al., 1995). Thus, short-lived rises in acetylcholine levels may not be sufficient to trigger synaptic toxicity in localized brain areas. Transient soman exposures likely require higher concentrations to influence a wider circuitry, leading to secondary episodes of excitotoxic activity.

Soman at 20 μM was used to show that, at higher agent concentration, transient exposures can cause synaptopathogenesis. Over the 7-day treatment regimen, synaptic markers were significantly reduced. The reduction in the synaptic proteins occurred in conjunction with evident excitotoxicity as indicated by the marked increase in an excitotoxic indicator BDP_N. BDP_N was labeled with antibodies directed against the proteolytic site in the spectrin sequence (Bahr et al., 1995b). The synaptic decline was found throughout the hippocampal subfields. The dendritic zone of hippocampal field CA1 (stratum radiatum) that normally exhibits dense staining for synaptophysin, was markedly reduced in the punctate immunolabeling after the soman treatment (Munirathinam and Bahr, 2004). A similar decline was evident in the molecular layer of the dentate gyrus. The synaptic effects occurred rather gradually since a single exposure to soman produced little or no change in presynaptic synaptophysin and postsynaptic GluR1 markers 24 h later.

Synaptic deterioration was apparent before neuronal loss, indicating selective vulnerability among synapses of soman-exposed brain tissue. The transient exposures that produced synaptic decline after 7 days of repeated contact had no obvious effect on neuronal density, nor did they produce any pyknotic changes in field CA1, hippocampal field CA3, and the hilus. Note that only sparse indications of pyknotic nuclei were found among granular neurons of the dentate gyrus of soman-treated slice cultures, which were not evident in control tissue. Analyses for glial fibrillary acidic protein determined that the soman exposures caused synaptic decline without producing secondary pathology in the form of an astroglial response (Munirathinam and Bahr, 2004).

Next, we tested whether the subtoxic soman exposures cause brain tissue to become susceptible to the type of synaptic decline that results from high levels of soman. Hippocampal slices that were treated daily with 150 nM soman exhibited enhanced vulnerability to a brief excitotoxic insult. Slices were harvested 7 days after the start of the soman exposures. Mild excitotoxicity was induced on day 6 by over-stimulating AMPA-type glutamate receptors for 3 min with 100 μM AMPA, a selective agonist known to cause neurodegeneration with longer treatment times in the slice model (Bahr et al., 1995b, 2002). The insult was rapidly quenched with receptor antagonists in parallel with washout of the excitotoxin. After a 24-h recovery period, the excitotoxic insult alone did not cause appreciable synaptic decline. In contrast, in slice cultures first treated daily with subtoxic soman, the 3-min excitotoxic insult caused a marked reduction in the vesicle protein synaptophysin (Munirathinam and Bahr, 2004). Immunoreactivity levels of synaptic markers were unchanged after 7 days of repeated soman exposures alone, but were significantly reduced in soman-treated slices 24 h after the AMPA insult ($p<0.01$).

Repeated exposures to subtoxic soman also leave hippocampal tissue vulnerable to excitotoxic activation of the protease calpain and resultant cytoskeletal damage. Calpain-mediated spectrin breakdown product BDP_N provides a sensitive marker for the protease activation that identifies neurotoxic conditions (see Vanderklish and Bahr, 2000). Persistent calpain activation is triggered by glutamatergic excitotoxicity and is thought to be a precursor of synaptic pathology and neurodegeneration (Siman et al., 1989; Bahr et al., 1995b, 2002; Bendiske et al., 2002). Corresponding with the enhanced synaptic vulnerability, subtoxic soman exposures caused a greater calpain response evident 24 h after the mild AMPA insult. The excitotoxic insult alone produced only trace levels of BDP_N, possibly explaining the lack of synaptic effects. Similarly, daily applications with 150 nM soman caused only a small, insignificant change in BDP_N. On the other hand, with the addition of the secondary excitotoxic insult, calpain-mediated BDP_N was markedly increased to levels similar to those found in slices repeatedly exposed to 20 μM soman alone.

While incidences of excitotoxic and synaptic vulnerability developed after a week of repeated soman contact, a single transient exposure also resulted in hippocampal tissue becoming susceptible to a disparate insult after only 24 h. A 1-h treatment with trimethyltin (TMT), a neurotoxin that causes excitotoxic damage in sensitive areas of the brain including the hippocampus (Feldman et al., 1993; Ishida *et al.*, 1997; Munirathinam et al., 2002), was found to be more effective at causing synaptic and cytoskeletal deterioration when followed by a single exposure to 150 nM soman. The brief TMT application followed by antagonist quenching and washout was too short to cause lasting signs of damage. Similarly treated slice cultures were then subjected to transient soman exposure and assessed for a presynaptic marker and the calpain-mediated spectrin fragment BDP_N 24 h later. Indicated by the enhanced synaptic decline and spectrin breakdown, it is clear that subtoxic soman increases neuronal vulnerability to toxic responses triggered before or after the nerve agent contact (Munirathinam and Bahr, 2004).

To test whether low-level soman exposures disrupt repair signaling, we attempted to offset the enhanced vulnerability by positive modulating endogenous survival signals. This was done with 1-(quinoxalin-6-ylcarbonyl)piperidine, a neuroprotectant that promotes basal glutamatergic responses and their connection to repair systems including the mitogen-activated protein kinase (MAPK) pathway (Wang et al., 1997; Hayashi et al., 1999; McKinney et al., 1999; Bahr et al., 2002; Limatola et al., 2002). The compound was introduced into the daily applications of sub-toxic soman, and a week later the hippocampal slices were assessed for excitotoxic vulnerability. The repeated soman exposures allowed a normally undamaging AMPA treatment to produce marked synaptic decline and

cytoskeletal breakdown. The addition of 1-(quinoxalin-6-ylcarbonyl)piperidine completely prevented the AMPA-induced pathogenic responses. Pre- and postsynaptic markers remained at levels similar to those in control slices, and calpain activation was not evident. These data indicate that soman-induced neuronal vulnerability does not involve disruption of endogenous repair responses.

This project has identified repair mechanisms that are able to counteract the effects of neurotoxin exposure. We have shown that AMPA-type glutamate receptors are linked to appropriate signaling events in order to prevent neuronal injury as well as enhance recovery. As reported in Bahr et al. (2002), AMPA stimulation in hippocampal slice cultures caused the selective activation of MAPK through the upstream activator MAPK kinase (MEK). Excessive glutamatergic activity through AMPA receptors is no doubt a critical feature of excitotoxic damage (Buchan et al., 1991; Sheardown et al., 1993). On the other hand, enhancing basal stimulation of AMPA receptors and associated MAPK signaling with the positive modulator 1-(quinoxalin-6-ylcarbonyl)piperidine (also known as Ampakine CX516), was found to promote neuronal survival after toxic exposure (Bahr et al., 2002; Munirathinam et al., 2002). As with AMPA receptors, we recently showed that stimulation of signals through cannabinoid receptors and proteoglycan-binding adhesion receptors also mediate neuroprotection in the slice model.

6. KEY RESEARCH ACCOMPLISHMENTS

- The extension of Specific Aim I led to the identification of multiple classes of receptors that elicit compensatory repair signals similar to those linked to the pro-survival MAPK pathway. Common signaling elements are potentially involved in such endogenous repair mechanisms through different receptors.

- We established that enhancing the signaling through AMPA receptors as well as cannabinoid receptors and adhesion-type receptors leads to neuroprotection in a tissue model of neurotoxin exposure. For this model, organotypic hippocampal slice cultures are used to provide a sensitive experimental system that exhibits toxic responses comparable to those expected from *in vivo* studies. The hippocampus is a brain region that has been extensively utilized to study the action of neurotoxins. The three-dimensional slice cultures possess features that are characteristic of the adult hippocampus *in vivo*, including circuitry, cellular interactions, morphological integrity, and organization of neuronal subfields. Interestingly, there is evidence of additive effects between distinct avenues of neuroprotection, e.g., enhancing MAPK compensatory responses vs. anti-inflammatory action.

- As reported in Bahr et al., 2002, up-regulation of AMPA receptor-MAPK repair signaling facilitated long-term cell survival and synaptic maintenance assessed 7-10 days post-insult *in vitro* and *in vivo*.

- Experiments of Specific Aim II further established that endogenous repair signals activated through different receptor systems protect against the effects of neurotoxin exposure. To be thorough, we added a mitochondrial toxin (3NP) to the list of toxic agents tested. Mitochondrial dysfunction has been implicated in stroke and age-related diseases such as Parkinsons, and may be involved in enhancing neuronal vulnerability after low-level toxin exposure. Recent work shows the same neuroprotectants that act against TMT and GD also protect against the action of the mitochondrial toxin (paper in preparation).

- Work from Specific Aim II also established that neuroprotectant can be applied to brain tissue after the toxic exposure and still elicit pronounced levels of cellular and synaptic repair. More importantly, we discovered that neurons become acutely vulnerable to damage after low-level chronic exposure to toxic agents such as TMT and GD. While pathogenic markers were not evident in brain tissue following the low-level exposure, the resultant increased vulnerability allowed an inconsequential minor insult to produce marked levels of cellular damage and synaptic decline (Munirathinam and Bahr, 2004).

- Specific Aim III found that endogenous repair responses involving MAPK signaling are still effective protection pathways when stimulated 3-6 hours after neurotoxin exposure. Thus, there appears to be a sizeable window of opportunity to activate recovery systems.

- As shown is last year's progress report, signaling experiments found that glutamate receptors as well as cannabinoid receptors and proteoglycan-binding adhesion receptors activate the MAPK pathway and focal adhesion kinase (FAK), the primary mediator of integrin signaling. Blocking integrin signaling disrupted MAPK and FAK activation and, correspondingly, enhanced neuronal vulnerability. These results indicate that adhesion responses contribute to endogenous signaling pathways underlying cellular recovery.

- Work under Specific Aim III utilized microarray and gene regulation analyses to study the cellular response to neurotoxin exposure. The cellular response is biphasic. Evidence suggests that the initial phase consists of neuroprotective changes, while the second phase consists of degenerative pathways and gene changes. Neuroprotectant-induced signaling overlaps with the second phase, offsetting the neurodegenerative chemistries with distinctive transcription factor activation and the upregulated expression of anti-apoptotic genes. The original idea that neuroprotection is mediated through blockage of the transcription factor NF-κB is not true. The first phase of NF-κB activation after a toxic insult appears to represent a compensatory repair response, while the second phase of the NF-κB response is consistent with delayed pathogenesis that may explain the increased vulnerability following chronic exposure to mild toxin levels. Indeed, genes activated during the delayed phase appear to be those that enhance neuronal vulnerability.

7. REPORTABLE OUTCOMES

presentations; patents and licenses applied for and/or issued; degrees obtained that are supported by this award; development of cell lines, tissue or serum repositories; infomatics such as databases and animal models, etc.; funding applied for based on work supported by this award; employment or research opportunities applied for and/or received based on experience/training supported by this award.

- MANUSCRIPTS

1. Bahr BA, Yilma S, and Suppiramaniam V (1999) Structural chemistries underlying synaptic signaling and regulation. *J Mol Biol Biotech* **1**:35-48.

2. Bahr BA (2000) Integrin-type signaling has a distinct influence on NMDA-induced cytoskeletal disassembly. *J Neuroscience Res* **59**:827-832.

3. Vanderklish PW and Bahr BA (2000) The pathogenic activation of calpain: A marker and mediator of cellular toxicity and disease states. *Internatl J Exp Pathol* **81**:323-339.

4. Hoffman KB, Murray BA, Lynch G, Munirathinam S, and Bahr BA (2001) Delayed and isoform-specific effect of NMDA exposure on neural cell adhesion molecules in hippocampus. *Neuroscience Res* **39**:167-173.

5. Suppiramaniam V, Bahr BA, Sinnarajah S, Owens K, Rogers G, Yilma S, and Vodyanoy V (2001) Member of the Ampakine class of memory enhancers prolongs the single channel open time of reconstituted AMPA receptors. *Synapse* (NY) **40**:154-158.

6. Wang X, Karlsson J-O, Zhu C, Hagberg H, Bahr BA, and Blomgren K (2001) Caspase activation after hypoxia-ischemia in neonatal rat brain. *Biol Neonate* **79**:172-179.

7. Blomgren K, Zhu C, Wang X, Karlsson J-O, Andersson A-L, Bahr BA, Mallard C, and Hagberg H (2001) Synergistic activation of caspase-3 by m-calpain after neonatal hypoxia-ischemia - A mechanism of "pathological apoptosis"? *J Biol Chem* **276**:10191-10198.

8. Bahr BA (2001) Adhesion chemistries and synaptic regulation. *Neurochemistry News* **1**:78-81.

9. Bahr BA, Bendiske J, Brown QB, Munirathinam S, Caba E, Rudin M, Urwyler S, Sauter A, and Rogers G (2002) Survival signaling and selective neuroprotection through glutamatergic transmission. *Exp Neurol* **174**:37-47.

10. Caba E, Brown QB, Kawasaki B, and Bahr BA (2002) Peptidyl α-keto amide inhibitors of calpain block excitotoxic damage without affecting signal transduction events. *J Neuroscience Res* **67**:787-794.

11. Bendiske J, Caba E, Brown QB, and Bahr BA (2002) Intracellular deposition, microtubule destabilization, and transport failure: An 'early' pathogenic cascade leading to synaptic decline. *J Neuropathol Exp Neurol* **61**:640-650.

12. Vicente JS, Munirathinam S, and Bahr BA (2002) Calpain-mediated spectrin breakdown identifies vulnerable brain regions at middle age. *J Mol Biol Biotech* **3**:1-9.

13. Ekdahl CT, Mohapel P, Weber E, Bahr BA, Blomgren K, and Lindvall O (2002) Caspase-mediated death of newly formed neurons in the adult rat dentate gyrus following status epilepticus. *Eur J Neurosci* **16**:1463-1471.

14. Munirathinam S, Rogers G, and Bahr BA (2002) Positive modulation of α-amino-3-hydroxy-5-methyl-4-isoxazolepropionic acid-type glutamate receptors elicits neuroprotection after trimethyltin exposure in hippocampus. *Toxicol Appl Pharmacol* **185**:111-118.

15. Bahr BA and Bendiske J (2002) The neuropathogenic contributions of lysosomal dysfunction. *J Neurochem* **83**:481-489.

16. Bendiske J and Bahr BA (2003) Lysosomal activation is a compensatory response against protein accumulation and associated synaptopathogenesis – An approach for slowing Alzheimer's disease? *J Neuropathol Exp Neurol* **62**:451–463.

17. Ferrand-Drake M, Zhu C, Gidö G, Hansen A, Karlsson J-O, Bahr BA, Zamzami N, Kroemer G, Chan P, Wieloch T, and Blomgren K (2003) Cyclosporin A prevents calpain activation despite increased intracellular calcium concentrations, as well as translocation of apoptosis-inducing factor, cytochrome c, and caspase-3 activation in neurons exposed to transient hypoglycemia. *J Neurochem* **85**:1431-1442.

18. Emgård M, Hallin U, Karlsson J, Bahr BA, Brundin P, and Blomgren K (2003) Both apoptosis and necrosis occur early after intracerebral grafting of ventral mesencephalic tissue: A role for protease activation. *J Neurochem* **86**:1223-1232.

19. Ekdahl CT, Zhu C, Bonde S, Bahr BA, Blomgren K, and Lindvall O (2003) Death mechanisms in status epilepticus-generated neurons and effects of additional seizures on their survival. *Neurobiol Dis* **14**:513-523.

20. Chicoine LM, Suppiramaniam V, Vaithianathan T, Gianutsos G, and Bahr BA (2004) Sulfate- and size-dependent polysaccharide modulation of AMPA receptor properties. *J Neurosci Res* **75**:408-416.

21. Caba E and Bahr BA (2004) Biphasic activation of NF-κB in the excitotoxic hippocampus. *Acta Neuropathologica* **108**: May online, in press.

22. Munirathinam S and Bahr BA (2004). Repeated contact with subtoxic soman leads to synaptic vulnerability in hippocampus. *J Neurosci Res*, July Online (DOI: 10.1002/jnr.20209), in press.

23. Caba E, Elliot RC, Giardina C, Wang H-W, Shin D-G, and Bahr BA (2004) Categorical informatics for identifying opposed gene profiles in the excitotoxic hippocampus. Submitted.

24. Chicoine LM and Bahr BA (2004) Polysaccharide modulation of AMPA receptors results in neuroprotection against excitotoxicity. Submitted.

25. Araújo IM, Verdasca MJ, Leal EC, Bahr BA, Ambrósio AF, and Carvalho CM (2004) Early calpain-mediated proteolysis following AMPA receptor activation compromises neuronal survival in cultured hippocampal neurons. J Neurochem. Submitted.

26. Volbracht C, Chua BT, Ng CP, Bahr BA, Hong W, and Li P (2004) Critical role of calpain activation in nitric oxide-induced neuronal apoptosis. Submitted.

27. Caba E, Giardina C, Elliot R, Rogers, and Bahr BA (2004) Early and delayed expression profiles of synapse-related genes in the excitotoxic hippocampus. In prep.

28. Karanian DA, Brown QB, Makriyannis A,and Bahr BA (2004) Blocking cannabinoid activation of FAK and ERK1/2 compromises synaptic integrity in hippocampus. Submitted to Eur J Pharmacol.

29. Caba E, Munirathinam S and Bahr BA (2004). Synaptic vulnerability after subtoxic soman exposures: Evidence of compromised compensatory systems. In prep.

- ABSTRACTS

1. Bendiske J, Rogers G, Rudin M, Urwyler S, Sauter A, and Bahr BA (1999) Ampakine Modulators of AMPA-Type Glutamate Receptors Promote Neuronal Recovery after Excitotoxic Injury in Brain Tissue. *Mol Biol Cell* **10** (Suppl.):230.

2. Bahr BA, Bendiske J, Rudin M, Urwyler S, Sauter A, and Rogers G (2000) Positive Modulation of AMPA Receptors Promotes Cellular Repair Following Excitotoxic Injury to Brain Tissue *In Vitro* and *In Vivo. The Toxicologist* **54**:179.

3. Bendiske J, Caba E, and Bahr BA (2000) Tau modifications and concomitant transport disturbances following lysosomal dysfunction, *J. Neurochem.*, **74** (Suppl.): S30C.

4. Brown QB and Bahr BA (2000) Phosphorylation of the ERK1/ERK2 MAP kinase can be influenced by AMPA-type glutamate receptors and their positive modulation in hippocampus. *J Neurochem* **74** (Suppl.):S20D.

5. Bahr BA, Bendiske J, Brown QB, Rogers G, Rudin M, Urwyler S, and Sauter A (2000) Multifaceted properties of AMPA receptors include links to neuroprotective signaling pathways. *J Neurochem* **74** (Suppl.):S50C.

6. Caba E, Brown QB, and Bahr BA (2000) Evaluation of mitogen-activated protein kinase and NF-κB in an *in vitro* model of neuroprotection. *J Neurochem* **74** (Suppl.):S20C.

7. Munirathinam S and Bahr BA (2000) Positive modulation of hippocampal AMPA receptors promotes recovery several hours after trimethyltin-induced excitotoxicity. *Soc Neurosci Abstr* **26**:#3459.

8. Bahr BA, Bendiske J, Brown QB, Caba E, Rogers G, Rudin M, Urwyler S, and Sauter A (2000) Links to metabotropic signaling allow AMPA receptors to counteract the neurodegeneration resulting from their own ionotropic over-activity. *Soc Neurosci Abstr* **26**:#2835.

9. Suppiramaniam V, Manivannan K, Subramaniam T, Dityatev A, and Bahr BA (2000) Interaction between AMPA receptor channels: A mechanism for modifying synaptic strength. *Soc Neurosci Abstr* **26**:#1898.

10. Bendiske J, Caba E, Lan S, Gianutsos G, and Bahr BA (2000) Tau deposition is linked to microtubule destabilization and concomitant synaptic decline. *Soc. Neurosci. Abstr.*, **26**:#2869.

11. Wang X, Karlsson J, Bahr BA, Hagberg H, Blomgren K, Caspase activity after hypoxia-ischemia in Rat Brain, *Professor Ingemar Kjellmer Symposium of the XIXth Internatl Conf. on Cerebral Blood Flow and Metabolism* (2000).

12. Blomgren K, Hallin U, Puka-Sundvall M, Bahr BA, Hagberg H, Selective interactions between caspase-3, calpain, and stress protein calpastatin in neonatal rat hypoxia-ischemia, *XIXth Internatl. Conf. on Cerebral Blood Flow and Metabolism* (2000).

13. Blomgren K, Hallin U, Puka-Sundvall M, Bahr BA, and Hagberg H, Caspase-Calpain Interaction and Calpastatin as a Stress Protein in Neonatal Rat Hypoxia-Ischimia, *XIXth International Symposium on Cerebral Blood Flow and Metabolism* (2000).

14. Blomgren K, Wang X-Y, Zhu C-L, Karlsson J-O, Bahr BA, Hagberg H, Activation of caspases in neonatal rat hypoxia-ischemia, *Soc. Neurosci. Abstr.*, **26**, 245 (2000).

15. Bahr BA, Bendiske J, Caba E, A link between microtubule and synaptic failure in a model of synaptopathogenesis, *Proc. Australian Neurosci. Soc.*, **12**, 50 (2001).

16. Bahr BA and Munirathinam S, A Novel Protective Signaling Pathway Identified in a Model of Neurotoxin Exposure, *Dept. of Defense Workshop of the Neurotoxin Exposure Treatment Research Program (NETRP)* (2001).

17. Caba E, Giardina C, and Bahr BA, Evidence of a Biphasic NF-κB Response to an Excitotoxin in Hippocampus, *The Toxicologist*, **55**, 1732 (2001).

18. Bahr BA and Munirathinam S, Multiple Avenues of Protection Identified in a Model of Neurotoxin Exposure, *The Toxicologist*, **55**, 899 (2001).

19. Chicoine L, Bahr BA, Sulfated glycosaminoglycan enhances the channel properties of calcium-permeable AMPA receptors, *New England Pharmacol Meeting* (2001).

20. Bahr BA, Structural Signals Underlying Plasticity and Protection Events, *J Neurochem* **75** (Suppl) (2001).

21. Brown QB, Bendiske J, Caba E, Munirathinam S, and Bahr BA, AMPA-type glutamate receptors are linked to endogenous protection mechanisms resulting in reduced excitotoxic risk, *J. Neurochem.*, **75** (Suppl.) (2001).

22. Caba E and Bahr BA, Biphasic response of NF-κB to stroke-type pathogenesis in organotypic hippocampal slice cultures, *GRASP Pharmacy Research Conference* (2001).

23. Bendiske J and Bahr BA, Characterization and slowing of the protein deposition and synaptic decay cascade in hippocampal slice cultures, *Second Neurobiology Conference: Identifying Accelerators and Brakes of Brain Aging* (2001).

24. Caba E, Giardina C, Rogers G, Bahr BA, Ampakine effects indicate that the biphasic NF-κB response to excitotoxicity denotes two opposing signaling pathways, *Soc. Neurosci. Abstr.*, **27**, 867.2 (2001).

25. Suppiramaniam V, Subramaniam T, Kanju PM, Kleene R, Moss A, Premkumar L, Brown Q, Bahr BA, and Dityatev A, Single channel recordings from mossy fiber synaptosomes: Evidence for the presence of high-affinity synaptic AMPA receptors, *Soc. Neurosci. Abstr.*, **27**, 502.10 (2001).

26. Subramaniam T, Kleene R, Manivannan K, Dityatev A, Bahr BA, and Suppiramaniam V, Polysialic acid modulates single channel properties of synaptosomal AMPA receptors, *Soc. Neurosci. Abstr.*, **27**, 610.5 (2001).

27. Chicoine L, Suppiramaniam V, Gianutsos G, Kawasaki BT, and Bahr BA, Sulfated polysaccharides modulate calcium permeability and binding properties of hippocampal AMPA receptors, *Soc. Neurosci. Abstr.*, **27**, 480.6 (2001).

28. Bahr BA, Bendiske J, Michaelis ML, Georg G, Caba E, and Brown Q, Compensatory responses in the brain yield new treatment strategies for neurodegenerative disorders, *Soc. Neurosci. Abstr.*, **27**, 581.2 (2001).

29. Bendiske J and Bahr BA, Positive lysosomal modulation reverses the PHF-tau accumulation <> microtubule destabilization <> transport failure <> synaptic deterioration cascade, *Soc. Neurosci. Abstr.*, **27**, 425.15 (2001).

30. Emgard M, Karlsson J, Bahr BA, Brundin P, and Blomgren K, The majority of cell death occurs early after intracerebral grafting of ventral mesencephalic tissue: A role for calpain activation. *Soc. Neurosci. Abstr.*, **27**, 197.4 (2001).

31. Bahr BA, Caba E, Giardina C, Brown QB, and Bendiske J, Biphasic NF-κB activation in brain tissue denotes protective and pathogenic signaling pathways, *Mol. Biol. Cell*, **12** (Suppl.), 2233 (2001).

32. Munirathinam S and Bahr BA, Low-level soman exposure leads to synaptic damage in the hippocampus and potentiates neuronal vulnerability. *The Toxicologist* (Society of Toxicology), **58**, 1551 (2002).

33. Bahr BA and Munirathinam S, Synaptic vulnerability following low-level soman exposures is reduced through glutamatergic signals. *FASEB J* (Suppl.), **16**, A947 (2002).

34. Bendiske J and Bahr BA, Lysosomal modulation leads to neuroprotection in a model of protein deposition and synaptic decline. *The Pharmacologist* (ASPET) (2002).

35. Ekdahl CT, Mohapel P, Weber E, Bahr BA, Blomgren K, and Lindvall O, The role of caspases, calpains, and cathepsins in the degeneration of newly formed neurons in the dentate gyrus following status epilepticus. *International Stem Cell Meeting (France)* (2002).

36. Volbracht C, Chua BT, Bahr BA, and Li P, Neuronal apoptosis dependent on calpain activation. *Cell Death Meeting, Australian Neuroscience Society - Noosaville* (2002).

37. Bahr BA, The pathogenic and protective contributions of lysosomal dysfunction and modulation, respectively. *Soc. Neurosci. Abstr.*, **28**, 192.15 (2002).

38. Caba E, Giardina C, and Bahr BA, The two phases of excitotoxic NF-κB activation have different effects on pro- and anti-apoptotic gene regulation. *Soc. Neurosci. Abstr.*, **28**, 250.9 (2002).

39. Karanian DA, Brown QB, Makriyannis A, and Bahr BA, Evidence that glutamatergic and endocannabinoid signaling utilize different pathways to promote neuronal survival. Soc. *Neurosci. Abstr.*, **28**, 202.16 (2002).

40. Ekdahl CT, Mohapel P, Weber E, Bahr BA, Blomgren K, and Lindvall O, Caspase-mediated death of newly formed neurons in the adult rat dentate gyrus following status epilepticus. *Soc. Neurosci. Abstr.*, **28**, 618.6 (2002).

41. Subramaniam T, Leshchynska I, Kanju PM, Bahr BA, Dityatev A, and Suppiramaniam V, AMPA receptor-mediated currents in trans-golgi network (TGN)-derived organelles. Soc. *Neurosci. Abstr.*, **28**, 139.10 (2002).

42. Suppiramaniam VD, Subramaniam T, Kanju PM, Coleman E, Bahr BA, and Wang Z, Modulation of synaptosomal AMPA receptors by a member of the Ampakine family of drugs. *Soc. Neurosci. Abstr.*, **28**, 540.4 (2002).

43. Kanju PM, Subramaniam T, Karanja P, Brown Q, Tyler J, Bahr BA, and Suppiramaniam V, Lysosomal dysfunction leads to altered AMPA channel properties in hippocampal neurons. *Soc. Neurosci. Abstr.*, **28**, 139.11 (2002).

44. Bahr BA and Brown QB, Lysosomal activation in guinea pig hippocampus: Compensatory signaling against protein accumulation events. *The Pharmacologist* (ASPET) (2003).

45. Karanian DA, Brown QB, Makriyannis A, and Bahr BA, Synaptic Maintenance in Hippocampus Appears to Require Endocannabinoid-Mediated Activation of MAPK and FAK Pathways. Soc. *Neurosci. Abstr.*, **29**, 464.9 (2003).

46. Brown QB, Baude AS, Gilling K, Bahr BA, and Parsons CG, Memantine and Neramexane Protect Against Semi-chronic 3-NP Toxicity in Organotypic Hippocampal Cultures. *Soc. Neurosci. Abstr.* **29**, 153.8 (2003).

47. Chicoine LM and Bahr BA, Neuroprotection Through Polysaccharide Modulation of AMPA Receptors, *Soc. Neurosci. Abstr.*, **29**, 895.2 (2003).

48. Bahr BA, Brown QB, and Hubbard AK, Pathogenic vs. Compensatory Activation of the Lysosomal System in the Hippocampal Slice Model of Protein Accumulation and Synaptopathogenesis. *Soc. Neurosci. Abstr.*, **29**, 877.11 (2003).

49. Caba E, Elliot R, Giardina C, and Bahr BA, Opposing early and delayed gene regulation events in the excitotoxic hippocampus. *Soc. Neurosci. Abstr.*, **29**, 545.10 (2003).

50. Wang Z, Clark R, Vaithianathan T, Kanju P, Bahr BA, Dey P, and Suppiramaniam V, Benzamide anticonvulsants modulate the channel properties of AMPA–glutamate receptors. *Soc. Neurosci. Abstr.*, (2003).

51. Bahr BA and Caba E, The threat of sub-toxic soman exposures: Enhanced vulnerability in brain tissue. *Internatl. Conf. on Advanced Technologies for Homeland Security* (2003).

- PRESENTATIONS

1. University of Connecticut Department of Psychology: "Development of a Model System to Study Age-Related Processes that Lead to Synaptic Pathology", Mansfield-Storrs, Connecticut (1999).

2. American Society for Neurochemistry Colloquium: "Multifaceted Properties of AMPA Receptors Include Links to Neuroprotective Signaling Pathways", Chicago, Illinois (2000).

3. Hewitt Symposium on Neurotherapeutic Research: "Advances in an *In Vitro* Model of Age-Related Neuropathogenesis", Storrs, Connecticut (2000).

4. Nathan Kline Institute/New York University Medical School Seminar: "Abnormal Protein Processing is Linked to Microtubule Destabilization and Concomitant Synaptic Decline", Orangeburg, New York (2000).

5. Pfizer Inc., Central Research Division Invited Speaker: "Alzheimer-Type Pathogenesis and Potential Neuroprotection Avenues: Unique Ideas from a Unique *In Vitro* System", Groton, Connecticut (2000).

6. University of Connecticut Health Center, Claude Pepper Center Research Seminar: "Development of a Model of Neurodegeneration for the Study of Potential Intervention Strategies", Farmington, Connecticut (2000).

7. Workshop on DoD Sponsored Parkinsons Research: "A Novel Protective Signaling Pathway Identified in a Model of Neurotoxin Exposure", Potomac, Maryland (2001).

8. Joint Asian Pacific Society for Neurochemistry/Australian Neuroscience Society, Alzheimers Pathology Symposium: "A Link Between Microtubule and Synaptic Failure in an I*n Vitro* Model of Neurodegeneration," Brisbane, Australia (2001).

9. Joint International Society for Neurochemistry/American Society for Neurochemistry Colloquium: "Therapeutic Strategies Identified with an *In Vitro* Model of Excitotoxicity", Rio de Janeiro, Brazil (2001).

10. International Society for Neurochem Colloquium: "Dynamic Structural Chemistries Underlying Synaptic Plasticity and Protection", Buenos Aires, Argentina (2001).

11. Pfizer Inc., CNS Program Invited Speaker: "Lypex-Mediated Reversal of Synaptopathogenesis in Hippocampus", Groton, Connecticut (2001).

12. Society for Neuroscience Annual Meeting: "Compensatory responses in the brain yield new treatment strategies for neurodegenerative disorders", San Diego, California (2001).

13. American Society of Cell Biology Annual Meeting: "Biphasic NF-κB activation in brain tissue denotes protective and pathogenic signaling pathways," Washington D.C. (2001).

14. Society of Toxicology Meeting: "Low-level soman exposure leads to synaptic damage in the hippocampus and potentiates neuronal vulnerability", Nashville, Tennessee (2002).

15. 9th Meeting of the International Neurotoxicology Association: "Enhanced vulnerability in hippocampus following repeated exposures to low-level soman", Germany (2003).

16. International Brain Research Organization: "Dysfunction and Activation of the Lysosomal System in the Central Nervous System", Czech Republic (2003).

17. University of Connecticut Health Center/Medical School Seminar Series: "Selective Compensatory Signaling in Response to Neuropathogenic Conditions", Farmington, Connecticut (2003).

8. CONCLUSIONS

Our findings have several important implications. Although acute exposure of animals to soman causes the death of neurons, the present data indicate that synapses express the initial damage elicited by repetitive contact with the nerve agent. Proteolytic activation and synaptic decline occurred after the soman exposure, both indicators of neurotoxicity (Bahr et al., 2002). In fact, inhibition of calpain proteolytic activity has been proposed as a treatment for exposure to neurotoxins including soman (Vanderklish and Bahr, 2000; Cowan et al., 2001). Persistent synaptopathogenesis in the hippocampal region may explain the delayed behavioral abnormalities and memory loss in exposed rodents and humans. Interestingly, hippocampal tissue treated with sub-toxic soman levels becomes markedly vulnerable to excitotoxic activation of glutamate receptors. Calpain is also a mediator of the toxic action of glutamate-based excitotoxicity (Siman et al., 1989; Bahr et al., 1995b, 2002; Caba et al., 2002), suggesting an initial role for the protease in the tissue vulnerability.

Hence, these findings imply that imperceptible soman contact can leave the brain susceptible to glutamate-based injuries of which there are many. Similarly, tissue compromised by a prior excitotoxic episode is made more sensitive to soman. The enhanced vulnerability does not appear to involve the disruption of cellular repair responses as determined through the potentiation of compensatory signaling. The results reported here emphasize the need for early indicators of low-level soman exposure so that subsequent brain injury can be adequately assessed and treatment/prevention measures executed in a timely manner.

Long after exposure to an environmental toxin or military threat agent, select brain regions can remain acutely vulnerable to stroke events and age-related neurodegenerative disorders such as Parkinson's disease. Similarly, low-level chronic exposure of slice cultures to toxic agents leads to increased vulnerability to subsequent insults. Compensatory responses including the activation of gene regulation events appear to be involved in offsetting the increased vulnerability. It may indeed be the case that exposures to differently acting toxicants can be treated with the same protection strategy that exploit endogenous repair systems.

As a result of the identified biphasic cellular response to toxin exposure, enhanced vulnerability may stem from disruption of the early gene regulation events that promote survival as part of the initial phase of the response. For example, IL-6, junB, Egr-1, HES-1, SOCS-3, MAPK phosphatase (cpg21), and HO-1 are upregulated while ICE is down-regulated early after neurotoxin exposure. Thus, besides protective genes being upregulated, the decrease in the expression levels of such apoptotic genes as ICE may also designate the early phase as protective. Disruption of these types of protective changes would affect neuronal vulnerability. BDNF stands out as a protective gene whose expression is disrupted by both NMDA-mediated excitotoxicity and repeated low-level soman exposures.

Alternatively, enhanced vulnerability may be due to exacerbation of the pathogenic phase of the cellular reponse. Among the genes upregulated early that may be contributing to injury were the pathogenic genes TNF-α, MIP1α, NGFI-B, NOR-1, fra-1 and ICAM-1. It is possible to envision that the survival genes are over-powered by the upregulated pathogenic genes, resulting in the initiation of a pathogenic phase that enhances the risk of onset of neuropathogenesis including

synaptic decline and loss of function. Evidence contributing to this hypothesis comes from pathogenic genes that are upregulated early after NMDA exposure (1 h post-insult) and remain upregulated over the course of the whole period such as MIP1α and C/EBP.

An array of apoptotic genes may be affected to alter neuronal vulnerability. Some are upregulated early while a different set of pathogenic genes is upregulated 24 h post-insult. Among the unique changes occurring 24 h post-insult, the potent pathogenic genes calpain and ICE were upregulated. Conversely, such genes as BDNF, trkB, Egr-1, neuroD4, and neuronatin α, which have been shown to be protective, were down-regulated in the delayed phase. It might be these changes whose effects are compounded by the slow upregulation of more pathogenic genes such as ICE and calpain.

Calpain, in particular, has been implicated in the pathogenesis of neurotoxin exposure. During such injury, calcium influx into the cell is increased resulting in the activation of calcium-dependent proteins, some of which will promote pathogenesis, such as calpain (for review see (Vanderklish and Bahr, 2000). It has been shown previously that delayed antagonism of calpain results in neuroprotection in response to excitotoxicity (Brorson et al., 1995). Accordingly, using a specific inhibitor for calpain we have shown that signaling cascades such as MAPK and NF-κB are not altered, therefore this may be an avenue of neuroprotection to follow in preventing the detrimental effects of neurotoxins (Caba et al., 2002). Pathogenic consequences of calpain upregulation are likely compounded by the down-regulation of the proteins involved in ion homeostasis (NVP, PC3, PEP-19, and hippocalcin) and has been proposed to make pathogenic proteins more potent (Toyota et al., 2003).

According to our findings, it may be possible to design specific treatment strategies where intervention or activation of specific signaling pathways may be beneficial at different times. This means of identification of gene regulation events that potentially are most influential to survival can be used to target treatment strategies appropriately. There are appropriate therapeutic targets to be explored, and it may be possible to further filter the gene data by examining the altered genes during effective neuroprotectant treatment. Additionally, these findings may enable us to construct the sequence of events following neurotoxin exposure and enhanced vulnerability.

9. REFERENCES

Bahr BA (1995) Long-term hippocampal slices: A model system for investigating synaptic mechanisms and pathologic processes. J Neuroscience Res 42:294-305.

Bahr, B. A., Abai, B., Gall, C., Vanderklish, P. W., Hoffman, K. B., and Lynch, G. (1994). Induction of β-amyloid-containing polypeptides in hippocampus: Evidence for a concomitant loss of synaptic proteins and interactions with an excitotoxin. *Exp. Neurol.* **129**, 81-94.

Bahr BA, Kessler M, Rivera S, Vanderklish PW, Hall RA, Singh Mutneja M, Gall C, and Hoffman KB (1995a) Stable maintenance of glutamate receptors and other synaptic components in long-term hippocampal slices. Hippocampus 5:425-439.

Bahr, B. A., Tiriveedhi, S., Park, G. Y., and Lynch, G. (1995b). Induction of calpain-mediated spectrin fragments by pathogenic treatment in long-term hippocampal slices. *J. Pharmacol. Exp. Ther.* **273**, 902-908.

Bahr, B. A., Hoffman, K. B., Kessler, M., Hennegriff, M., Park, G. Y., Yamamoto, R. S., Kawasaki, B. T., Vanderklish, P. W., Hall, R. A., and Lynch, G. (1996). Distinct distributions of α-amino-3-hydroxy-5-methyl-4-isoxazolepropionate (AMPA) receptor subunits and a related 53,000 M_R antigen (*GR53*) in brain tissue. *Neuroscience* **74**, 707-721.

Bahr, B. A., Bendiske, J., Brown, Q. B., Munirathinam, S., Caba, E., Rudin, M., Urwyler, S., Sauter, A., and Rogers, G. (2002). Survival signaling and selective neuroprotection through glutamatergic transmission. *Exp. Neurol.* **174**, 37-47.

Brorson, J. R., Marcuccilli, C. J., and Miller, R. J. (1995) Delayed Antagonism of Calpain Reduces Excitotoxicity in Cultured Neurons. Stroke 26(7), 1259-1267.

Buchan AM, H Li, S Cho, WA Pulsinelli 1991. Blockade of AMPA receptor prevents CA1 hippocampal injury following transient forebrain ischemia. *Neurosci. Lett.* **132**: 255-258.

Caba E and Bahr BA (2003) Biphasic activation of NF-κB in the excitotoxic hippocampus. Submitted to *J Neuropathol Exp Neurol.*

Caba, E., Brown, Q. B., Kawasaki, B., and Bahr, B. A. (2002). Peptidyl α-keto amide inhibitors of calpain block excitotoxic damage without affecting signal transduction events. *J Neuroscience Res* **67**, 787-794.

Carpentier, P., Lambrinidis, M., and Blanchet, G. (1991). Early dendritic changes in hippocampal pyramidal neurons (field CA1) of rats subjected to acute soman intoxication: A light microscopic study. *Brain Res.* **541**, 293–299.

Choi, D. W. (1988). Glutamate neurotoxicity and diseases of the nervous system. *Neuron* 1, 623-634.

Cowan, F. M., Broomfield, C. A., Lenz, D. E., and Shih, T. M. (2001). Protective action of the serine protease inhibitor N-tosyl-L-lysine chloromethyl ketone (TLCK) against acute soman poisoning. *J. Appl. Toxicol.* **21**, 293-296.

de Groot, D. M., Bierman, E. P., Bruijnzeel, P. L., Carpentier, P., Kulig, B. M., Lallement, G., Melchers, B. P., Philippens, I. H., and van Huygevoort, A. H. (2001). Beneficial effects of TCP on soman intoxication in guinea pigs: Seizures, brain damage and learning behaviour. *J. Appl. Toxicol.* **21**, S57-65.

Feldman, R. G., White, R. R., and Eriator, I. I. (1993). Trimethyltin encephalopathy. *Arch. Neurol.* **50**, 1320-1324.

Filliat, P., Baubichon, D., Burckhart, M. F., Pernot-Marino, I., Foquin, A., Masqueliez, C., Perrichon, C., Carpentier, P., and Lallement, G. (1999). Memory impairment after soman intoxication in rat: Correlation with central neuropathology: Improvement with anticholinergic and antiglutamatergic therapeutics. *Neurotoxicology* **20**, 535–549.

Granger, R., Deadwlyer, S., Davis, M., Moskovitz, B., Kessler, M., Rogers, G., and Lynch, G. (1996). Facilitation of glutamate receptors reverses age-associated memory impairment in rats. Synapse 22, 332-337.

Hampson, R. E., Rogers, G., Lynch, G., and Deadwyler, S. A. (1998). Facilitative effects of the ampakine CX516 on short-term memory in rats: correlations with hippocampal neuronal activity. J. Neurosci. 18, 2748-2763.

Hayashi, T., Umemori, H., Mishina, M., and Yamamoto, T. (1999). The AMPA receptor interacts with and signals through the protein tyrosine kinase Lyn. Nature 397, 72-76.

Ishida, N., Akaike, M., Tsutsumi, S., Kanai, H., Masui, A., Sadamatsu, M., Kuroda Y., Watanabe, Y., McEwen, B. S., and Kato, N. (1997). Trimethyltin syndrome as a hippocampal degeneration model: temporal changes and neurochemical features of seizure susceptibility and learning impairment. *Neuroscience* **81**, 1183-1191.

Lallement, G., Carpentier, P., Collet, A., Pernot-Marino, I., Baubichon, D., and Blanchet, G. (1991). Effects of soman-induced seizures on different extracellular amino acid levels and on glutamate uptake in rat hippocampus. *Brain Res.* **563**, 234-240.

Lallement, G., Denoyer, M., Collet, A., Pernot-Marino, I., Baubichon, D., Monmaur, P., and Blanchet, G. (1992). Changes in hippocampal acetylcholine and glutamate extracellular levels during soman-induced seizures: Influence of septal cholinoceptive cells. *Neurosci. Lett.* **139**, 104–107.

Lallement, G., Delamanche, I. S., Pernot-Marino, I., Baubichon, D., Denoyer, M., Carpentier, P., and Blanchet, G. (1993). Neuroprotective activity of glutamate receptor antagonists against soman-induced hippocampal damage: Quantification with a w3-site ligand. *Brain Res.* **618**, 227–237.

Lebrun, C., Pilliere, E., and Lestage, P. (2000). Effects of S 18986-1, a novel cognitive enhancer, on memory performances in an object recognition task in rats. Eur. J. Pharmacol. 401, 205-212.

Lemercier, G., Carpentier, P., Sentenac-Roumanou, H., and Morelis, P. (1983). Histological and histochemical changes in the central nervous system of the rat poisoned by an irreversible anticholinesterase organophosphorous compound. *Acta Neuropathol.* **61**, 123-129.

Limatola, C., Ciotti, M. T., Mercanti, D., Santoni, A., and Eusebi, F. (2002). Signaling pathways activated by chemokine receptor CXCR2 and AMPA-type glutamate receptors and involvement in granule cells survival. J. Neuroimmunol. 123, 9-17.

Mattson, M. P. (1990). Antigenic changes similar to those seen in neurofibrillary tangles are elicited by glutamate and Ca^{2+} influx in cultured hippocampal neurons. *Neuron* **4**, 105-117.

McKinney, R. A., Capogna, M., Durr, R., Gahwiler, B. H., and Thompson, S. M. (1999). Miniature synaptic events maintain dendritic spines via AMPA receptor activation. Nat. Neurosci. 2, 44-49.

Munirathinam, S., and Bahr, B. A. (2002). Low-level soman exposure leads to synaptic damage in the hippocampus and potentiates neuronal vulnerability. *Toxicol. Sci.* **58** (Suppl.), 1551 (Abstract).

Munirathinam, S., Rogers, G., and Bahr, B. A. (2002). Positive modulation of α-amino-3-hydroxy-5-methyl-4-isoxazolepropionic acid-type glutamate receptors elicits neuroprotection after trimethyltin exposure in hippocampus. *Toxicol. Appl. Pharmacol.* **185**, 111-118.

Pazdernik, T. L., Cross, R. S., Giesler, M., Samson, F. E., and Nelson, S. R. (1985). Changes in local cerebral glucose utilization induced by convulsants. *Neuroscience* **14**, 823-835.

Raveh, L., Weissman, B. A., Cohen, G., Alkalay, D., Rabinovitz, I., Sonego, H., and Brandeis, R. (2002). Caramiphen and scopolamine prevent soman-induced brain damage and cognitive dysfunction. *Neurotoxicology* **23**, 7–17.

Raveh, L., Brandeis, R., Gilat, E., Cohen, G., Alkalay, D., Rabinovitz, I., Sonego, H., and Weissman B. A. (2003). Anticholinergic and antiglutamatergic agents protect against soman-induced brain damage and cognitive dysfunction. *Toxicol. Sci.* **75**, 108-116.

Sheardown, M. J., Nielsen, E. O., Hansen, A. J., Jacobsen, P., and Honore, T. (1990). 2,3-Dihydroxy-6-nitro-7-sulfamoyl-benzo(F)quinoxaline: A neuroprotectant for cerebral ischemia. *Science* **247**, 571-574.

Siman, R., Noszek J. C., and Kegerise, C. (1989). Calpain I activation is specifically related to excitatory amino acid induction of hippocampal damage. *J. Neurosci.* **9**, 1579-1590.

Slemmon JR, Feng B, and Erhardt JA (2000) Small proteins that modulate calmodulin-dependent signal transduction: effects of PEP-19, neuromodulin, and neurogranin on enzyme activation and cellular homeostasis. *Mol Neurobiol* **22**:99-113.

Sparenborg, S., Brennecke, L. H., Jaax, N. K., and Braitman, D. J. (1992). Dizocilpine (MK-801) arrests status epilepticus and prevents brain damage induced by soman. *Neuropharmacol.* **31**, 357-368.

Staubli U, Ambros-Ingerson J, Lynch G. (1992) Receptor changes and LTP: an analysis using aniracetam, a drug that reversibly modifies glutamate (AMPA) receptors. Hippocampus 2(1):49-57.

Staubli, U., Rogers, G. and Lynch, G. (1994). Facilitation of glutamate receptors enhances memory. Proc. Natl. Acad. Sci. U.S.A. 91, 777-781.

Taylor, P. (2001). Anticholinesterase agents. In The Pharmacological Basis of Therapeutics, 10th ed. (J. G. Hardman, L. E. Limbird, and A. G. Gilman, Eds.), pp. 175–191. McGraw-Hill Companies, Inc., New York.

Toyota H, Yanase N, Yoshimoto T, Moriyama M, Sudo T, and Mizuguchi J (2003) Calpain-induced Bax-cleavage product is a more potent inducer of apoptotic cell death than wild-type Bax. *Cancer Lett* **189** :221-230.

Vanderklish, P. W., and Bahr, B. A. (2000). The pathogenic activation of calpain: A marker and mediator of cellular toxicity and disease states. *Internatl. J. Exp. Pathol.* **81**, 323-339.

Wade, J. V., Samson, F. E., Nelson, S. R., and Pazdernik, T. L. (1987). Changes in extracellular amino acids during soman- and kainic acid-induced seizures. *J. Neurochem. 49*, 645-650.

Wang, Y., D. L. Small, D. B. Stanimirovic, P. Morley, and J. P. Durkin. 1997. AMPA receptor-mediated regulation of the G_i-protein in cortical neurons. *Nature* **389**: 502-504.

10. APPENDICE

- RECENT MANUSCRIPTS

Munirathinam S and Bahr BA (2004). Repeated contact with subtoxic soman leads to synaptic vulnerability in hippocampus. *J Neurosci Res.*, in press.

11. PERSONNEL RECEIVING PAY FROM THE RESEARCH EFFORT

Ben A. Bahr, Ph.D., P.I.

Ebru Caba, Ph.D., postdoctoral researcher

Queenie Brown, M.S., research technician

David Karanian, B.S., graduate student/research assistant

tapraid5/z3p-neuro/z3p-neuro/z3p01504/z3p2471d04g | gockleyj | S=11 | 6/11/04 | 13:47 | Art: P-182

Journal of Neuroscience Research 00:000–000 (2004)

Repeated Contact With Subtoxic Soman Leads to Synaptic Vulnerability in Hippocampus

Subramani Munirathinam and Ben A. Bahr*
Department of Pharmaceutical Sciences, Center for Drug Discovery, University of Connecticut, Storrs, Connecticut

Soman, an anticholinesterase and dangerous nerve agent, produces convulsions, memory impairment, and cell loss in the brain, especially in the hippocampus. Soman-induced accumulation of acetylcholine initiates mechanisms responsible for the development of incapacitating seizures. The prolonged epileptiform nature of these seizures causes the release of another excitatory neurotransmitter, glutamate, which has been linked to the toxic action of the nerve agent. Here, we tested whether subtoxic soman exposures influence the brain's sensitivity to glutamate-based excitotoxicity. Over a 1-week period, hippocampal slice cultures were exposed daily to a transient level of soman that produced no evidence of synaptic deterioration. After subtoxic soman treatments, however, the tissue became vulnerable to a brief episode of glutamate receptor overstimulation that normally resulted in little or no excitotoxic damage. In those slice cultures treated with subtoxic soman, a decline in synaptic markers as well as an increase in spectrin breakdown occurred 24 hr after the mild excitotoxic event. Exposure to high soman concentrations alone produced similar synaptic degeneration, but without evident cell death, suggesting that synaptic decline is an early neurotoxicological response to the nerve agent. Interestingly, enhanced excitotoxic sensitivity caused the brain tissue to become susceptible to disparate insults initiated before or after the soman contact. These findings indicate that seemingly innocuous soman exposures leave the brain sensitive to the types of insults implicated in traumatic injury and stroke. They also warn that asymptomatic contact with soman may lead to progressive synaptopathogenesis and that early indicators of soman exposure are critical to prevent potential brain injury. © 2004 Wiley-Liss, Inc.

Key words: excitotoxicity; hippocampal slice culture; soman; spectrin breakdown product; synaptic decline

Acute exposure to soman, a military-threat agent in the same family as sarin, causes seizure activity and long-term damage in the central nervous system (Lemercier et al., 1983; Pazdernik et al., 1985; Taylor, 2001). Soman is a serious concern to soldiers as well as civilians during the threat of a chemical attack and the unpredictable movement of the airborne toxin. As an irreversible inhibitor of acetylcholinesterase, exposure to the nerve agent leads to acetylcholine levels that initiate the early expression of seizures (see McDonough and Shih, 1997). Prolonged epileptiform action of such seizures promotes the release of excitatory amino acids such as glutamate. It is believed that the released glutamate can both reinforce seizure discharges and cause related excitotoxic neurodegeneration in vulnerable brain regions (Wade et al., 1987; Lallement et al., 1991, 1992; Deshpande et al., 1995; Raveh et al., 2003). Evidence suggests that septohippocampal areas of the glutamatergic system are recruited early after soman exposure and the resultant accumulation of extracellular acetylcholine. The excess glutamatergic stimulation in turn causes distinct damage to brain tissue, and blocking specific glutamate receptors reduces neuropathogenic responses, including soman toxicity (see Sheardown et al., 1990; Sparenborg et al., 1992; Lallement et al., 1993; Deshpande et al., 1995; de Groot et al., 2001).

Excitotoxic levels of glutamate are thought to be involved in the dendritic and synaptic damage following acute soman exposure, and this may be the early toxicological response that leads to neuronal dysfunction and memory impairment (Carpentier et al., 1991; Filliat et al., 1999; de Groot et al., 2001; Munirathinam and Bahr, 2002; Raveh et al., 2002, 2003). Overstimulation of glutamate receptors indeed causes synaptic and cellular deterioration in the hippocampus (Siman et al., 1989; Bahr et al., 1995b, 2002), a brain region involved in information processing and one that exhibits early degeneration following ischemia and related brain trauma. In addition,

Contract grant sponsor: U.S. Army; Contract grant number: DAMD17-99-C9090.

*Correspondence to: Ben A. Bahr, Department of Pharmaceutical Sciences, University of Connecticut, Storrs, CT 06269-2092.
E-mail: bahr@uconn.edu

Received 7 January 2004; Revised 14 April 2004; Accepted 12 May 2004

Published online 00 Month 2004 in Wiley InterScience (www.interscience.wiley.com). DOI: 10.1002/jnr.20209

© 2004 Wiley-Liss, Inc.

events of excitotoxicity in hippocampal neurons enhance the vulnerability to other types of neuropathogenesis (see, e.g., Mattson, 1990; Bahr et al., 1994). Hence, hippocampal circuitries important for memory encoding exhibit a distinct susceptibility to excitotoxic insults, particularly affecting the synaptic integrity that is required for stable neuronal connections.

The hippocampus is a brain region that has been extensively utilized to study the action of neurotoxins. Organotypic hippocampal slice cultures provide a sensitive model system that exhibits toxic responses comparable to those found in animal studies (Bahr et al., 1995b, 2002; Munirathinam et al., 2002). The three-dimensional slice cultures possess features that are characteristic of the adult hippocampus in vivo, including circuitry, cellular interactions, and the morphological integrity and organization of neuronal subfields (Stopinni et al., 1991; Bahr, 1995; Bahr et al., 1995a). Using this model, we found that levels of soman exposure that do not elicit signs of damage promote synaptic vulnerability. The hippocampus becomes susceptible to excitotoxicity, resulting in the selective deterioration of synapses in association with proteolytic activation and cytoskeletal damage.

MATERIALS AND METHODS

Chemicals and Antibodies

Soman (pinacolyl methylphosphonofluoridate) was synthesized and supplied by the U.S. Army Medical Research Institute of Chemical Defense. The glutamate receptor agonist AMPA and antagonists MK801 and CNQX were from Tocris (Ballwin, MO). Trimethyltin (TMT) was from Aldrich Chemicals (Milwaukee, WI). The monoclonal antibody against synaptophysin was obtained from Boehringer Mannheim (Indianapolis, IN), and antiactin was from Sigma (St. Louis, MO). Affinity-purified antibodies to the AMPA receptor subunit GluR1 were prepared as described elsewhere (Bahr et al., 1996). The spectrin breakdown product BDP_N was measured by using affinity-purified antibodies against end residues Gln-Gln-Glu-Val-Tyr of the aminoterminal fragment produced by calpain I (Bahr et al., 1995b). Cell culture supplies and protease inhibitors were obtained from Sigma and Boehringer Mannheim. Nitrocellulose paper was from Osmonics, Inc. (Westborough, MA). Alkaline phosphatase-conjugated and horseradish peroxidase-conjugated antibodies and appropriate substrate kits were purchased from Bio-Rad Laboratories (Richmond, CA) and Vector Laboratories (Burlingame, CA).

Organotypic Hippocampal Slice Cultures

Conventional methods were used to prepare hippocampal slices from rat pups (Bahr et al., 1995a). Sprague-Dawley rat litters (Charles River Laboratories, Wilmington, MA) were housed in accordance with guidelines from the National Institutes of Health. The brains from 11–12-day postnatal rats were rapidly removed and cooled in ice-cold buffer containing 124 mM NaCl, 3 mM KCl, 2 mM $CaCl_2$, 4 mM $MgSO_4$, 1.25 mM KH_2PO_4, 26 mM $NaHCO_3$, 10 mM D-glucose, 2 mM ascorbic acid, and 75 μM adenosine (pH 7.2). Hippocampi were quickly dissected and cooled, and transverse slices of 400 μm were collected from the septal to the temporal end. Groups of eight to ten slices were distributed on Millicell-CM culture inserts (Millipore, Bedford, MA). The Biopore insert membrane was maintained in contact with culture media consisting of 50% basal medium Eagle, 25% and Earl's salt solution, 25% horse serum, supplemented to the following final concentrations: 136 mM NaCl, 2 mM $CaCl_2$, 2.5 mM $MgSO_4$, 4 mM $NaHCO_3$, 3 mM glutamine, 40 mM glucose, 0.4 mM ascorbic acid, 20 mM HEPES buffer (pH 7.3 at 23°C), 1 mg/liter insulin (24 IU/mg), 5 U/ml penicillin, and 5 mg/liter streptomycin. The slices were maintained for 14–18 days in culture before use, at 37°C, in a humid incubator supplied with 5% CO_2, with the media being changed every 2–3 days.

The slice cultures were transiently exposed to different concentrations of soman. A single treatment of freshly prepared agent was applied to both surfaces of the cultured slices, and this was repeated daily for up to 1 week. For vulnerability tests in separate cultures, induction of an excitotoxic insult was conducted on day 6 of subtoxic soman exposures using a 3-min AMPA (100 μM) application. During washout of the excitotoxin, the cultures were rapidly quenched with 40 μM CNQX and 20 μM MK-801 to stop further glutamate receptor stimulation (total procedure used two 10-min washes). All slice groups were harvested 7 days after the start of the soman exposures. Alternatively, different cultures were subjected to a 1-hr TMT (100 μM) exposure *before* the initial soman contact. The brief TMT application was followed by rapid quenching and washout, and the slices were subsequently exposed to subtoxic soman and harvested 24 hr later. All treatment groups (n = 4–6 per condition) were staggered so that all slices were harvested on the same day, at which time they were washed thoroughly in serum-free media and prepared for subsequent analyses.

Immunoblot Analysis

Cultured slices were gently removed with a soft brush and homogenized by sonication in groups of six to eight slices each using ice-cold buffer containing 8 mM HEPES buffer (pH 7.4), 1 mM EDTA, 1 mM EGTA, 0.02% NaN_3, 10 μg/liter antipain, and 2 μg/liter each of leupeptin, aprotinin, and pepstatin. Samples were assessed for protein content with a bovine serum albumin (BSA) standard, and equal protein aliquots (85 μg) were denatured in sodium dodecyl sulfate (SDS) and β-mercaptoethanol for 5 min at 100°C, then separated by 6–16% SDS-PAGE and blotted to nitrocellulose. The nitrocellulose membrane was incubated with primary antibodies at 4°C overnight with gentle agitation. Secondary antibody incubation utilized anti-IgG-alkaline phosphatase conjugates, and color development used the 5-bromo-4-chloro-3-indolyl phosphate and nitroblue tetrazolium substrate system. Development of immunoreactive bands was terminated before maximal intensity was reached to avoid saturation and to ensure a linear relationship with increasing amount of sample protein. Single immunoblots were used for comparative studies between different treatment groups and across multiple antigens. Bands were scanned at high resolution and assessed for integrated density with Bioquant software (R & M Biometrics, Nashville, TN).

Histology

Slices were rinsed with 0.1 M phosphate buffer, pH 7.4 (PB), and fixed for 2 hr in PB plus 4% paraformaldehyde. Slices were then cryoprotected in 20% sucrose for 1 hr and carefully removed from the insert, and serial sections were prepared at 20-μm thickness and mounted on Superfrost plus-coated slides (Fisher Scientific, Pittsburgh, PA). Sections were immunolabeled with antisynaptophysin by using the avidin-biotin-peroxidase technique and 3,3′-diaminobenzidine as the chromogen. Alternatively, separate sections were stained with cresyl violet. Bioquant image analysis included the use of a computerized deconvolution system with motorized Z-focus drive. For routine screening of slice culture quality, synaptic density was assessed with antisynaptophysin staining.

Statistical Analysis

Immunoreactivity levels were expressed as means ± SEM, and statistical significance was determined by unpaired *t*-tests and by one-way analyses of variance, followed by the Tukey-Kramer multiple-range tests.

RESULTS

Different concentrations of soman (nerve agent code GD) were administered to cultured hippocampal slices to determine levels that do not cause synaptic degeneration after an extended exposure period. Single daily applications produced transient exposure of the chemical agent before rapid hydrolysis in the culture medium, and this was repeated over a 7-day schedule. Slice cultures treated with up to 150 nM soman for 7 days of exposure exhibited no appreciable change in the synaptic vesicle component synaptophysin (left graph in Fig. 1B; see also left sample pair in Fig. 2A) or in the AMPA receptor subunit GluR1 (Fig. 1B, middle graph). Similar concentrations of soman have been shown to inhibit acetylcholinesterase by >90% while having no effect on cell viability in cultured hippocampal neurons (Deshpande et al., 1995). Thus, short-lived rises in acetylcholine levels may not be sufficient to trigger synaptic toxicity in localized brain areas. Transient soman exposures likely require higher concentrations to influence a wider circuitry, leading to secondary episodes of excitotoxic activity.

Soman at 20 μM was used to show that, at a higher agent concentration, transient exposures can cause synaptopathogenesis. Over the 7-day treatment regimen, presynaptic (Fig. 1B, left graph) and postsynaptic markers (Fig. 1B, middle graph) were significantly reduced. The reduction in the synaptic proteins occurred in conjunction with evident excitotoxicity as indicated by the marked increase in an excitotoxic indicator, BDP_N (right graph in Fig. 1B; also see immunoblots in Fig. 1A). BDP_N was labeled with antibodies directed against the proteolytic site in the spectrin sequence (Bahr et al., 1995b). The synaptic decline was found throughout the hippocampal subfields. The dendritic zone of hippocampal field CA1 (stratum radiatum), which normally exhibits dense staining for synaptophysin (Fig. 3A), was markedly reduced in the punctate immunolabeling after the soman treatment (Fig. 3B).

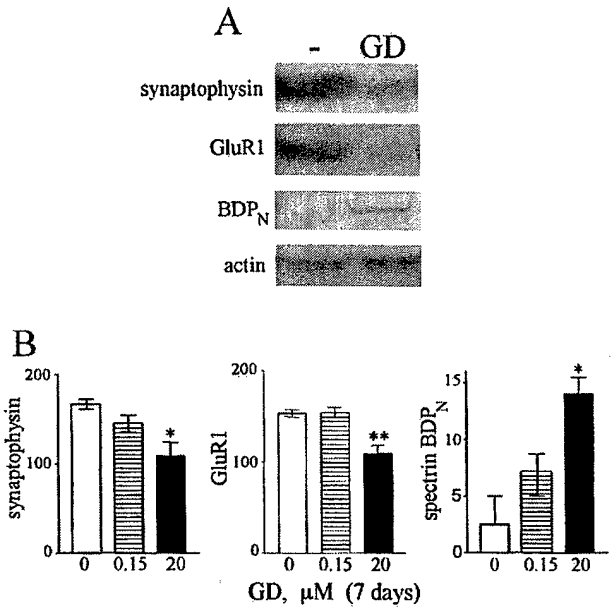

Fig. 1. Synaptic decline and cytoskeletal breakdown after transient soman exposures. **A:** Hippocampal slice cultures were prepared from postnatal day 12 Sprague-Dawley rats and maintained in culture for 3 weeks, after which a single treatment of 20 μM soman was applied each day for 7 days (GD). Equal protein aliquots from slice homogenates were used to determine amounts of synaptophysin, AMPA receptor subunit GluR1, and calpain-mediated spectrin breakdown product BDP_N by immunoblotting. Blots were also reprobed for β-actin to verify equal protein load. **B:** Integrated optical density levels of the immunoreactive bands were determined for slices subjected to repeated exposures to 0, 0.15, or 20 μM soman over 7 days (mean ± SEM; n = 5–9 groups of 6–8 slices each). Post hoc tests compared with nontreated control: $*P < 0.01$, $**P < 0.001$.

A similar decline was evident in the molecular layer of the dentate gyrus (Fig. 3D; compare with control in Fig. 3C). The synaptic effects occurred rather gradually; a single exposure to 20 μM soman produced little or no change in presynaptic synaptophysin and postsynaptic GluR1 markers 24 hr later (not shown).

Synaptic deterioration was apparent before neuronal loss, indicating selective vulnerability among synapses of soman-exposed brain tissue. The transient exposures that produced synaptic decline after 7 days of repeated contact had no obvious effect on neuronal density, nor did they produce any pyknotic changes in field CA1 (Fig. 4B; control tissue in Fig. 4A), hippocampal field CA3 (Fig. 4D; control in Fig. 4C), and the hilus (Fig. 5B; control in Fig. 5A). Note that, in Figure 5D, only sparse indications of pyknotic nuclei (arrows) were found among granular neurons of the dentate gyrus of soman-treated slice cultures, which were not evident in control tissue (Fig. 5C). Analyses for glial fibrillary acidic protein determined that the repeated soman exposures caused synaptic decline without producing secondary pathology in the form of an astroglial response (not shown).

tapraid5/z3p-neuro/z3p-neuro/z3p01504/z3p2471d04g | gockleyj | S=11 | 6/11/04 | 13:47 | Art: P-182

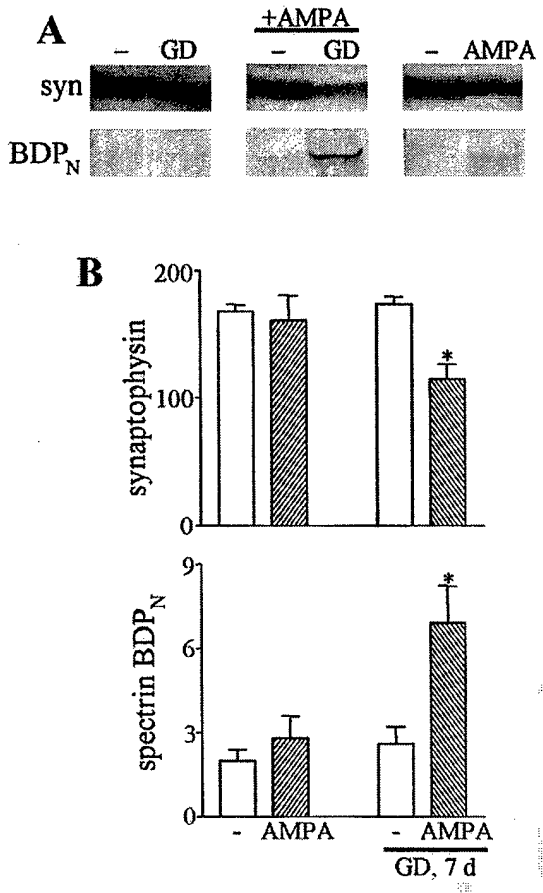

Fig. 2. Enhanced vulnerability in hippocampal slices exposed repeatedly to subtoxic soman. **A:** Slice cultures were treated 1) with or without 150 nM soman (GD) for 1 week of daily exposures (left lanes), 2) with or without a 3-min excitotoxic insult using 100 μM AMPA 24 hr before harvesting slices (right lanes), and 3) with or without the repeated soman exposures in conjunction with the AMPA insult on the sixth day of soman treatment (middle lanes). Slices were harvested on the same day and assessed for synaptophysin (syn) and the spectrin breakdown product BDP$_N$ by immunoblotting. **B:** Integrated optical density levels were determined for synaptophysin and BDP$_N$ in the different treatment groups (mean ± SEM; n = 7–15 groups of 6–8 slices each). Unpaired, two-tailed *t*-test: $*P < 0.01$.

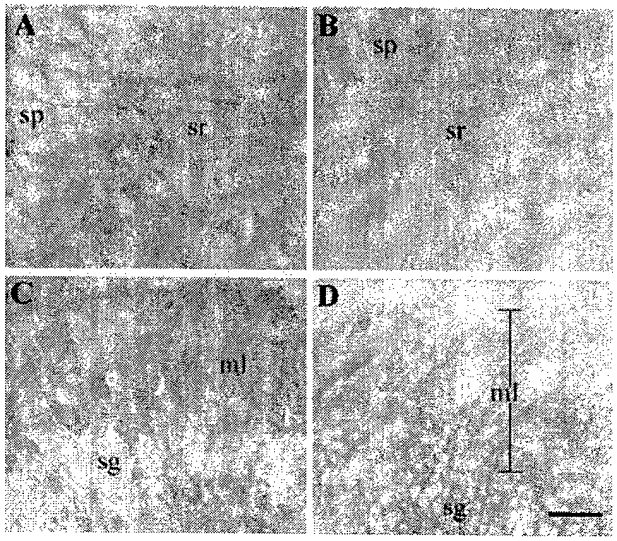

Fig. 3. Synaptic decline in soman-treated hippocampus. Hippocampal slice cultures were repeatedly treated without (**A,C**) or with (**B,D**) 20 μM soman for 7 days, after which they were fixed, sectioned, and stained with a monoclonal antibody against the synaptic vesicle protein synaptophysin. The immunoreactivity in the hippocampal subfield CA1 (A,B) and dentate gyrus (C,D) is shown. ml, Molecular layer; sg, stratum granulosum; sp, stratum pyramidale; sr, stratum radiatum. Scale bar = 35 μm for A,B, 50 μm for C,D.

COLOR

Next, we tested whether the subtoxic soman exposures cause brain tissue to become susceptible to the type of synaptic decline that results from high levels of soman. Hippocampal slices that were treated daily with 150 nM soman exhibited enhanced vulnerability to a brief excitotoxic insult. Slices were harvested 7 days after the start of the soman exposures. Mild excitotoxicity was induced on day 6 by overstimulating AMPA-type glutamate receptors for 3 min with 100 μM AMPA, a selective agonist known to cause neurodegeneration with longer treatment times in the slice model (Bahr et al., 1995b, 2002). The insult was rapidly quenched with receptor antagonists in parallel with wash-out of the excitotoxin. After a 24-hr recovery period, the excitotoxic insult alone did not cause appreciable synaptic decline (Fig. 2A, right sample pair). In contrast, in slice cultures first treated daily with subtoxic soman, the 3-min excitotoxic insult caused a marked reduction in the vesicle protein synaptophysin (Fig. 2A, middle pair of immunoblot samples). Immunoreactivity levels of the presynaptic marker were unchanged after 7 days of repeated soman exposures alone (leftmost sample pair) but were significantly reduced in soman-treated slices 24 hr after the AMPA insult ($P < 0.01$; upper graph in Fig. 2B). A similar reduction was evident for the postsynaptic marker GluR1 (not shown).

Repeated exposures to subtoxic soman also leave hippocampal tissue vulnerable to excitotoxic activation of the protease calpain and resultant cytoskeletal damage. The calpain-mediated spectrin breakdown product BDP$_N$ provides a sensitive marker for the protease activation that identifies neurotoxic conditions (see Vanderklish and Bahr, 2000). Persistent calpain activation is triggered by glutamatergic excitotoxicity and is thought to be a precursor of synaptic pathology and neurodegeneration (Siman et al., 1989; Bahr et al., 1995b, 2002; Bendiske et al., 2002). Subtoxic soman exposures caused a greater calpain response evident 24 hr after the mild AMPA insult (lower graph in Fig. 2B), corresponding to the enhanced synaptic vulnerability. The excitotoxic insult alone produced only trace levels of BDP$_N$ (right sample pair in Fig. 2A), possibly explaining the lack of synaptic effects. Similarly, daily

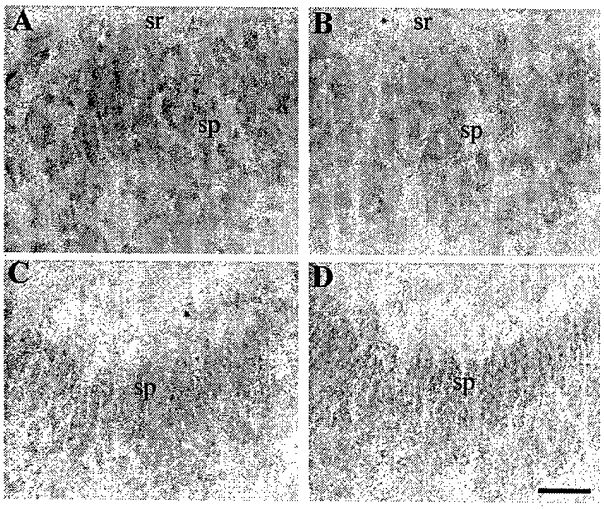

Fig. 4. Normal density of pyramidal neurons in soman-treated slice cultures. Hippocampal cultures were repeatedly treated without (**A,C**) or with (**B,D**) 20 μM soman for 7 days, after which they were fixed, sectioned, and stained with cresyl violet. Photomicrographs show pyramidal neurons in CA1 (A,B) and in field CA3 (C,D). sp, Stratum pyramidale; sr, stratum radiatum. Scale bar = 35 μm for A,B, 110 μm for C,D. Figure can be viewed in color online via www.interscience.wiley.com.

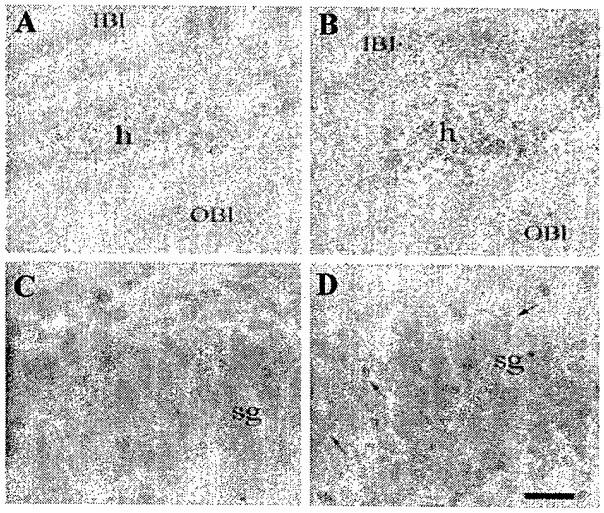

Fig. 5. Normal cellular densities in the dentate gyrus of soman-treated hippocampus. Hippocampal slice cultures were repeatedly treated without (**A,C**) or with (**B,D**) 20 μM soman for 7 days, after which they were fixed, sectioned, and stained with cresyl violet. Photomicrographs show the dentate gyrus zone (A,B) as well as granular neurons from the inner blade at high power (C,D). Sparse pyknotic nuclei are noted with arrows. h, Hilus; IBl, inner blade; OBl, outer blade; sg, stratum granulosum. Scale bar = 150 μm for A,B, 30 μm C,D. Figure can be viewed in color online via www.interscience.wiley.com.

applications with 150 nM soman caused only a small, insignificant change in BDP_N (Fig. 2A, leftmost sample pair). On the other hand, with the addition of the secondary excitotoxic insult, calpain-mediated BDP_N was markedly increased (middle immunoblot samples in Fig. 2A) to levels similar to those found in slices repeatedly exposed to 20 μM soman alone (see Fig. 1A).

Whereas incidences of excitotoxic and synaptic vulnerability developed after 1 week of repeated soman contact, a single transient exposure also resulted in hippocampal tissue becoming susceptible to a disparate insult after only 24 hr. A 1-hr treatment with TMT, a neurotoxin that causes excitotoxic damage in sensitive areas of the brain, including the hippocampus (Feldman et al., 1993; Ishida et al., 1997; Munirathinam et al., 2002), was found to be more effective at causing synaptic and cytoskeletal deterioration when followed by a single exposure to 150 nM soman (Fig. 6). The brief TMT application followed by antagonist quenching and wash-out was too short to cause lasting signs of damage (Fig. 6, rightmost sample pair). Similarly treated slice cultures were then subjected to transient soman exposure and assessed for a presynaptic marker and the calpain-mediated spectrin fragment BDP_N 24 hr later. As indicated by the enhanced synaptic decline and spectrin breakdown (middle pair of immunoblot samples in Fig. 6), it is clear that subtoxic soman increases neuronal vulnerability to toxic responses triggered before or after the nerve agent contact.

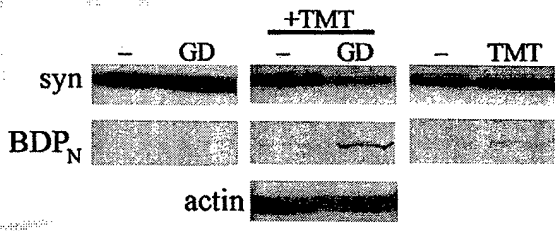

Fig. 6. Enhanced vulnerability with a single exposure to subtoxic soman. Slices were subjected to three different conditions: 1) treated with or without a single application of 150 nM soman (GD; left lanes), 2) with or without 100 μM TMT for 1 hr followed by rapid quenching and wash-out (right lanes), and 3) with or without the TMT exposure followed by the single soman treatment (middle lanes). The slices were harvested 24 hr postinsult and pooled into groups of six to eight slices each on the same culture day. Immunoblotting was conducted to assess the levels of synaptophysin (syn) and the spectrin breakdown product BDP_N. Blots were reprobed with an antibody to β-actin to indicate the relative amount of protein loaded in each lane.

DISCUSSION

Our results have several important implications regarding nerve agent exposure. First, the data indicate that, after repetitive, transient contact with high soman levels, synapses express the initial pathogenic response before overt signs of cellular atrophy. A distinct decline in synaptic markers occurred before neuronal loss in the hippocampus. The exposed hippocampal slice cultures re-

vealed intact, densely packed neurons and the absence of pyknotic changes in the major pyramidal fields. Among granular neurons of the dentate gyrus, the sparse distribution of pyknotic nuclei is an unlikely explanation of the soman-induced synaptic decline. Studies using subtoxic levels of soman showed no evidence of synaptopathogenesis, but the repeated exposures caused hippocampal tissue to become acutely sensitive to mild, disparate insults. The seemingly unaffected hippocampus was in fact susceptible to excitotoxic synaptic decline and cytoskeletal damage, both indicators of early and progressive neurotoxicity (Bahr et al., 1995b, 2002). Most importantly, the enhanced excitotoxic vulnerability was evident after 1 week or as little as 1 day of transient soman exposure, causing the hippocampus to become susceptible to insults occurring before or after nerve agent contact.

Hippocampal slices repeatedly treated with subtoxic soman became vulnerable to a brief AMPA exposure that usually has no lasting effects on synaptic or cellular integrity. The findings reveal a possible synergy between the excitotoxic activation of AMPA-type glutamate receptors and the release of glutamate following soman exposure. In support of this, Pavlovsky et al. (2003) reported acetylcholine-dependent enhancement of glutamategic excitatory transmission. AMPA receptors also have been found to play a key role in prompting hyperexcitability of population responses and spontaneous discharges in soman-treated hippocampal-entorhinal cortex slices (Wood and Tattersall, 2001). As noted, the excessive excitatory activity brought about by soman-induced increases in brain acetylcholine is thought to generate neurotoxic levels of glutamate. In addition to the overstimulation of AMPA receptors, the released glutamate may also cause the pathogenic activation of N-methyl-D-aspartate (NMDA)-type glutamate receptors (see McDonough and Shih, 1997). Deshpande et al. (1995) reported that soman and acetylcholine do not potentiate glutamate toxicity, in contrast to the enhanced excitotoxic vulnerability shown here in organotypic cultures. This may be because the authors did not use repeated exposures or because of the difference in pathogenic responsiveness between dissociated neurons and slice cultures.

Enhanced excitotoxic sensitivity was evident even when the subtoxic soman contact occurred after a brief episode of excitotoxicity. Hippocampal slices treated first with a mild TMT insult were made more sensitive to synaptic and cytoskeletal compromise upon a subsequent, single application of soman. The subtoxic soman exposure caused increased levels of excitotoxic damage 24 hr later. Note that longer insult durations with AMPA or TMT produced a degree of synaptic decline similar to that found in slices treated with high levels of soman alone (Harry et al., 1985; Brock and O'Callaghan, 1987; Bahr et al., 2002). This further suggests that a synergistic relationship underlies the disruption of synaptic maintenance produced by the combination of subtoxic soman exposure and a brief excitotoxic insult. The resultant synaptic deterioration would disrupt memory systems, and enhanced excitotoxic sensitivity would exacerbate the problem, especially insofar as memory impairment is a common outcome after exposures to AMPA (see Wenk et al., 1996; Kalivas et al., 2001), TMT (Kreyberg et al., 1992; Ishida et al., 1997; Ishikawa et al., 1997), or soman (Filliat et al., 1999; de Groot et al., 2001; Raveh et al., 2003). Persistent synaptopathogenesis in the hippocampus is likely part of the behavioral abnormalities and memory loss in soman-exposed animals and humans.

Accompanying the enhanced synaptic vulnerability was the activation of the protease calpain. Calpain mediates excitotoxic pathology, including the damage produced by AMPA and TMT insults, and is thought to instigate synaptopathogenesis and neuronal death (see Siman et al., 1989; Bahr et al., 1995b, 2002; Munirathinam et al., 2002). Calpain is involved in the neurodegeneration mediated by another family of cysteine proteases, the caspases (see Wang, 2000; Blomgren et al., 2001). Calpain and various caspases both promote cellular compromise during different types of excitotoxic episodes, including related seizure activity. The calpain response associated with subtoxic soman and enhanced sensitivity was similar to that found after repeated contact with high soman concentrations alone. Thus, subtoxic soman exposures may decrease the threshold for the excitotoxic activation of calpain, thereby increasing synaptic vulnerability to brief insults. Indeed, calpain-mediated proteolysis has been linked to toxin-induced synaptopathogenesis, and inhibition of proteolytic processes is a proposed treatment for exposure to neurotoxins, including soman (see Vanderklish and Bahr, 2000; Cowan et al., 2001). The present findings also suggest that excitotoxic protease activation plays a role in the initial action of nerve agents, leading to neuronal dysfunction and decay.

Although there are many examples of subtoxic or mildly toxic conditions that promote neuronal tolerance (known as *preconditioning*), e.g., ischemia, hypoxia, excitotoxin exposure (see Schaller and Graf, 2002; Raval et al., 2003), subtoxic soman contact leads to a dramatic decrease in tolerance. This is an important issue, in that, although acute toxicity is easily detected, low-level toxicity is difficult to identify and can last for an extended period after the initial exposure (for an excellent review of the subject see Somani and Romano, 2001). The enhanced synaptic vulnerability described here may explain some of the toxicological complications that persist for months or years, making treatment very challenging. Adding to this challenge is that imperceptible soman contact can leave the brain susceptible to excitotoxic episodes, of which there are many examples, including stroke and traumatic brain injury. Criteria for exposure that involve memory or cognitive tests may not detect those individuals who are distinctly vulnerable to damage but lack obvious signs of neuronal dysfunction. The present results emphasize the need for early indicators to measure any level of soman exposure, so that subsequent brain injury can be ade-

quately assessed and treatment/prevention measures executed in a timely manner.

REFERENCES

Bahr BA. 1995. Long-term hippocampal slices: a model system for investigating synaptic mechanisms and pathologic processes. J Neurosci Res 42:294–305.

Bahr BA, Abai B, Gall C, Vanderklish PW, Hoffman KB, Lynch G. 1994. Induction of β-amyloid-containing polypeptides in hippocampus: evidence for a concomitant loss of synaptic proteins and interactions with an excitotoxin. Exp Neurol 129:81–94.

Bahr BA, Kessler M, Rivera S, Vanderklish PW, Hall RA, Singh Mutneja M, Gall C, Hoffman KB. 1995a. Stable maintenance of glutamate receptors and other synaptic components in long-term hippocampal slices. Hippocampus 5:425–439.

Bahr BA, Tiriveedhi S, Park GY, Lynch G. 1995b. Induction of calpain-mediated spectrin fragments by pathogenic treatment in long-term hippocampal slices. J Pharmacol Exp Ther 273:902–908.

Bahr BA, Hoffman KB, Kessler M, Hennegriff M, Park GY, Yamamoto RS, Kawasaki BT, Vanderklish PW, Hall RA, Lynch G. 1996. Distinct distributions of α-amino-3-hydroxy-5-methyl-4-isoxazolepropionate (AMPA) receptor subunits and a related 53,000 M_R antigen (GR53) in brain tissue. Neuroscience 74:707–721.

Bahr BA, Bendiske J, Brown QB, Munirathinam S, Caba E, Rudin M, Urwyler S, Sauter A, Rogers G. 2002. Survival signaling and selective neuroprotection through glutamatergic transmission. Exp Neurol 174: 37–47.

Bendiske J, Caba E, Brown QB, Bahr BA. 2002. Intracellular deposition, microtubule destabilization, and transport failure: an 'early' pathogenic cascade leading to synaptic decline. J Neuropathol Exp Neurol 61:640–650.

Blomgren K, Zhu C, Wang X, Karlsson J-O, Andersson A-L, Bahr BA, Mallard C, Hagberg H. 2001. Synergistic activation of caspase-3 by m-calpain after neonatal hypoxia-ischemia—a mechanism of "pathological apoptosis"? J Biol Chem 276:10191–10198.

Brock TO, O'Callaghan JP. 1987. Quantitative changes in the synaptic vesicle proteins synapsin I and p38 and the astrocyte-specific protein glial fibrillary acidic protein are associated with chemical-induced injury to the rat central nervous system. J Neurosci 7:931–942.

Carpentier P, Lambrinidis M, Blanchet G. 1991. Early dendritic changes in hippocampal pyramidal neurons (field CA1) of rats subjected to acute soman intoxication: a light microscopic study. Brain Res 541: 293–299.

Cowan FM, Broomfield CA, Lenz DE, Shih TM. 2001. Protective action of the serine protease inhibitor N-tosyl-L-lysine chloromethyl ketone (TLCK) against acute soman poisoning. J Appl Toxicol 21:293–296.

de Groot DM, Bierman EP, Bruijnzeel PL, Carpentier P, Kulig BM, Lallement G, Melchers, BP, Philippens IH, van Huygevoort AH. 2001. Beneficial effects of TCP on soman intoxication in guinea pigs: Seizures, brain damage and learning behaviour. J Appl Toxicol 21:S57–S65.

Deshpande SS, Smith, CD, Filbert MG. 1995. Assessment of primary neuronal culture as a model for soman-induced neurotoxicity and effectiveness of memantine as a neuroprotective drug. Arch Toxicol 69:384–390.

Feldman RG, White RR, Eriator II. 1993. Trimethyltin encephalopathy. Arch Neurol 50:1320–1324.

Filliat P, Baubichon D, Burckhart MF, Pernot-Marino I, Foquin A, Masqueliez C, Perrichon C, Carpentier P, Lallement G. 1999. Memory impairment after soman intoxication in rat: correlation with central neuropathology: improvement with anticholinergic and antiglutamatergic therapeutics. Neurotoxicology 20:535–549.

Harry GJ, Goodrum JF, Krigman MR, Morell P. 1985. The use of synapsin I as a biochemical marker for neuronal damage by trimethyltin. Brain Res 326:9–18.

Ishida N, Akaike M, Tsutsumi S, Kanai H, Masui A, Sadamatsu M, Kuroda Y, Watanabe Y, McEwen BS, Kato N. 1997. Trimethyltin syndrome as a hippocampal degeneration model: temporal changes and neurochemical features of seizure susceptibility and learning impairment. Neuroscience 81:1183–1191.

Ishikawa K, Kubo T, Shibanoki S, Matsumoto A, Hata H, Asai S. 1997. Hippocampal degeneration inducing impairment of learning in rats: model of dementia? Behav Brain Res 83:39–44.

Kalivas PW, Jackson D, Romanidies A, Wyndham L, Duffy P. 2001. Involvement of pallidothalamic circuitry in working memory. Neuroscience 104:129–136.

Kreyberg S, Torvik A, Bjorneboe A, Wiik-Larsen W, Jacobsen, D. (1992). Trimethyltin poisoning: report of a case with postmortem examination. Clin Neuropathol 11:256–259.

Lallement G, Carpentier P, Collet A, Pernot-Marino I, Baubichon D, Blanchet G. 1991. Effects of soman-induced seizures on different extracellular amino acid levels and on glutamate uptake in rat hippocampus. Brain Res 563:234–240.

Lallement G, Denoyer M, Collet A, Pernot-Marino I, Baubichon D, Monmaur P, Blanchet G. 1992. Changes in hippocampal acetylcholine and glutamate extracellular levels during soman-induced seizures: influence of septal cholinoceptive cells. Neurosci Lett 139:104–107.

Lallement G, Delamanche IS, Pernot-Marino I, Baubichon D, Denoyer M, Carpentier P, Blanchet G. 1993. Neuroprotective activity of glutamate receptor antagonists against soman-induced hippocampal damage: quantification with a w3-site ligand. Brain Res 618:227–237.

Lemercier G, Carpentier P, Sentenac-Roumanou H, Morelis P. 1983. Histological and histochemical changes in the central nervous system of the rat poisoned by an irreversible anticholinesterase organophosphorous compound. Acta Neuropathol 61:123–129.

Mattson MP. 1990. Antigenic changes similar to those seen in neurofibrillary tangles are elicited by glutamate and Ca^{2+} influx in cultured hippocampal neurons. Neuron 4:105–117.

McDonough J Jr, Shih T. 1997. Neuropharmacological mechanisms of nerve agent-induced seizure and neuropathology. Neurosci Biobehav Rev 21:559–579.

Munirathinam S, Bahr BA. 2002. Low-level soman exposure leads to synaptic damage in the hippocampus and potentiates neuronal vulnerability. Toxicol Sci 58(Suppl):1551.

Munirathinam S, Rogers G, Bahr BA. 2002. Positive modulation of α-amino-3-hydroxy-5-methyl-4-isoxazolepropionic acid-type glutamate receptors elicits neuroprotection after trimethyltin exposure in hippocampus. Toxicol Appl Pharmacol 185:111–118.

Pavlovsky L, Browne RO, Friedman A. 2003. Pyridostigmine enhances glutamatergic transmission in hippocampal CA1 neurons. Exp Neurol 179:181–187.

Pazdernik TL, Cross RS, Giesler M, Samson FE, Nelson SR. 1985. Changes in local cerebral glucose utilization induced by convulsants. Neuroscience 14:823–835.

Raval AP, Dave KR, Mochly-Rosen DM, Sick TJ, Perez-Pinzon MA. 2003. εPKC is required for the induction of tolerance by ischemic and NMDA-mediated preconditioning in the organotypic hippocampal slice. J Neuroscience 23:384–391.

Raveh L, Weissman BA, Cohen G, Alkalay D, Rabinovitz I, Sonego H, Brandeis R. 2002. Caramiphen and scopolamine prevent soman-induced brain damage and cognitive dysfunction. Neurotoxicology 23:7–17.

Raveh L, Brandeis R, Gilat E, Cohen G, Alkalay D, Rabinovitz I, Sonego H, Weissman BA. 2003. Anticholinergic and antiglutamatergic agents protect against soman-induced brain damage and cognitive dysfunction. Toxicol Sci 75:108–116.

Schaller B, Graf R. 2002. Cerebral ischemic preconditioning. An experimental phenomenon or a clinical important entity of stroke prevention? J Neurol 249:1503–1511.

Sheardown MJ, Nielsen EO, Hansen AJ, Jacobsen P, Honore T. 1990. 2,3-Dihydroxy-6-nitro-7-sulfamoyl-benzo(F)quinoxaline: a neuroprotectant for cerebral ischemia. Science 247:571–574.

Siman R, Noszek JC, Kegerise C. 1989. Calpain I activation is specifically related to excitatory amino acid induction of hippocampal damage. J Neurosci 9:1579–1590.

Somani SM, Romano J. 2001. Chemical warfare agents: low level toxicity. Boca Raton, FL: CRC Press.

Sparenborg S, Brennecke LH, Jaax NK, Braitman DJ. 1992. Dizocilpine (MK-801) arrests status epilepticus and prevents brain damage induced by soman. Neuropharmacology 31:357–368.

Stoppini L, Buchs PA, Muller D. 1991. A simple method for organotypic cultures of nervous tissue. J Neurosci Methods 37:173–182.

Taylor P. 2001. Anticholinesterase agents. In: Hardman JG, Limbird LE, Gilman AG, editors. The pharmacological basis of therapeutics, 10th ed. New York: McGraw Hill. p 175–191.

Vanderklish PW, Bahr BA. 2000. The pathogenic activation of calpain: a marker and mediator of cellular toxicity and disease states. Int J Exp Pathol 81:323–339.

Wade JV, Samson FE, Nelson SR, Pazdernik TL. 1987. Changes in extracellular amino acids during soman- and kainic acid-induced seizures. J Neurochem 49:645–650.

Wang KK. 2000. Calpain and caspase: can you tell the difference? Trends Neurosci 23:20–26.

Wenk GL, Stoehr JD, Mobley SL, Gurney J, Morris RJ. 1996. Age-related decrease in vulnerability to excitatory amino acids in the nucleus basalis. Neurobiol Aging 17:1–7.

Wood SJ, Tattersall JE. 2001. An improved brain slice model of nerve agent-induced seizure activity. J Appl Toxicol 21:S83–S86.

Author Proof

Acta Neuropathol (2004) 108 : 173–182
DOI 10.1007/s00401-004-0876-5

REGULAR PAPER

Ebru Caba · Ben A. Bahr

Biphasic NF-κB activation in the excitotoxic hippocampus

Received: 10 December 2003 / Revised: 24 March 2004 / Accepted: 2 April 2004 / Published online: 8 May 2004
© Springer-Verlag 2004

Abstract Excitotoxic stimulation of NMDA receptors results in the activation of a variety of cellular responses. The inducible transcription factor NF-κB is known to be involved in excitotoxic responses by neurons. Here, we show that NF-κB activation occurs in a biphasic manner in hippocampal slices following a 20-min *N*-methyl-D-aspartate (NMDA) exposure. The biphasic activation profile consists of an early, rapid phase at 0.5–1 h post-insult, and a delayed phase evident 10–24 h post-insult. Endogenous inhibitors of NF-κB, IκBs, were examined for their involvement in the biphasic activation. IκBβ exhibited marked degradation in response to the excitotoxity, while changes in the levels of IκBα and p105 isoforms were not detected. The initial decline in IκBβ occurred in as little as 30 min post-NMDA exposure, coinciding with early NF-κB activity. A second, more gradual phase of IκBβ degradation was also evident, possibly giving rise to the delayed activation of the transcription factor. While both phases of NF-κB activation were disrupted by the NMDA receptor antagonist AP5, they were distinct with regard to the composition of activated complexes and their responsiveness to altered culture conditions. The two phases of NF-κB activity also were associated with distinct gene regulation events. Up-regulation of bcl-2 message occurred early after the excitotoxic insult and remained up-regulated for an extended period. In contrast, bax message initially remained unchanged after the insult, but then exhibited an increase 24 h later, corresponding with the second phase of the NF-κB response. These results indicate that distinct phases of NF-κB activation are generated in the excitotoxic hippocampus, and that the phases may be involved in opposing cellular responses.

E. Caba · B. A. Bahr (✉)
Department of Pharmaceutical Sciences
and the Neurosciences Program, University of Connecticut,
Storrs, CT 06269-2092, USA
Tel.: +1-860-4866043, Fax: +1-860-4866858,
e-mail: Bahr@uconn.edu

Keywords bcl-2 · bax · Excitotoxicity · Hippocampal slice cultures · NF-κB

Introduction

Excessive or prolonged activation of *N*-methyl-D-aspartate (NMDA)- and α-amino-3-hydroxy-5-methyl-4-isoxazolepropionate (AMPA)-type glutamate receptors in the brain induces sustained levels of intracellular calcium, causing neuronal impairment and death, particularly in the hippocampus. This phenomenon, referred to as glutamate excitotoxicity, is characterized by damage of cellular components and disruption, or at times activation, of signal transduction events including those involving nuclear factor-κB (NF-κB) [10, 18, 22, 36, 58]. NF-κB is a ubiquitous, inducible transcription factor that is activated by a wide range of stimuli [16, 23, 37]. The complexity of this transcription factor is not only a result of the variety of signals that regulate it, but the vast number of genes that are regulated by NF-κB.

NF-κB has been extensively studied because it is a pleiotropic factor that, depending on the stimulus [37, 53], cell type [2, 3], and stage of development [19], can initiate the transcription of many genes. The diversity of NF-κB activation is illustrated by its involvement in promoting apoptosis as well as cell survival. Numerous studies have assigned such opposing roles to NF-κB in the same cell and tissue types [21, 27, 33, 57, 60], thus suggesting that the pathway mediated by NF-κB is determined not by the tissue type but by the stimulus. In the brain, however, a controversy exists in the fact that NF-κB activation leads to opposing pathways after the same type of stimulus. For example, several studies implicate NF-κB in apoptosis in response to excitotoxicity and global ischemia [1, 11, 17, 41, 46], while others point to the anti-apoptotic role played by NF-κB during the same type of excitotoxic episodes [15, 31, 35, 49, 55]. The present study approached the dual role issue by testing for distinct events of NF-κB activation that may be involved in pro- and anti-apoptotic pathways in the excitotoxic hippocampus.

The hippocampus is particularly vulnerable to stroke-type excitotoxicity, hence we sought to explore the role of NF-κB in the established hippocampal slice model of excitotoxicity [4, 6, 7, 25, 42, 48, 59]. To study the transcription factor, we evaluated the activation profile of NF-κB in interface slice cultures that were subjected to a 20-min NMDA exposure. The brief insult resulted in a biphasic activation profile for NF-κB. Interestingly, we show that the biphasic NF-κB response in the excitotoxic hippocampus coincides with early up-regulation of an anti-apoptotic gene and delayed up-regulation of a pro-apoptotic gene.

Methods and materials

Organotypic hippocampal slice cultures

Sprague-Dawley rat litters (Charles River Laboratories, Wilmington, MA) were housed in accordance with guidelines from the National Institutes of Health and Institutional Animal Care and Use Committee. Interface hippocampal slice cultures were prepared from animals at 11–12 days postnatal. The methodology used has been approved by the Animal Care and Use Committee. Transverse slices of hippocampus (400 μm) were quickly prepared, maintained on Millicell-CM inserts (Millipore Corporation, Bedford, MA), and periodically supplied with fresh media composed of 50% basal medium Eagle, 25% Earle's balanced salts, 25% horse serum, and defined supplements [5, 6]. Slices were maintained at 37°C in a 5% CO_2-enriched atmosphere and fed every other day until use. Slices were allowed to mature for 10–15 days in culture before being used in experiments.

Induction of excitotoxicity

Brief excitotoxicity was achieved by incubating the cultured slices with media containing 200 μM NMDA (Tocris, Ellisville, MO) for 20 min. The agonist was then removed using multiple media washes containing 40 μM each of MK801 and CNQX (Tocris), selective antagonists that quench any further activity of NMDA- and AMPA-type glutamate receptors, respectively. The slice cultures were then placed in fresh media for the recovery period of 0.5–24 h. In a separate group of cultures, a control experiment was conducted in which the NMDA receptor antagonist AP5 (Tocris) was present before (5-min pre-treatment), during, and after the excitotoxic insult. Continual presence of the antagonist throughout the treatment paradigm was to verify that the measured results were indeed mediated by NMDA receptors. Additional experiments were conducted in the presence of the neuroprotective agent Ampakine (20 μM) or in the absence of serum to measure changes in NMDA-induced effects.

Immunohistochemistry

Slices were fixed on the Millicell membranes in 4% paraformaldehyde for 2 h and cryoprotected with 20% sucrose for 1 h or overnight. The fixed tissue was then sectioned at 20 μm and mounted on coated slides (Fisher Scientific, Pittsburgh, PA). The mounted tissue was Nissl stained or probed with antibodies that selectively recognize activated NF-κB. These include antibodies to the nuclear localization signal in the p50 subunit (anti-p50/NLS or anti-p50/D17; Santa Cruz Biotechnology, Santa Cruz, CA). Avidin-biotin-peroxidase technique and the chromogen 3,3'-diaminobenzidine (Vector Laboratories, Burlingame, California) showed the location of the bound primary antibody.

Nuclear extraction and electrophoretic mobility shift assay

Nuclear extraction was carried out as previously described [10]. Briefly, harvested slices were homogenized in ice-cold nuclear extract buffer (20 mM HEPES pH 7.9, 100 mM NaCl, 1.5 mM $MgCl_2$, 0.5 mM EDTA, 0.7% IGEPAL CA630, 10% glycerol, 2 μg/ml leupeptin, 5 μg/ml aprotinin, 0.1 mM phenylmethanesulfonyl fluoride, and 0.5 mM dithiothreitol). Homogenates were centrifuged at 6,500 rpm, and the pellets washed. The pellets were suspended in 35 μl high-salt buffer and centrifuged so that supernatant could be collected and protein concentrations determined. Equal amounts of nuclear protein (7.5 μg) were subjected to electrophoretic mobility shift assay (EMSA) as outlined previously [10]. The samples were incubated with 2.5 μg poly-dI·dC (Sigma-Aldrich Corporation; St. Louis, MO) and 0.75 μg BSA in 15 μl total volume for 20 min, then incubated at room temperature for 15 min with ^{32}P-labeled NF-κB consensus oligonucleotide (5'-AGT TGA GGG GAC TTT CCC AGG C-3'; Promega, Madison, WI). Protein-DNA complexes were then resolved by 4% PAGE and visualized by Kodak X-OMAT film autoradiography. Supershift analyses entailed incubating samples with antibodies to p50, p52, and p65 (Santa Cruz Biotechnology) for 20 min on ice before electrophoretic separation. NF-κB binding activity was determined by integrated optical density using BIOQUANT software (R & M Biometrics, Nashville, TN). Mean densities from slice samples treated with or without NMDA were compared using unpaired, two-tailed *t*-tests or ANOVA.

SDS-PAGE and immunoblot analysis

Control and NMDA-treated slice cultures were gently removed with a soft brush and homogenized, in groups of six to eight, using ice-cold homogenization buffer. Protein content was determined with a BSA standard and equal aliquots of the slice samples were denatured in sampling buffer for 5 min at 100°C, then separated by 4–16% SDS-PAGE, and blotted onto nitrocellulose. Immunodetection was accomplished by incubating blots at 4°C with antibodies that recognize IκBα, IκBβ, p105 (Santa Cruz Biotechnology), and the phosphorylated active form of IκB kinase (IKK; Cell Signaling, Beverly, MA). Secondary antibody incubation utilized anti-IgG-alkaline phosphatase conjugates, and band intensity was determined using 5-bromo-4-chloro-3-indolyl phosphate and nitroblue tetrazolium. Color development of immunoreactive bands was terminated before maximal intensity was reached to avoid saturation and to ensure a linear relationship with increasing amount of sample protein. Bands were scanned at high resolution and assessed for integrated density with BIOQUANT software (R & M Biometrics). Mean integrated densities for antigens in slice samples treated with or without NMDA were compared using unpaired, two-tailed *t*-tests or ANOVA.

Reverse transcriptase-PCR

RNA was isolated from control and NMDA-exposed hippocampal slices using RNeasy Mini kit according to manufacturer's recommendations (Qiagen; Valencia, California). cDNA was generated using 2.5 μM random hexamers, 1 X PCR reaction buffer, 2.5 mM $MgCl_2$, 1 mM of each dNTP, 1U/μl MuLV reverse transcriptase (RT) (Applied Biosystems, Branchburg, NJ). Using 200 ng cDNA as the template, PCR was carried out in a total volume of 25 μl containing 1× PCR reaction buffer, 2.5 mM $MgCl_2$, 0.2 mM of each dNTP, 1.25 U/μl Taq DNA polymerase (Eppendorf Scientific, Westbury, NY), and 0.25 mM each of forward and reverse primers. The primer sequences were as follows: bcl-2 5' strand CAC CCC TGG CAT CTT CTC CTT, bcl-2 3' strand AGC GTC TTC AGA GAC AGC CAG, bax 5' strand CCA CCA GCT CTG AAC AGA TCA TGA, and bax 3' strand TCA GCC CAT CTT CTT CCA GAT GGT (Sigma Genosys, The Woodlands, TX). Rat β-actin primers were purchased from Promega. Reaction mixture without DNA template was used as a negative control. Twenty-four cycles

of amplification, for both bax and bcl-2, were determined to generate products in the linear dynamic range. PCR products were resolved on 2% agarose gels and their images captured and analyzed using the Kodak EDAS120 system (Rochester, NY).

In situ hybridization

Experiments used the in situ hybridization/detection kit and manufacturer's recommendations from Maxim Biotech, Inc. (San Francisco, CA). The biotin-labeled oligonucleotide probe for rat bcl-2 (235 bp) was constructed according to the sequence from the GenBank database (accession no. L144680). Control and treated slices were fixed in 4% paraformaldehyde, sectioned at 20 μm thickness, and dried. The tissue was rehydrated, then incubated with proteinase K for 1 h to deproteinize the samples. The sections were air-dried, denatured at 70°C, followed by overnight incubation with the diluted probe in a humidity chamber. After subsequent washes, the biotinylated probe was detected through signal amplification and a streptavidin-alkaline phosphatase conjugate. Color development utilized appropriate substrates and the tissue was cover-slipped and examined by light microscopy.

Results

To monitor excitotoxic activation of NF-κB, hippocampal slice cultures were infused with NMDA, an agonist of a class of excitatory glutamate receptors. After 20 min, the NMDA was thoroughly washed out in the presence of selective antagonists to quench any further glutamatergic stimulation, thus providing a defined insult. The NMDA-treated slices were probed with anti-p50/NLS antibodies, which recognize the nuclear localization signal in the p50

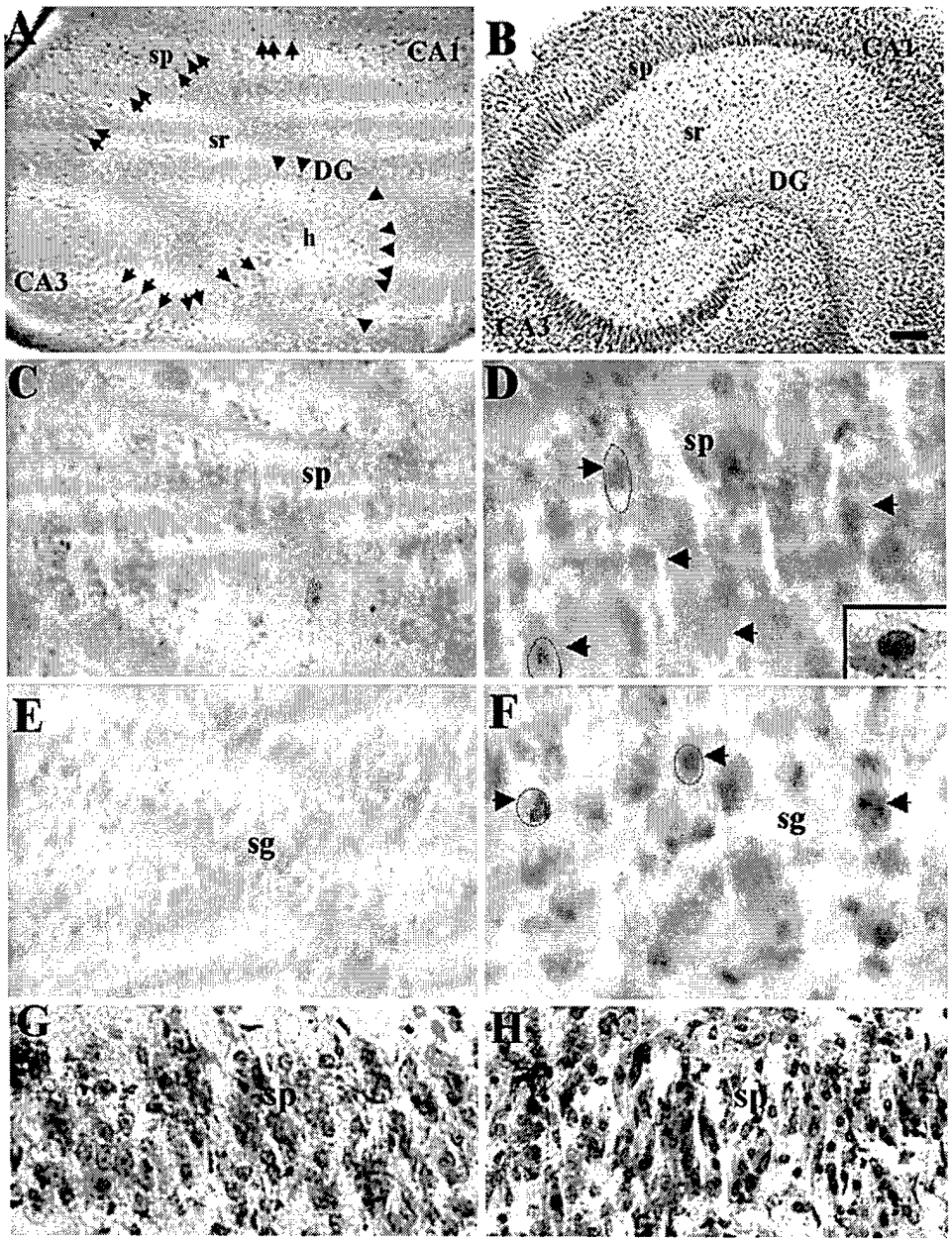

Fig. 1 Excitotoxicity causes NF-κB activation in neuronal subfields of hippocampus. NMDA (200 μM) was infused into slice cultures for 20 min, followed by rapid washout and quenching of glutamatergic receptors. Slices were subsequently fixed at 24 h post-insult, then assessed for active NF-κB with anti-p50/NLS as described in Materials and Methods (**A**). Anti-p50/NLS antibodies labeled a wide distribution of nuclei in pyramidal neurons of CA1 and CA3 (*arrows*) and in the stratum granulosum of the dentate gyrus (see *arrowheads*). Additional excitotoxic slices were Nissl stained (**B**). Control cultures (**C**, **E**) and slices harvested 1 h post-insult (**D**, **F**) were fixed, sectioned, and probed with anti-p50/NLS. Pyramidal neurons (**C**, **D**) and granular neurons (**E**, **F**) were examined at high magnification, revealing NMDA-induced nuclear localization of active NF-κB (see outline of selected cell bodies). Nissl staining of the CA1 region is shown at 1 h (**G**) and 24 h post-insult (**H**) (*DG* dentate gyrus, *h* hilus, *sg* stratum granulosum, *sp* stratum pyramidale, *sr* stratum radiatum). *Bar* (in **B**) **A**, **B** 250 μm; **C**, **D** 20 μm; *inset* in **D** 12 μm; **E**, **F** 14 μm; **G**, **H** 35 μm

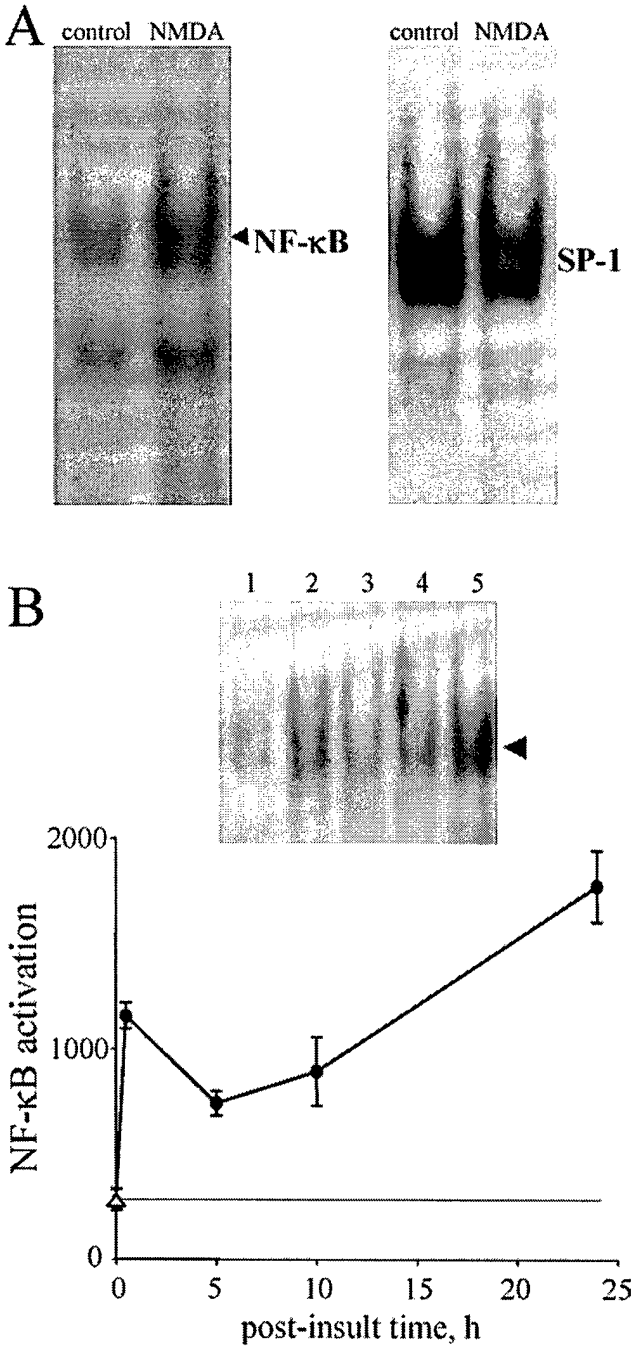

Fig. 2 Specific and biphasic activation of NF-κB in the excitotoxic hippocampus. NMDA was infused into hippocampal slice cultures for 20 min, followed by washout and antagonist quenching. Nuclei were isolated 1 h post-insult and NF-κB activation was assessed for probe binding (**A**, *left lanes*). The EMSA shows that NF-κB binding activity is increased following the insult. Nuclei from similarly treated slices were assessed for SP-1 binding (**A**, *right lanes*). In **B**, NF-κB activation (*arrow*) was quantified in nuclei extracted from non-treated control slices (*lane 1*) and from NMDA-treated slices harvested 1, 5, 10, and 24 h post-insult (*lanes 2–5*, respectively). The plotted integrated optical densities (means ± SEM) represent NF-κB-DNA binding activity of control slices (*triangle*; see *dotted baseline*) and the NMDA-induced activation profile (*circles*) determined from 4 to 13 separate groups of slices. The data were subjected to a one-way analysis of variance ($P<0.0001$). (*EMSA* electrophoretic mobility shift assay)

subunit normally masked by IκBs. Punctate nuclear staining of the activated p50 subunit was evident 24 h post-insult, particularly in the wide band of pyramidal neurons in fields CA1 and CA3 (Fig. 1A, arrows), as well as in the granular cell layer of the dentate gyrus (arrowheads) (see the Nissl-stained slice in Fig. 1B for position references). In the hilus and the dendritic fields of CA1, there was evidence of staining of other cell types including perhaps interneurons and astrocytes. In addition, p50-containing NF-κB complexes were translocated into neuronal nuclei as early as 1 h post-insult. Morphologically defined neurons in the stratum pyramidale exhibited nuclear staining of the active transcription factor (see arrows and inset in Fig. 1D), whereas control tissue exhibited mostly cytoplasmic staining and perhaps low-level basal activation (Fig. 1C). Granular neurons also exhibited NMDA-induced nuclear staining of activated NF-κB (arrows in Fig. 1F), while control slices did not (Fig. 1E). Note that NF-κB activation occurs as the major neuronal subfields remain intact in the excitotoxic hippocampus (Fig. 1B). While vulnerable CA1 neurons are without overt signs of atrophy 1 h post-insult (Fig. 1G), initial pyknotic changes as well as intact neurons are evident at 24 h post-insult (Fig. 1H).

In further experiments, nuclei preparations were extracted from control and NMDA-treated slices and subsequently assessed for the activity of transcription factors NF-κB and SP-1. The excitotoxic exposure caused an increase in NF-κB binding of the consensus sequence (Fig. 2A, left lanes), as expected from the immunocytochemistry results showing NF-κB complexes translocated into neuronal nuclei. No such increase in activity was exhibited by SP-1 in NMDA-treated slice cultures (Fig. 2A, right lanes). In fact, the SP-1 activity was lower than that measured in control slices (70±15% of control; $n=6$ groups of 20 slices each), but the change was not statistically significant. To better determine the activation profile for NF-κB, slices were harvested and nuclei isolated at different times post-insult. As shown in Fig. 2B, biphasic activation of NF-κB is evident following the induced excitotoxicity. The initial increase above basal activity, which occurred at 0.5–1 h post-insult time, was reduced by almost 50% 4 h later, followed by a gradual second phase of activation between 10–24 h post-insult. To confirm the biphasic profile, imaging data from control and NMDA-treated slice groups were assessed by a one-way analysis of variance ($P<0.0001$).

Next, we tested whether IκB degradation events can account for the early and delayed phases of NF-κB activation. Specific antibodies were used to monitor IκB family members, namely IκBα, IκBβ and p105, in control and NMDA-treated slices. As shown in Fig. 3A, a significant decline in IκBβ (lower graph) coincided with the early activation of NF-κB (upper graph). IκBβ levels also exhibited a gradual decline from initially restored levels (Fig. 3B, lower graph) that coincided with the delayed phase of NF-κB activation (Fig. 3B, upper graph). As determined from post-hoc tests, the decrease in IκBβ was not significant until the 10 h post-insult time and was more obvious after 24 h, perhaps giving rise to the increase in NF-κB activity that occurs between 10–24 h post-insult. Interestingly, the two phases of IκBβ decline corre-

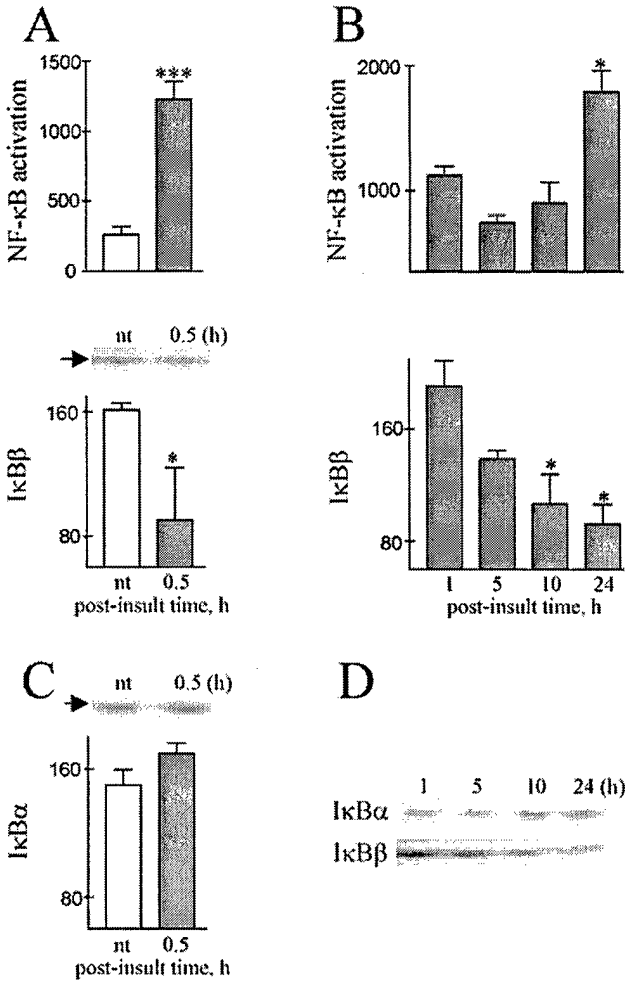

Fig. 3 IκBβ degradation corresponds with NF-κB activation in the excitotoxic hippocampus. Non-treated control tissue (*nt*) and NMDA-treated slices harvested 0.5 h post-insult were analyzed for nuclear NF-κB binding activity (mean ± SEM; n=8–12), while slice homogenate samples were assessed for IκBβ immunoreactivity by Western blot (**A**); unpaired, two-tailed t-test: *P<0.05, ***P<0.0001. The same slice homogenates were assessed for IκBα (**C**). Mean immunoreactivity levels were determined from integrated density imaging measures (± SEM). NF-κB activation and IκBβ levels were also determined in slice samples that were harvested 1, 5, 10, and 24 h post-insult (n=3–12 each) (**B**). The gradual decrease in IκBβ (ANOVA: P=0.016) corresponds with the increased nuclear translocation of NF-κB (ANOVA: P<0.001) (*Tukey's post-hoc test compared to 1 h point: *P<0.05). Representative immunoblots stained for IκBα and IκBβ are shown (**D**)

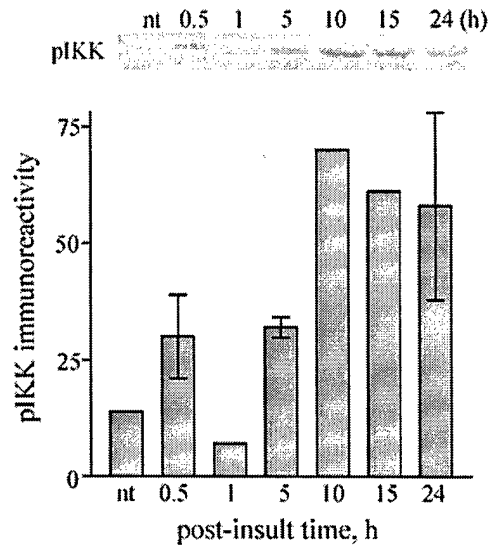

Fig. 4 Activation of IκB kinase (*IKK*) in the excitotoxic hippocampal slice model. The homogenate samples used to measure IκBβ in Fig. 3 were assessed for IKK activation. Antibodies that selectively recognize the phosphorylated active form of the kinase (*pIKK*) stained the immunoblot samples from non-treated slices (*nt*) and NMDA-treated slices harvested at the noted post-insult times. Immunoreactivity levels were determined by image analysis, and mean integrated optical densities are shown (± SEM). The plotted data were subjected to ANOVA (P<0.05)

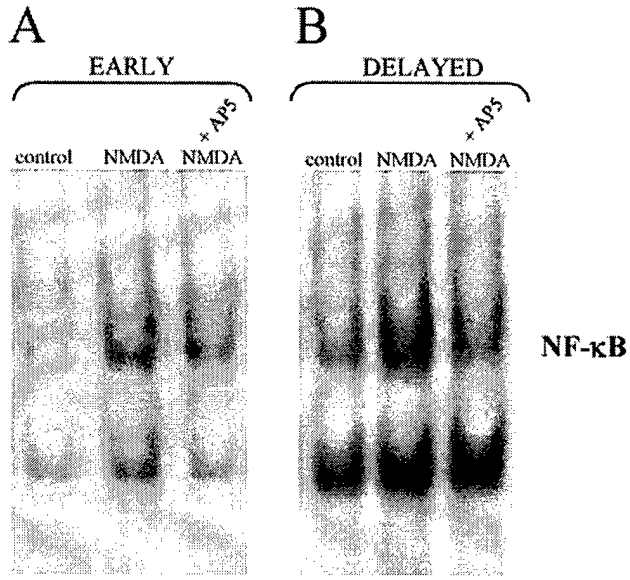

Fig. 5 NF-κB activation is mediated through NMDA-type glutamate receptors. Hippocampal slices were treated with the NMDA insult alone or, in a separate group of slices, AP5 was applied to the slices before, during, and after the insult. Nuclear extractions were carried out on slices harvested 0.5–1 h (**A**) and 24 h post-insult (**B**) and the preparations used for EMSA

sponded closely in time with early and delayed activation of IKK evident in Fig. 4. Note that experiments with purified IKK indicate that the activated form of the kinase, pIKK, can phosphorylate both IκBα and IκBβ at the appropriate regulatory residues [40, 64], causing their rapid degradation. However, IκBα did not exhibit evidence of degradation in the excitotoxic hippocampal slices. In the same slice samples that expressed early and delayed reductions in IκBβ, no such decline in IκBα immunoreactivity occurred at the early time point (Fig. 3C), nor was there a change in IκBα levels at 10–24 h post-insult (99± 3% of control, n=12; see representative blots in Fig. 3D). The p105 isoform also exhibited stable levels in slices harvested 1–24 h post-insult (not shown).

Further studies were conducted to determine whether the two phases of NF-κB activation have distinctive features other than the temporal one. First, control experiments were done to verify that the NMDA effects were specific in both phases. Previous studies reported that NMDA-induced NF-κB activation is blocked by the NMDA receptor antagonist AP5 [18]. Similarly, we found that AP5, when present before, during, and after the excitotoxic insult, disrupted both the early phase of NF-κB activity at 1 h post-insult (Fig. 5A) and the delayed phase at 24 h post-insult (Fig. 5B). Also, competition studies with non-radiolabeled probe indicated that the binding activity in either phase was specific for NF-κB (data not shown). While the two phases are similar with regard to the inhibitory effect of AP5, they appear to involve distinct subunit compositions of the activated NF-κB complex. EMSAs of sufficient resolution indicate that early activation results from the nuclear translocation of both p50-containing and p65-containing complexes (Fig. 6A). As shown by supershift analysis, anti-p50 antibodies essentially eliminated the p50/p50 complex (closed arrow) and markedly reduced the heterodimeric p65/p50 (open arrow), while shifting the binding activity to a higher molecular weight (see p50 lane). The involvement of p65 was verified with anti-p65 antibodies that nearly eliminated p65/p50 and shifted binding activity to a higher position (asterisk in the p65 lane). While the early phase of NF-κB activation exhibits the doublet pattern of activated p50/p50 and p65/p50, the delayed phase consists primarily of the p50/p50 homodimer (Fig. 6B). Only a single band of activity was evident in nuclei prepared 24 h post-insult, whose mobility was retarded by anti-50 antibodies (p50 lane). Correspondingly, anti-p65 antibodies caused no evident reduction in the protein-DNA complex (see p65 lane). Neither of the two phases of activity exhibits the presence of the p52 subunit as anti-p52 antibodies had no influence in supershift analyses.

In addition to the makeup of activated complexes, differential responses to protective and pathogenic conditions provide further evidence that the NF-κB activation profile consists of two distinct phases. When the excitotoxic insult was conducted in the presence of the neuroprotective agent Ampakine, the induced activation of NF-κB was enhanced in the delayed phase, while no significant change occurred in the early phase (Fig. 7A). Note that Ampakine positively modulates mitogen-activated protein kinase and other protective signaling pathways [7], and alone causes at least a twofold increase in NF-κB activity in hippocampal slice cultures ($P<0.0001$). The opposite result was found when the excitotoxic insult was conducted under serum-free conditions, causing an enhanced level of NF-κB activation only in the early phase (Fig. 7B). Removal of serum had no effect on the delayed phase, although serum deprivation alone produced a twofold increase in NF-κB activity that was sustained across a 24-h period.

Lastly, we tested for evidence that the early and delayed excitotoxic responses involving NF-κB lead to distinct gene regulation events. Since NF-κB has been implicated in compensatory repair signaling as well as programmed cell death (see [43] for a review), representa-

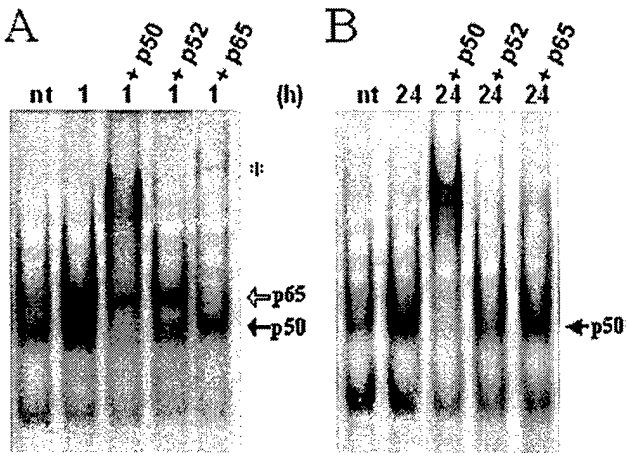

Fig. 6 The two phases of NF-κB activation involve distinct subunit compositions. Non-treated control slices (*nt*) and NMDA-treated slices harvested 1 h (**A**) or 24 h post-insult (**B**) were analyzed for the nuclear binding activity of p50/p50 homodimers (*closed arrow*) and p65/p50 heterodimers (*open arrow*). Separate aliquots of the nuclear extracts were pre-incubated with antibodies to p50, p52, and p65 for supershift analyses in adjacent lanes. Anti-p50 clearly reduced the mobility of the early and delayed binding activity, while anti-p65 shifted binding activity in the early phase only (*asterisk*). Antibodies to p52 had no effect in either phase

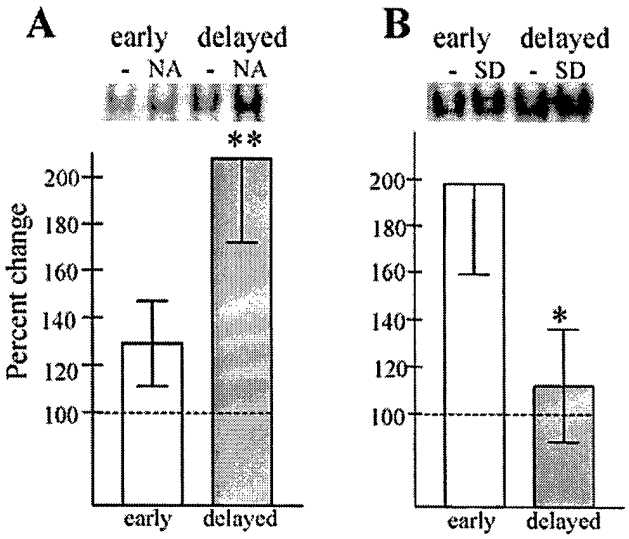

Fig. 7 Differential responses expressed by the two phases of NF-κB activation. Slice cultures were subjected to the NMDA insult in conjunction with the presence of the neuroprotective agent Ampakine (**A**; n=11–13) or the absence of serum in the media (**B**; n=4). Separate groups of slices were harvested 1 h (*early*) or 24 h post-insult (*delayed*) to be analyzed for nuclear NF-κB activity. Binding activity levels were determined from integrated optical density measures, and percent change in activation (mean ± SEM) was assessed by normalizing the data to that expressed by insult-alone samples (set at 100%). The EMSAs shown illustrate the effect the neuroprotective agent (*NA*) or serum deprivation (*SD*) has on NMDA-induced NF-κB activation

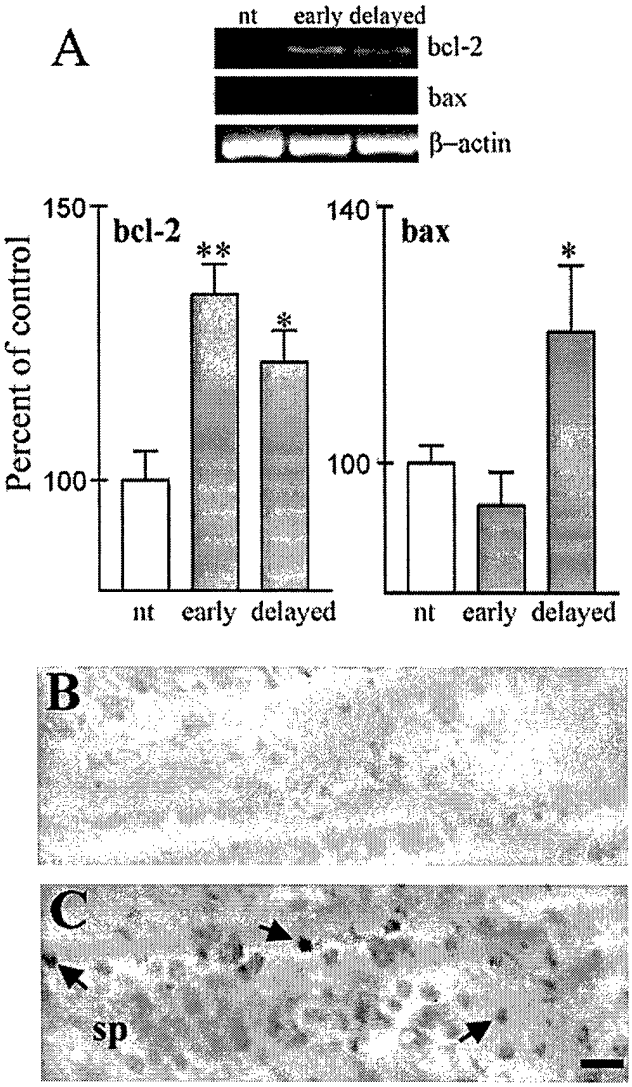

Fig. 8 Differential gene regulation is evident in the two phases of NF-κB activation. **A** RNA was isolated from groups of non-treated slices (*nt*) and from NMDA-insulted slices harvested in the early (1 h post-insult) or delayed (24 h) phase of NF-κB activation. RT-PCR products of bcl-2, bax, and β-actin, amplified from the same RNA preparations, were quantified by image analysis, normalized to respective β-actin message, and plotted as percent of the non-treated control level (mean ± SEM). Early up-regulation of the bcl-2 message corresponds with the initial activation of NF-κB. Analyses of variance were applied to bcl-2 (P=0.002) and bax data (P=0.03). Tukey's post-hoc test compared to non-treated control: *P<0.05, **P<0.01. **B, C** In situ hybridization analysis for bcl-2 mRNA was conducted in control tissue (**B**) and in NMDA-treated slices at 1 h post-insult (**C**). After being fixed and sectioned, the tissue was incubated with a biotinylated cDNA probe, assessed for hybridization through streptavidin-conjugate binding, and pyramidal neurons (*arrows*) were visualized by associated alkaline phosphatase activity (*sp* stratum pyramidale). *Bar* 45 μm

tives of both anti-apoptotic (bcl-2) and pro-apoptotic (bax) pathways were examined. We chose bcl-2 and bax because these genes are thought to be regulated by NF-κB (e.g., [52, 55]). Specific primers were used for RT-PCR analyses of gene expression levels. Early after the excitotoxic NMDA exposure, bcl-2 message was increased and it remained at the up-regulated level (Fig. 8A, left graph; ANOVA: P=0.002). The NMDA-induced early increase in bcl-2 message, confirmed by in situ hybridization (Fig. 8C; control in Fig. 8B), corresponds with the early phase of NF-κB activation. Bax, on the other hand, did not exhibit early regulation, but did express a delayed increase in message level at 24 h post-insult (Fig. 8A, right graph). These findings lead to the idea that the NF-κB activation profile may result in anti-apoptotic as well as pro-apoptotic chemistries in the excitotoxic hippocampus.

Discussion

The results of this study show that NMDA-mediated excitotoxicity in hippocampus leads to distinct phases of NF-κB activation. The data provide evidence that NF-κB responds to an excitotoxic insult in a biphasic manner to promote opposing pathways. The transcription factor indeed has been reported to have a dual role in promoting both life and death in neurons [28, 30, 34, 36, 37, 43], thus implicating it in compensatory repair signaling as well as pathogenic cellular responses.

NF-κB exhibits at least two activation phases in the excitotoxic hippocampal slice model, and both were shown to be specifically mediated by the over-stimulation of NMDA receptors. Biphasic activation of the transcription factor has been described in other model systems [20, 24, 29, 56]. For instance, Lille et al. [29] reported a comparable activation profile in response to ischemia/reperfusion in rat muscle. Similar to our results, they found an initial peak between 0.5–3 h post-perfusion, and a second wave of activation between 6 and 16 h. However, while the level of NF-κB activation in ischemic muscle diminished by 24 h post-injury, it continued to increase in the excitotoxic hippocampus, evident particularly in the major neuronal subfields as well as indications of activity in other cells. The biphasic NF-κB profile does not appear to involve differential activation across the three neuronal subfields, and more extensive studies will be needed to determine whether the two phases represent distinct responses by different cell types. Note that in astrocytes, biphasic NF-κB activity is apparent, but follows a much shorter time course than our results [24].

Differential IκB degradation has been implicated in the NF-κB responses in astrocyte and neuroblastoma experiments [24], as well as in other studies illustrating biphasic activation of the transcription factor. Thompson et al. [56] have suggested that two different IκBs give rise to two types of NF-κB activation: a transient phase mediated primarily through IκBα degradation, and a persistent phase regulated by both IκBα and IκBβ. Alternatively, there is evidence that, while IκBβ is involved in a delayed phase of activation, it also contributes to an initial phase of NF-κB activity [20]. These findings correspond with our results that implicate IκBβ in both phases of the excitotoxic NF-κB response.

The present report shows that biphasic IκBβ degradation occurs in the excitotoxic hippocampus, consisting of rapid degradation as early as 30 min post-insult and a second, much slower phase of degradation. The NF-κB response to the insult does not appear to involve IκBα or p105, for they did not exhibit post-insult declines in immunoreactivity. This is somewhat surprising since the neuroprotective NF-κB response in excitotoxic hippocampal neurons has been shown to be controlled, at least in part, by IκBα [9]. Although unlikely, it may be the case that the immunoassays used in the present study are not sensitive enough to detect IκBα or p105 degradation in neurons. Perhaps IκBα expression is enhanced in the excitotoxic hippocampus, thereby masking its potential involvement. Related to this, transfected T lymphocytes were shown to exhibit decreased levels of IκBβ protein, while NF-κB-directed transcription of the IκBα gene was stimulated [39]. With that said, IκBβ appears to play a major role in the biphasic activation of NF-κB. Other IκB molecules cannot be excluded from playing a role, although they are unlikely candidates since IκBγ expression is only found in mouse B cells [8], IκBδ associates with RelB/p52 complexes [8], and IκBε selectively inhibits complex between p65 (RelA) and cRel [62].

Perhaps the IκBβ degradation events occur through two distinct mechanistic pathways. Indeed, it has been proposed that IκB proteins are degraded by a variety of mechanisms, and that degradation of IκBα and IκBβ goes through different pathways involving the calcium-dependent protease calpain and the ubiquitine/proteosome degradation system [20]. Although calpain has been implicated in the degradation of the inhibitory proteins [32, 44, 51], our previous work provides evidence that calpain is not involved in the early response of NF-κB [10]. Hence, the ubiquitine/proteosome pathway is a strong candidate for playing a role in the early activation. Calpain, on the other hand, may be responsible for the delayed phase, a finding that is consistent with the study of Han and Brasier [20], who reported that calpain is involved in the second phase of the biphasic activation observed during their treatment paradigm. Calpain has also been implicated in IκBα degradation during oxidative stress-induced NF-κB activation [50]. Further, more extensive studies would be needed to rule out additional potential pathways. For instance, the lysosomal system may rapidly degrade both IκBα and IκBβ [12]. More interesting with respect to the current study, previous reports identified an unphosphorylated, non-degradable or slowly degraded form of IκBβ that is involved in the persistent activation of NF-κB [54, 61]. This novel form of IκBβ may explain the apparent rapid re-synthesis of IκBβ and its gradual degradation in the delayed phase of NF-κB activation.

Inducible transcription factors such as NF-κB are important for communicating changes in the cellular environment into specific signaling responses. For example, neurons are known to activate a number of defense mechanisms in response to injury. Survival depends on the ability to repair or remove damaged cells, and while many cellular mechanisms are predominantly protective or predominantly pathogenic, a few, including NF-κB, are linked to both (for review see [34]). Correspondingly, the present study implicates NF-κB in such a dual role involving opposing pathways. We found that increased levels of bcl-2 message correspond with the rapid early phase of NF-κB translocation in the excitotoxic hippocampus. This is in agreement with several studies that point to a role for NF-κB in anti-apoptotic mechanisms [15, 31, 35, 49, 55] and in neuroprotective responses to excitotoxicity in hippocampal neurons [9]. Moreover, expression of the bcl-2 gene was found similarly regulated in excitotoxicity-related models of hypoxia and reperfusion [45, 55]. Excitotoxic hippocampal slices did not exhibit increased message for the pro-apoptotic gene bax until the delayed phase of NF-κB activation, coinciding with initial pyknotic changes expressed by vulnerable neurons. This also is in accordance with many reports linking NF-κB signaling to apoptosis [1, 11, 17, 41, 46] and showing that bax is up-regulated in response to glutamate-induced neurotoxicity [13, 14, 17, 26, 38, 47, 63]. While bcl-2 and bax represent opposing pathways of protection and death, respectively, the expression of both genes appears to be associated with the excitotoxic NF-κB response.

The involvement of NF-κB in neuronal survival as well as neuronal death makes this transcription factor quite unique. Together with previous reports, the present findings suggest that biphasic NF-κB activation leads to the regulation of opposing cellular responses. This dual nature of NF-κB would explain how the transcription factor influences both degenerative and regenerative pathways. The results also support the hypothesis that degenerative and compensatory mechanisms are triggered by a stroke-type insult, and that the opposing pathways together determine the extent of neurodegeneration.

Acknowledgements The authors would like to extend their gratitude to Professor Charles Giardina for invaluable insight and for the use of his laboratory for EMSA procedures. This work was supported by U.S. Army Medical Research grant DAMD17-99-C9090, and a Boehringer Ingelheim pre-doctoral fellowship.

References

1. Bachis A, Colangelo AM, Vicini S, Doe PP, De Bernardi MA, Brooker G, Mocchetti I (2001) Interleukin-10 prevents glutamate-mediated cerebellar granule cell death by blocking caspase-3-like activity. J Neurosci 21:3104–3112
2. Baeuerle PA (1991) The inducible transcription activator NF-κB: Regulation by distinct protein subunits. Biochim Biophys Acta 1072:63–80
3. Baeuerle PA, Baltimore D (1996) NF-κB: Ten years after. Cell 87:13–20
4. Bahr BA (1995) Long-term hippocampal slices: a model system for investigating synaptic mechanisms and pathologic processes. J Neurosci Res 42:294–305
5. Bahr BA, Arai B, Gall CM, Vanderklish PW, Hoffman KB, Lynch G (1994) Induction of β-amyloid-containing polypeptides in hippocampus: evidence for a concomitant loss of synaptic proteins and interactions with an excitotoxin. Exp Neurol 129:81–94

6. Bahr BA, Kessler M, Rivera S, Vanderklish PW, Hall RA, Mutneja MS, Gall C, Hoffman KB (1995) Stable maintenance of glutamate receptors and other synaptic components in long-term hippocampal slices. Hippocampus 5:425–439
7. Bahr BA, Bendiske J, Brown QB, Munirathinam S, Caba E, Rudin M, Urwyler S, Sauter A, Rogers G (2002) Survival signaling and selective neuroprotection through glutamatergic transmission. Exp Neurol 174:37–47
8. Baldwin AS Jr (1996) The NF-κB and IκB proteins: new discoveries and insights. Annu Rev Immunol 14:649–683
9. Barger SW, Mattson MP (1996) Induction of neuroprotective kappa B-dependent transcription by secreted forms of the Alzheimer's β-amyloid precursor. Mol Brain Res 40:116–126
10. Caba E, Brown QB, Kawasaki B, Bahr BA (2002) Peptidyl α-keto amide inhibitor of calpain blocks excitotoxic damage without affecting signal transduction events. J Neurosci Res 67:787–794
11. Clemens JA, Stephenson DT, Dixon EP, Smalstig EB, Mincy RE, Rash KS, Little SP (1997) Global cerebral ischemia activates nuclear factor-κB prior to evidence of DNA fragmentation. Mol Brain Res 48:187–196
12. Cuervo AM, Hu W, Lim B, Dice JF (1998) IκB is a substrate for a selective pathway of lysosomal proteolysis. Mol Biol Cell 9:1995–2010
13. Djebaili M, Rondouin G, Baille V, Bockaert J (2000) p53 and bax implication in NMDA induced-apoptosis in mouse hippocampus. Neuroreport 11:2973–2976
14. Furukawa K, Mattson MP (1998) The transcription factor NF-κB mediates increases in calcium currents and decreases in NMDA- and AMPA/kainate-induced currents induced by tumor necrosis factor-alpha in hippocampal neurons. J Neurochem 70:1876–1886
15. Goodman Y, Mattson MP (1996) Ceramide protects hippocampal neurons against excitotoxic and oxidative insults, and amyloid β-peptide toxicity. J Neurochem 66:869–872
16. Grilli M, Memo M (1999) Nuclear factor-κB/Rel proteins: a point of convergence of signaling pathways relevant in neuronal function and dysfunction. Biochem Pharmacol 57:1–7
17. Grilli M, Pizzi M, Memo M, Spano P (1996) Neuroprotection by aspirin and sodium salicylate through blockade of NF-κB activation. Science 274:1383–1385
18. Guerrini L, Blasi F, Denis-Donini S (1995) Synaptic activation of NF-κB by glutamate in cerebellar granule neurons in vitro. Proc Natl Acad Sci USA 92:9077–9081
19. Guerrini L, Molteni A, Wirth T, Kistler B, Blasi F (1997) Glutamate-dependent activation of NF-κB during mouse cerebellum development. J Neurosci 17:6057–6063
20. Han Y, Brasier AR (1997) Mechanism for biphasic relA NF-κB1 nuclear translocation in tumor necrosis factor α-stimulated hepatocytes. J Biol Chem 272:9825–9832
21. Iimuro Y, Nishiura T, Hellerbrand C, Behrns KE, Schoonhoven R, Grisham JW, Brenner DA (1998) NF-κB prevents apoptosis and liver dysfunction during liver regeneration. J Clin Invest 101:802–811
22. Kaltschmidt C, Kaltschmidt B, Baeuerle PA (1995) Stimulation of ionotropic glutamate receptors activates transcription factor NF-κB in primary neurons. Proc Natl Acad Sci USA 92:9618–9622
23. Kaplan DR, Miller FD (2000) Neurotrophin signal transduction in the nervous system. Curr Opin Neurobiol 10:381–391
24. Kemler I, Fontana A (1999) Role of IκBα and IκBβ in the biphasic nuclear translocation of NF-κB in TNFα-stimulated astrocytes and in neuroblastoma cells. Glia 26:212–220
25. Knopfel T, Gähwiler BH (1992) Activity-induced elevations of intracellular calcium concentration in pyramidal and nonpyramidal cells of the CA3 region of rat hippocampal slice cultures. J Neurophysiol 68:961–963
26. Ko HW, Park KY, Kim H, Han PL, Kim YU, Gwag BJ, Choi EJ (1998) Ca^{2+}-mediated activation of c-Jun N-terminal kinase and nuclear factor-κB by NMDA in cortical cell cultures. J Neurochem 71:1390–1395
27. Kuhnel F, Zender L, Paul Y, Tietze MK, Trautwein C, Manns M, Kubicka S (2000) NF-κB mediates apoptosis through transcriptional activation of fas (CD95) in adenoviral hepatitis. J Biol Chem 275:6421–6427
28. Lezoualc'h F, Sagara Y, Holsboer F, Behl C (1998) High constitutive NF-κB activity mediates resistance to oxidative stress in neuronal cells. J Neurosci 18:3224–3232
29. Lille ST, Lefler SR, Mowlavi A, Suchy H, Boyle EMJ, Farr AL, Su CY, Frank N, Mulligan DC (2001) Inhibition of the initial wave of NF-κB activity in rat muscle reduces ischemia/reperfusion injury. Muscle Nerve 24:534–541
30. Lin B, Williams-Skipp C, Tao Y, Schleicher MS, Cano LL, Duke RC, Scheinman RI (1999) NF-κB functions as both a pro-apoptotic and anti-apoptotic regulatory factor within a single cell type. Cell Death Differ 6:570–582
31. Lipsky RH, Xu K, Zhu D, Kelly C, Terhakopian A, Novelli A, Marini AM (2001) Nuclear factor κB is a critical determinant in *N*-methyl-D-aspartate receptor-mediated neuroprotection. J Neurochem 78:254–264
32. Liu ZQ, Kunimatsu M, Yang JP, Ozaki Y, Sasaki M, Okamoto T (1996) Proteolytic processing of nuclear factor κ B by calpain in vitro. FEBS Lett 385:109–113
33. Manna SK, Aggarwal BB (1999) Lipopolysaccharide inhibits TNF-induced apoptosis: role of nuclear factor-κB activation and reactive oxygen intermediates. J Immunol 162:1510–1518
34. Martindale JL, Holbrook NJ (2002) Cellular response to oxidative stress: signaling for suicide and survival. J Cell Physiol 192:1–15
35. Mattson MP (1997) Neuroprotective signal transduction: relevance to stroke. Neurosci Biobehav Rev 21:193–206
36. Mattson MP, Camandola S (2001) NF-κB in neuronal plasticity and neurodegenerative disorders. J Clin Invest 107:247–254
37. Mattson MP, Culmsee C, Yu Z, Camandola S (2000) Roles of nuclear factor κB in neuronal survival and plasticity. J Neurochem 74:443–456
38. McInnis J, Wang C, Anastasio N, Hultman M, Ye Y, Salvemini D, Johnson KM (2002) The role of superoxide and nuclear factor-κB signaling in *N*-methyl-D-aspartate-induced necrosis and apoptosis. J Pharmacol Exp Ther 301:478–487
39. McKinsey TA, Brockman JA, Scherer DC, Al-Murrani SW, Green PL, Ballard DW (1996) Inactivation of IκBβ by the tax protein of human T-cell leukemia virus type 1: a potential mechanism for constitutive induction of NF-κB. Mol Cell Biol 16:2083–2090
40. Mercurio F, Murray BW, Shevchenko A, Bennett BL, Young DB, Li JW, Pascual G, Motiwala A, Zhu H, Mann M, Manning AM (1999) IκB kinase (IKK)-associated protein 1, a common component of the heterogeneous IKK complex. Mol Cell Biol 19:1526–1538
41. Nakai M, Qin ZH, Chen JF, Wang Y, Chase TN (2000) Kainic acid-induced apoptosis in rat striatum is associated with nuclear factor-κB activation. J Neurochem 74:647–658
42. Newell DW, Malouf AT, Franck JE (1990) Glutamate-mediated selective vulnerability to ischemia is present in organotypic cultures of hippocampus. Neurosci Lett 116:325–330
43. Perkins ND (2000) The Rel/NF-κB family: friend and foe. Trends Biochem Sci 25:434–440
44. Pianetti S, Arsura M, Romieu-Mourez R, Coffey RJ, Sonenshein GE (2001) Her-2/neu overexpression induces NF-κB via a PI3-kinase/Akt pathway involving calpain-mediated degradation of IκB-α that can be inhibited by the tumor suppressor PTEN. Oncogene 20:1287–1299
45. Poulaki V, Mitsiades CS, Joussen AM, Lappas A, Kirchhof B, Mitsiades N (2002) Constitutive nuclear factor-κB activity is crucial for human retinoblastoma cell viability. Am J Pathol 161:2229–2240
46. Qin ZH, Wang Y, Nakai M, Chase TN (1998) Nuclear Factor-κB contributes to excitotoxin-induced apoptosis in rat striatum. Mol Pharmacol 53:33–42

47. Qin ZH, Chen RW, Wang Y, Nakai M, Chuang DM, Chase TN (1999) Nuclear factor κB nuclear translocation upregulates c-Myc and p53 expression during NMDA receptor-mediated apoptosis in rat striatum. J Neurosci 19:4023–4033
48. Rimvall K, Keller F, Waser PG (1987) Selective kainic acid lesions in cultured explants of rat hippocampus. Acta Neuropathol 74:183–190
49. Rosenberger J, Petrovics G, Buzas B (2001) Oxidative stress induces proorphanin FQ and proenkephalin gene expression in astrocytes through p38- and ERK-MAP kinases and NF-κB. J Neurochem 79:35–44
50. Schoonbroodt S, Ferreira V, Best-Belpomme M, Boelaert JR, Legrand-Poels S, Korner M, Piette J (2000) Crucial role of the amino-terminal tyrosine residue 42 and the carboxyl-terminal PEST domain of IκB α in NF-κB activation by an oxidative stress. J Immunol 164:4292–4300
51. Shen J, Channavajhala P, Seldin DC, Sonenshein GE (2001) Phosphorylation by the protein kinase CK2 promotes calpain-mediated degradation of IκBα. J Immunol 167:4919–4925
52. Shou Y, Li N, Li L, Borowitz JL, Isom GE (2002) NF-κB-mediated up-regulation of Bcl-X(S) and Bax contributes to cytochrome c release in cyanide-induced apoptosis. J Neurochem 81:842–852
53. Sonenshein GE (1997) Rel/NF-κB transcription factors and the control of apoptosis. Semin Cancer Biol 8:113–119
54. Suyang H, Phillips R, Douglas I, Ghosh S (1996) Role of unphosphorylated, newly synthesized IκBβ in persistent activation of NF-κB. Mol Cell Biol 16:5444–5449
55. Tamatani M, Mitsuda N, Matsuzaki H, Okado H, Miyake S, Vitek MP, Yamaguchi A, Tohyama M (2000) A pathway of neuronal apoptosis induced by hypoxia/reoxygenation: roles of nuclear factor-κB and Bcl-2. J Neurochem 75:683–693
56. Thompson JE, Phillips RJ, Erdjument-Bromage H, Tempst P, Ghosh S (1995) IκB-β regulates the persistent response in a biphasic activation of NF-κB. Cell 80:573–582
57. Usami I, Kubota M, Bessho R, Kataoka A, Koishi S, Watanabe K, Sawada M, Lin YW, Akiyama Y, Furusho K (1998) Role of protein tyrosine phosphorylation in etoposide-induced apoptosis and NF-κB activation. Biochem Pharmacol 55:185–191
58. Vanderklish PW, Bahr BA (2000) The pathogenic activation of calpain: a marker and mediator of cellular toxicity and disease states. Int J Exp Pathol 81:323–339
59. Vornov JJ, Tasker RC, Coyle JT (1991) Direct observation of the agonist-specific regional vulnerability to glutamate, NMDA, and kainate neurotoxicity in organotypic hippocampal cultures. Exp Neurol 114:11–22
60. Wang Y, Qin ZH, Nakai M, Chen RW, Chuang DM, Chase TN (1999) Co-stimulation of cyclic-AMP-linked metabotropic glutamate receptors in rat striatum attenuates excitotoxin-induced nuclear factor-κB activation and apoptosis. Neuroscience 94: 1153–1162
61. Weil R, Laurent-Winter C, Israel A (1997) Regulation of IκBβ degradation. Similarities to and differences from IκBα. J Biol Chem 272:9942–9949
62. Whiteside ST, Epinat JC, Rice NR, Israel A (1997) IκBε, a novel member of the IκB family, controls RelA and cRel NF-κB activity. EMBO J 16:1413–1426
63. Xiang H, Kinoshita Y, Knudson CM, Korsmeyer SJ, Schwartzkroin PA, Morrison RS (1998) Bax involvement in p53-mediated neuronal cell death. J Neurosci 18:1363–1373
64. Zandi E, Chen Y, Karin M (1998) Direct phosphorylation of IκB by IKKα and IKKβ: discrimination between free and NF-κB-bound substrate. Science 281:1360–1363

Journal of Neuroscience Research 75:408–416 (2004)

Sulfate- and Size-Dependent Polysaccharide Modulation of AMPA Receptor Properties

Linda M. Chicoine,[1,2] Vishnu Suppiramaniam,[3] Thirumalini Vaithianathan,[3] Gerald Gianutsos,[1] and Ben A. Bahr[1,4]*

[1]Department of Pharmaceutical Sciences and the Neurosciences Program, University of Connecticut, Storrs
[2]Cognetix, Inc., Salt Lake City, Utah
[3]Department of Pharmacal Sciences, Auburn University, Auburn, Alabama
[4]Center for Drug Discovery, University of Connecticut, Storrs

Previous work found evidence that α-amino-3-hydroxy-5-methylisoxazole-4-propionic acid (AMPA)-type glutamate receptors interact with and are functionally regulated by the glycosaminoglycan heparin. The present study tested whether dextran species affect ligand binding, channel kinetics, and calcium permeability of AMPA receptors. Dextran sulfate of 500 kDa markedly reduced high affinity [^{3}H]AMPA binding in solubilized hippocampal membranes. In isolated receptors reconstituted in a lipid bilayer, the same dextran sulfate prolonged the lifetime of open states exhibited by AMPA-induced channel fluctuations. The large polysaccharide further changed the single channel kinetics by increasing the open channel probability five- to sixfold. Such modulation of channel activity corresponded with enhanced levels of calcium influx as shown in hippocampal neurons loaded with Fluo3AM dye. With an exposure time of <1 min, AMPA produced a dose-dependent increase in intracellular calcium that was blocked by 6-cyano-7-nitroquinoxaline-2,3-dione disodium (CNQX). Dextran sulfate, at the same concentration range that modified ligand binding (EC_{50} of 5–10 nM), enhanced the AMPA-induced calcium influx by as much as 60%. The enhanced influx was blocked by CNQX, although unchanged by the *N*-methyl-D-aspartate (NMDA) receptor antagonist AP5. Confocal microscopy showed that the increase in calcium occurred in neuronal cell bodies and their processes. Interestingly, smaller 5–8-kDa dextran sulfate and a non-sulfated dextran of 500 kDa had little or no effect on the binding, channel, and calcium permeability properties. Together, these findings suggest that synaptic polysaccharide species modulate hippocampal AMPA receptors in a sulfate- and size-dependent manner. © 2003 Wiley-Liss, Inc.

Key words: AMPA-type glutamate receptors; glycosaminoglycans; dextran sulfate; synaptic modulation

α-Amino-3-hydroxy-5-methylisoxazole-4-propionic acid (AMPA) receptors are involved in excitatory synaptic transmission in the brain, and their regulation is thought to be responsible for many types of neuronal functions. Most notable, AMPA receptors are thought to be involved in memory encoding (Staubli et al., 1994, 1996; Mahanty and Sah, 1998; Shapiro, 2001; Riedel et al., 2003), synaptogenesis (Launey et al., 1998; König et al., 2001), and neuronal maintenance (McKinney et al., 1999; Lauterborn et al., 2000; Bahr et al., 2002). The regulation of AMPA receptors during these activity-dependent events leads to alterations in AMPA receptor properties and changes at the synapse. Perhaps providing insight into possible mechanisms of regulation, AMPA receptor binding and channel properties have been shown to be modulated by subunit phosphorylation (e.g., see Correia et al., 2003), interactions with certain lectins (Lin and Levitan, 1991; Wong and Mayer, 1993), adhesion responses (Lüthi et al., 1994; Bahr et al., 1997; Kramar et al., 2002), and polysaccharides (Hall et al., 1996; Hoffman et al., 1997). The latter is of particular interest because synapses are known to contain polysaccharides implicated in plasticity events and receptor regulation (see Lander et al., 1998; Bahr et al., 1999; Lauri et al., 1999).

Understanding polysaccharide modulation of plasticity events and receptor regulation is important because it provides a plausible explanation of how the environment of the synapse may alter synaptic function. As an example, polysialic acid-containing synaptic adhesion molecules are thought to play a role in hippocampal plasticity (Lüthi et al., 1994; Rønn et al., 1995, 1998; Staubli et al., 1998), and selective removal of the polysaccharide component of cell adhesion molecules disrupts different forms of synaptic regulation (Muller et al., 1996). Correspondingly, plasticity induction stimuli have been shown to increase the levels of polysaccharide-laden adhesion molecules in the

Contract grant sponsor: NIH; Contract grant number: 1R43NS38404-01; Contract grant sponsor: US Army Medical Research; Contract grant number: DAMD17-99-C9090.

*Correspondence to: Ben A. Bahr, Department of Pharmaceutical Sciences, University of Connecticut, Storrs, CT 06269-2092.
E-mail: Bahr@uconn.edu

Received 2 July 2003; Revised 7 October 2003; Accepted 9 October 2003

© 2003 Wiley-Liss, Inc.

hippocampus (Muller et al., 1996; Hoffman, 1998). Such activity-dependent regulation was found for another polysaccharide carrier protein, the syndecan-3 proteoglycan, which is expressed at the processes of pyramidal neurons (Lauri et al., 1999). This transmembrane proteoglycan is expressed prominently in adult hippocampus and contains glycosaminoglycans that interact with cell surface receptors and components of the extracellular matrix. Providing further evidence of polysaccharides that regulate activity-dependent events, it was found that mice deficient in select proteoglycan species display altered plasticity properties (Brakebusch et al., 2002; Kaksonen et al., 2002). Together, these reports suggest that polysaccharide-containing elements of central synapses have critical influences on synaptic function.

The present report focuses on the ability of glycosaminoglycans to modulate synaptic properties. The glycosaminoglycan component of proteoglycans is of interest because enzymatic removal of glycosaminoglycans prevented activity-induced synaptic plasticity in hippocampal slices (Lauri et al., 1999). Surprisingly, the addition of heparin-type polysaccharides in the rat brain blocked plasticity events, and heparin has also been reported to influence high-affinity AMPA binding (Hall et al., 1996). Although heparin negatively influenced binding affinity, however, it positively modulated AMPA channel kinetics to prolong the open state, possibly occluding subsequent regulation by plasticity processes (Hall et al., 1996; Sinnarajah et al., 1999). As AMPA receptors attach to heparin-agarose during purification steps (Bahr et al., 1992; Hall et al., 1996), the polysaccharide modulation seems to be through direct interaction.

In the experiments described here, dextran sulfate of 500 kDa was tested for its ability to modulate AMPA receptor properties. Dextran sulfate is a freely soluble polyanion that mimics natural mucopolysaccharides including chondroitin sulfate and heparan sulfate. The described results show that dextran sulfate alters binding, channel and calcium-permeability properties of AMPA receptors in a sulfate- and size-dependent manner.

MATERIALS AND METHODS

Binding Assay

Using Sprague-Dawley rats (Charles River Laboratories, Inc., Wilmington, MA), hippocampal membrane preparations, solubilization, and [^{3}H]AMPA binding assays were conducted as described (Bahr et al., 1992; Hall et al., 1992). In brief, membranes were prepared by differential centrifugation and osmotic lysis, and suspended in a buffer of 50 mM Tris acetate, pH 7.2. Membranes were solubilized with 0.4% Triton X-100 and non-solubilized material was removed by centrifugation (48,000 × *g* for 2 hr). Samples were assayed for binding of 10 nM [^{3}H]AMPA in the absence or presence of various polysaccharides (Sigma, St. Louis, MO). A range of ligand concentrations was used for Scatchard analysis. Binding parameters from one- and two-site fits were assessed by computer-assisted nonlinear regression analysis, using the *Prism2* program (GraphPad Software, Inc.). The basic equilibrium formula (L)(Bmax)/(B) = K_D was used, where L is the free ligand concentration.

Purification of AMPA Receptors and Single Channel Recording

Brains from adult Sprague-Dawley rats were removed rapidly after anesthesia and decapitation, and membranes were prepared as described previously (Hall et al., 1992). The membranes were solubilized in ice-cold buffer A (30 mM HEPES, 5 mM EDTA, 1 mM EGTA, and 0.02% NaN_3, pH 7.4) with 1% (wt/vol) Triton X-100, 20% (wt/vol) glycerol, and 80 mM KSCN, at a detergent:protein ratio of 3:2. Particulate matter was removed by centrifugation at 30,000 × *g* for 3 hr. The supernatant was diluted with an equal volume of buffer A and applied to a diethylaminoethyl-Sepharose column equilibrated at 4°C with buffer A containing 1% *n*-octylglucoside (Roche, Basil, Switzerland), and 0.05% phosphatidylcholine (buffer B). The column was washed with four column volumes of buffer B and eluted with a KSCN gradient. AMPA receptors were then reconstituted, as reported previously, in small "tip-dip" bilayers (Bahr et al., 1992; Vodyanoy et al., 1993). AMPA (Tocris, Ellisville, MO) was delivered to the *cis* side of the bilayer in the absence or presence of dextran sulfate of different sizes and sulfate content. The AMPA specific antagonist, 6-cyano-7-nitroquinoxaline-2,3-dione disodium (CNQX; Tocris), was also delivered in the presence of AMPA and large 500-kDa dextran sulfate (DS-L). Single channel events were recorded with a VCR system and subjected to computer analysis of amplitude and time distributions (pCLAMP; Axon Instruments, Union City, CA). Recorded signals were filtered at 1–5 kHz and digitized between 5–25 kHz, after which they were reduced to series of datasets each containing 2,000–125,000 data points. The minimum detectable dwell time (0.1 msec) was calibrated by detection of brief events.

Calcium Influx in Primary Hippocampal Cell Culture

Hippocampi were obtained from postnatal Day 9 Sprague-Dawley rat pups and dissociated enzymatically using 1.8% (v/v) papain, 15 mM $CaCl_2$, 100 nM cysteine, and 5 mM EDTA. Cultures were seeded on poly-D-lysine-coated coverslips or 96-well tissue culture panels at 25,000 cells/200 μl, using a TomTec Quadra96 fluid-handling robot (TomTec, Hamden, CT). Cultures were grown in a 5% CO_2 environment with Dulbecco's modified Eagle medium (DMEM) containing B-27 and F-12 supplements (Gibco/BRL), 10% fetal bovine serum (FBS), 20 mM glucose, and 1× penicillin/streptomycin (Gibco/BRL), and used for experiments on Days 8–10 of culture. They were then rinsed and incubated in Fluo3AM calcium dye (Molecular Probes, Eugene, OR) for 35 min at 37°C and excess dye was removed. For confocal studies, dye-loaded hippocampal cultures on coverslips were perfused sequentially at approximately 0.5 ml/min with an AMPA solution, followed by AMPA plus DS-L in the presence or absence of CNQX. In the 96-well plate experiments, a baseline reading of dye-loaded cells was measured with a fluorimeter at 485 nm emission/530 nm excitation (Perseptives Biosystems, Stafford, TX). Then cells were treated with AMPA alone or with various polysaccharide agents, and the experimental reading was taken immediately. In the 96-well plates, eight wells were used for each treatment and

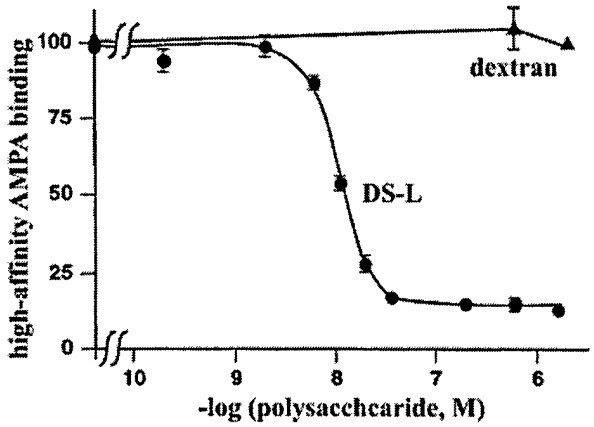

Fig. 1. Inhibition by DS-L of [^{3}H]AMPA binding to detergent-solubilized AMPA receptors from rat hippocampal membranes. The [^{3}H]AMPA concentration used (10 nM) was far below the K_D value for low-affinity binding to assess primarily high-affinity sites. The percentage of control [^{3}H]AMPA binding remaining in the presence of increasing concentrations of DS-L and sulfate-free dextran is shown. The data represent the mean ± SEM for 3 experiments.

individual responses from the eight wells were averaged to represent the value for a single experiment. Plate experiments were repeated to obtain an n = 3–13. Total time for reading a single 96-well plate was 45 sec, and the calcium-dye complex was stable for at least 5 min. Raw data was collected and percent changes in fluorescence were graphed using the *Origin* macro-analysis program. Statistical analysis was done using one-way analysis of variance (ANOVA) and Tukey's post-tests.

TABLE I. Parameters of [^{3}H]AMPA Binding in Solubilized Rat Hippocampal Membranes: Scatchard Analysis in the Absence or Presence of DS-L

Parameter	Control	+10 nM DS-L
High-affinity K_D (nM)	30 ± 4	25 ± 8
High-affinity Bmax (pmol/mg)	9.0 ± 0.7	1.4 ± 0.7
Low-affinity K_D (nM)	—	290 ± 48
Low-affinity Bmax (pmol/mg)	—	7.8 ± 0.5

TABLE II. Relative Potencies of Various Species on Inhibiting High-Affinity [^{3}H]AMPA Binding in Solubilized Rat Hippocampal Membranes*

Agent	Decreased high-affinity [^{3}H]AMPA binding (IC_{50})
DS-L (500 kDa)	11 ± 0.45 nM[a]
Fucoidan	150 ± 27 nM
DS-S (5–8 kDa)	720 ± 71 nM
Heparin	1,900 ± 400 nM
Hyaluronate	>30 μM
De-N-sulfate heparin	>30 μM
Dextran (18 kDa)	>30 μM
Dextran (260 kDa)	>30 μM
Dextran (500 kDa)	>30 μM
Glucosamine 2,3-disulfate	>10 mM
Na_2SO_4	>50 mM

*The respective IC_{50} values were determined from the binding inhibition of 10 nM [^{3}H]AMPA to assess primarily high-affinity sites. If no decrease in binding was detected, the IC_{50} is given as greater than the highest concentration tested.

[a]The titration curve for DS-L exhibited a Hill coefficient (2.8 ± 0.32) that was significantly different than 1.

RESULTS

Initial experiments tested whether dextran sulfate reduces high-affinity AMPA binding as found previously for heparin (Hall et al., 1996; Sinnarajah et al., 1999). To assess primarily high-affinity sites, the assay used a low ligand concentration that was far below the receptor's low-affinity K_D. Figure 1 shows the effect of a large, 500-kDa dextran sulfate (DS-L) on such [^{3}H]AMPA binding. DS-L decreased the high-affinity [^{3}H]AMPA binding in solubilized hippocampal membranes from rat with an IC_{50} of 11 nM. Similar effects on binding were found using Triton-solubilized, homomeric AMPA receptors expressed in HEK-293 cells from cDNAs encoding $GluR1_{flop}$ or $GluR2_{flip}$ (see Bahr et al., 1996; Hennegriff et al., 1997), as well as in human hippocampal receptors (not shown). With rat hippocampal receptors, Scatchard analysis confirmed that the DS-L effect was due to a decrease in the apparent affinity of AMPA binding sites, as found previously for another sulfated polysaccharide (Hall et al., 1996). In the absence of DS-L, a single high-affinity state was evident by linear regression (r = 0.98). The Bmax of this state was reduced by 84% in the presence of 10 nM DS-L, along with a concomitant exposure of a low-affinity state (K_D = 290 nM) that accounts for almost all of the lost binding sites (Table I).

As shown in a prior study (Sinnarajah et al., 1999), sulfate-free dextran of the same 500-kDa size had no effect on binding at up to 30 μM in concentration (Fig. 1). This indicates that the polysaccharide modulation of AMPA binding is sulfate-dependent. In addition, the sulfates must be an integral part of the polysaccharide because up to 50 mM sodium sulfate had no detectable influence on the high-affinity [^{3}H]AMPA binding (see Table II).

Other polysaccharide molecules were also examined for their potential to influence AMPA receptor binding affinity (Table II). As expected, non-sulfated dextrans of three different sizes all had no effect. Heparin also lost its ability to affect binding when sulfates were removed, as was the case for de-N-sulfate heparin. Interestingly, a small 5–8-kDa version of dextran sulfate (DS-S) exhibited much less effectiveness at inhibiting the high-affinity binding (IC_{50} = 720 nM) as compared to DS-L. A smaller monomeric species, glucosamine 2,3-disulfate, was completely ineffective (Table II), further suggesting that a size factor is associated with the sulfate component of polysaccharide modulation. Across the several agents tested, DS-L was most potent at altering AMPA binding to rat hippocampal receptors, and similar results were found using solubilized P2 membranes from human hippocampus. The

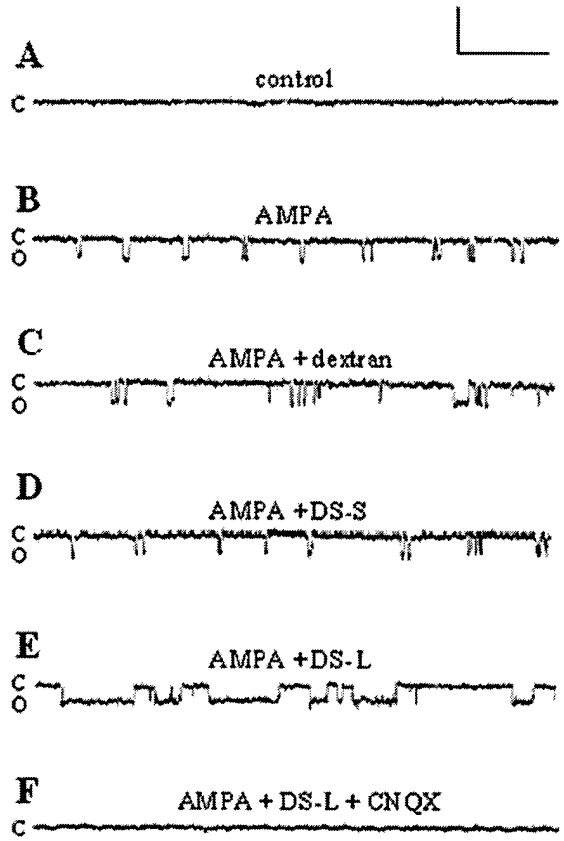

Fig. 2. Effects of DS-L on AMPA channel activity. Channel fluctuations were elicited by 150 nM AMPA in isolated AMPA receptors reconstituted in a lipid bilayer and voltage clamped at −72 mV. The closed state (c) was predominantly in the control trace (**A**), whereas numerous opening events (o) were induced by AMPA in the absence (**B**) or presence of 5 nM dextran (**C**) or 5 nM DS-S (**D**). Increased channel open time occurred with the addition of 5 nM DS-L (**E**), and the modulated channels were blocked by 1 μM CNQX (**F**). Calibration bar: 2.3 pA, 960 msec.

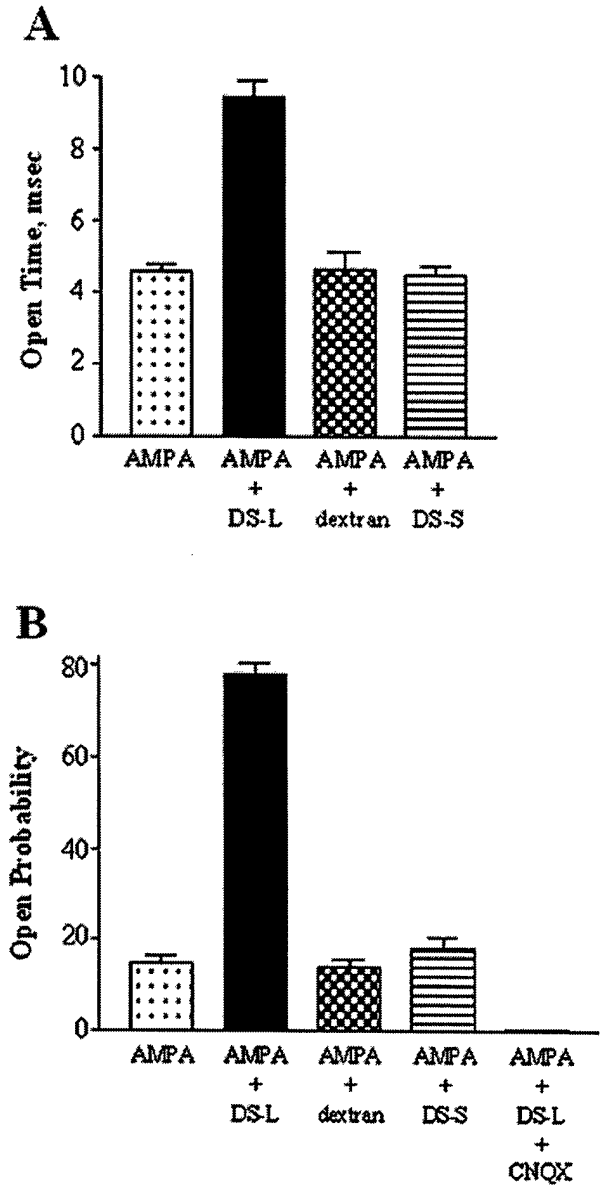

Fig. 3. Effects of polysaccharides on AMPA-elicited single channel open time (**A**) and probability of open channel state (**B**). From bilayer experiments in Figure 2, AMPA-induced single channel open time was found to be increased only by DS-L (ANOVA; $P < 0.0001$). The open time is the mean dwell time τ. Similarly, only in the presence of DS-L was there an increase in probability of the channel to be open ($P < 0.0001$). The probability of open channels is expressed as a percentage of all open and closed events within a recording segment of 0.6–1 sec consisting of 6,150–10,000 points sampled at intervals of 0.1 msec. The data represent means ± SEM from 5–6 different experiments.

rat and human receptors expressed the same rank order of potency: DS-L > fucoidan > DS-S > heparin.

As found in previous studies (Hall et al., 1996; Sinnarajah et al., 1999), polysaccharide modulation of AMPA binding was accompanied by modulated channel kinetics. Figure 2 shows portions of recordings from patch bilayers containing AMPA receptors exposed to AMPA agonist (trace B; compare to control trace A) with the voltage clamped at −72 mV. AMPA was used at 150 nM, which produces consistent channel activation events. Although the reconstituted receptors express high and low conductance states (Vodyanoy et al., 1993), the DS-L-modified channel activity was most obvious among the high-conductance events (trace E). The typical open time of 20–70 msec in control receptors was increased to 300–900 msec by DS-L. As shown in Figure 3, DS-L also causes a significant increase in the channel open time for the subtle low-conductance fluctuations that are similar to those expressed by AMPA receptors residing in their native environment ($P < 0.001$; graph A). In addition, DS-L application resulted in a nearly sixfold increase in their

open state probability ($P < 0.001$; graph B). The probability measures were expressed as a percentage of all open and closed events within a recording segment of 0.6–1 sec. Both of the modified conductance states were blocked completely by the AMPA receptor antagonist CNQX (trace F; also see Fig. 3B). Thus, DS-L does not have an effect on antagonism of the AMPA receptor's active site.

Although positive modulation of the channel kinetics is mediated by the large polysaccharide, the smaller DS-S polysaccharide and sulfate-free dextran (see respective traces in Fig. 2) had no effect on AMPA-induced current fluctuations. Together with previous work showing no effect on channel kinetics by monomeric glucosamine 2,3-disulfate, the results indicate that the channel modulation is similar to binding changes with regard to sulfate- and size-dependence.

To test if polysaccharide modulation of the channel activity affects calcium influx through AMPA receptors, primary hippocampal cultures were pre-loaded with Fluo3AM calcium ion dye. Note that postnatal Day 9 rat hippocampi were used to ensure sufficient levels of calcium-permeable AMPA receptors (Pellegrini-Giampietro et al., 1992). Results in Figure 4A show that AMPA produced a dose-dependent increase in fluorescence that was quenched by CNQX. In addition, time-lapse confocal movies revealed background fluorescence in dye-loaded neurons treated with saline (Fig. 4B), a subsequent increase in cellular fluorescent signal upon addition of AMPA (Fig. 4C), and quenching of the AMPA-mediated signal by the specific antagonist (Fig. 4D). AMPA at 60 μM produced a rapid fluorescent signal throughout the neuronal structure, allowing consistent measurements. The AMPA effect was pronounced in neuronal processes, and there was evidence of increased calcium at synaptic contacts (Fig. 5B).

Figure 6B shows that DS-L potentiates the calcium signal in hippocampal cell bodies and processes as compared to AMPA alone (Fig. 6A). DS-L had no effect on the few glial cells that exhibit a calcium response (<2% of total cells), and neurons made up the majority of AMPA responders (>90%). Pellegrini-Giampietro et al. (1992) indeed showed that the hippocampus contains increasing levels of calcium-permeable AMPA receptors during the developmental time from which tissue was harvested for culture preparation. By measuring the percent change in AMPA-induced calcium-Fluo3AM fluorescence, the DS-L effect was found to be dose-dependent (Fig. 7), causing up to a 60% increase in the response to 60 μM AMPA. As shown in Figure 6C and Figure 8, the DS-L effect was completely blocked by CNQX, indicating that DS-L-modulated calcium signals involve influx through AMPA receptors.

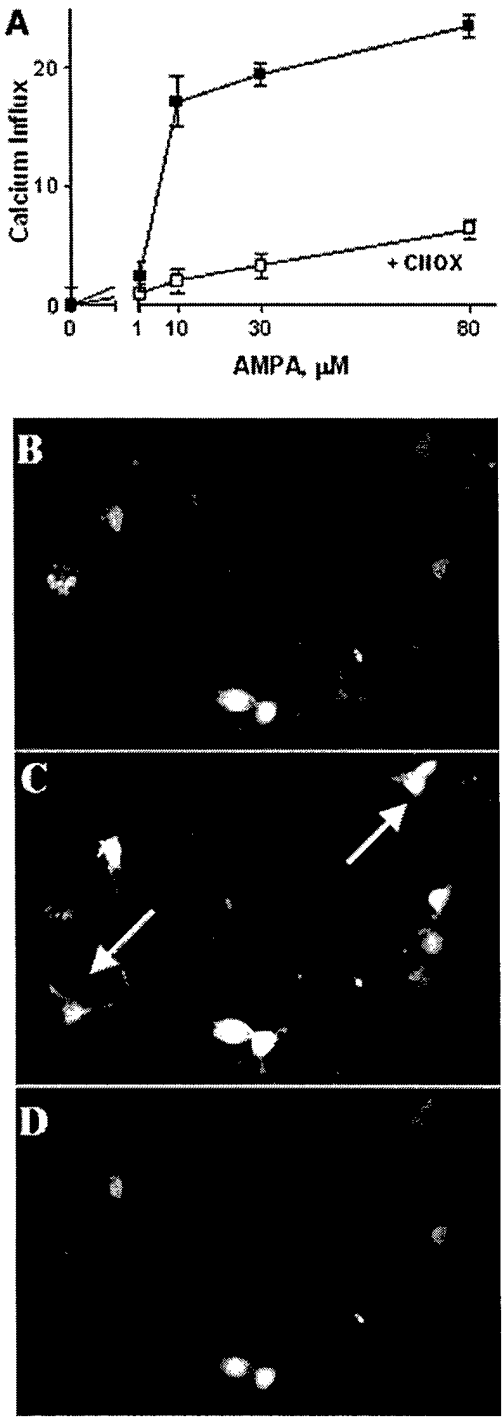

Fig. 4. AMPA induces an increase in calcium influx. AMPA-induced fluorescence was measured from Fluo3AM-loaded hippocampal cultures and background was subtracted (**A**). The data represent the mean ± SEM ($n = 3$ for the lowest concentration of AMPA; $n = 5$–10 for all other treatment conditions). Increasing AMPA concentrations caused an increase in fluorescent signal ($P < 0.0001$; closed squares). Time-lapse confocal images from the same field of dye-loaded hippocampal cells show the background fluorescence in non-treated cells (**B**), the subsequent increase in fluorescent signal when exposed to 60 μM AMPA (**C**), and blockage of the AMPA-mediated increase in fluorescent signal by 30 μM CNQX (**D**).

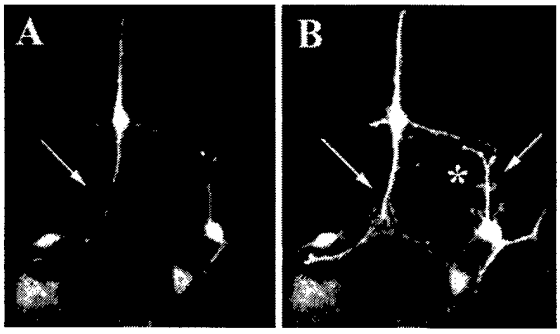

Fig. 5. AMPA increases calcium concentrations in the cell bodies and processes of hippocampal neurons, and at synaptic contacts along dendritic processes. Time-lapse confocal movies were made from dye-loaded hippocampal cells. Confocal images show saline control (**A**) and the subsequent increase in fluorescence intensity upon exposure to 60 μM AMPA (**B**). Arrows point to increases in intracellular calcium along cellular processes and the asterisk indicates evidence of synaptic contacts where AMPA mediated an increase in calcium influx.

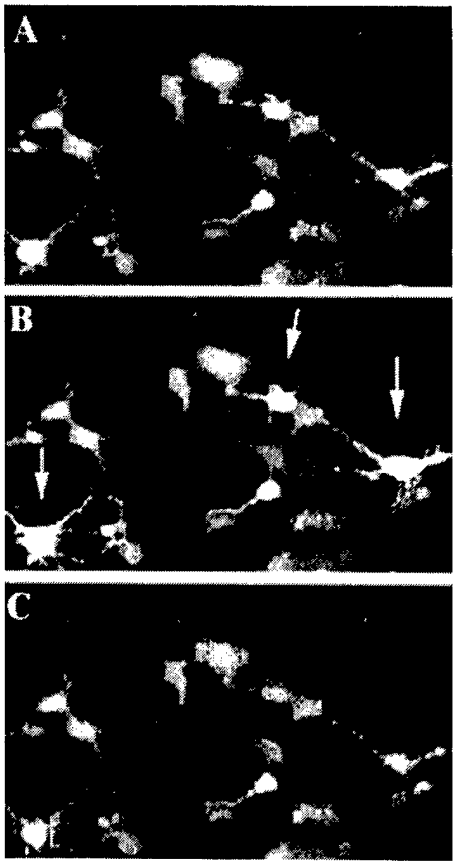

Fig. 6. DS-L enhances the AMPA-mediated calcium influx in primary hippocampal cell cultures. **A:** Still images from confocal movies from a single neuronal field show the Fluo3AM signal obtained by the 60 μM AMPA-mediated calcium influx. **B:** The fluorescent signal in the field is intensified with the addition of 10 nM DS-L, indicating an enhancement of the AMPA-mediated calcium influx. **C:** The addition of 30 μM CNQX quenches the fluorescence intensity generated by DS-L enhancement of the AMPA-mediated calcium influx.

In control experiments, the AMPA response and the DS-L enhancement of the AMPA response were not affected by the NMDA receptor antagonist AP5 (Fig. 8), and were not due to the release of internal calcium stores (Fig. 9). Further experiments using an L-type voltage-gated calcium channel inhibitor, nifedipine (1 μM), showed that voltage-gated calcium channels do not contribute to the DS-L-mediated increase in the AMPA response (−4.6% ± 7.1% change by nifedipine). Nifedipine did, on the other hand, block the calcium influx mediated by KCl (−85 ± 5.1% change). Together, these data indicate further that the modulated calcium signal involves stimulated AMPA channels.

As with the modulation of AMPA binding and channel kinetics, the effect of DS-L on calcium influx also exhibited sulfate- and size-dependencies. Whereas 10 nM DS-L markedly increased AMPA-induced calcium influx (post-hoc test: $P < 0.02$), 1 μM of the small DS-S species and 1 μM sulfate-free dextran had little to no effect (see Fig. 7). Also with no influence on the AMPA response were 10 μM glucosamine 2,3-disulfate (−0.9 ± 2% change) and 1 mM sodium sulfate (−4 ± 6% change), adding further to the common specificities across the binding, channel kinetics, and calcium influx properties.

DISCUSSION

The present report indicates that the glycosaminoglycan component of proteoglycans has the potential to modulate multiple AMPA receptor properties. A related polysaccharide, dextran sulfate, was found to lower the binding affinity of AMPA receptors, and to increase their single channel open time and probability of opening. In addition, the potentiated channel activity was associated with an enhancement of the AMPA-mediated calcium influx in hippocampal neurons. These findings strongly indicate that synaptic proteoglycans and polysaccharides are positioned appropriately to interact with and regulate AMPA-type glutamate receptors. Although the exact mechanisms for these events are not understood completely, polysaccharide modulation of neurotransmitter receptors may help explain the relationships between synaptic structure and function.

Dextran sulfate was shown to stabilize the open conformation of isolated AMPA channels, along with a receptor state that favors a low-affinity ligand interaction. Previous reports have shown that other polysaccharides promote similar changes in channel kinetics and binding properties (Hall et al., 1996; Hoffman et al., 1997; Sinnarajah et al., 1999), perhaps acting through an allosteric regulatory site on AMPA receptors (e.g., see Kessler et al., 1998; Bahr et al., 1999; Arai et al., 2000; Nagarajan et al., 2001; Suppiramaniam et al., 2001). Thus, it is possible that the dextran sulfate-induced changes in AMPA receptor

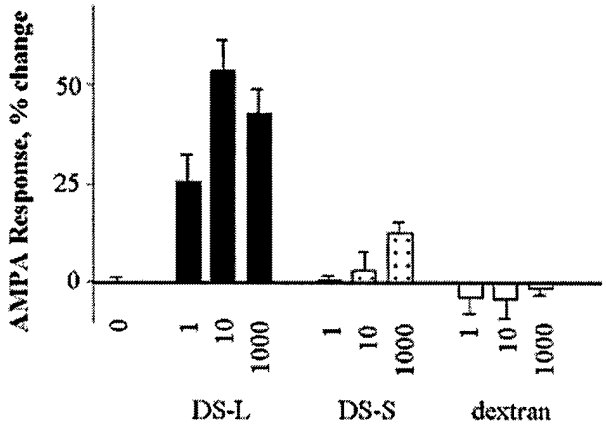

Fig. 7. Dose-dependent effects of DS-L on AMPA response in Fluo3AM-loaded hippocampal cells. Fluorimetry experiments were assessed for percent change in AMPA-mediated calcium response by different dextran species at stated nanomolar concentrations. DS-L increased the calcium influx in a dose-dependent manner (ANOVA; $P < 0.0001$). The smaller DS-S polysaccharide was much less effective at influencing the AMPA-mediated calcium influx ($P < 0.01$), and no change was found with sulfate-free dextran. The data represent means ± SEM ($n = 3$ for the lowest concentration of non-sulfated dextran; $n = 7$–10 for all other treatment conditions).

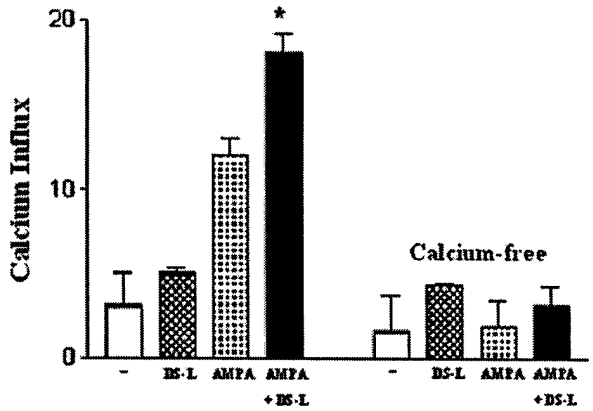

Fig. 9. Calcium signals modulated by DS-L require extracellular calcium. Fluo3AM-loaded hippocampal cells were assessed for AMPA and DS-L effects in normal media and in calcium-free media. Induced calcium signals were evident only in normal media (ANOVA; $P < 0.0001$), indicating that the intracellular signal was not from release of internal stores of calcium. Response to AMPA ligand (60 μM) was modulated positively by 10 nM DS-L (*post-hoc test; $P < 0.01$), whereas DS-L alone had no effect on the calcium signal in the absence or presence of extracellular calcium. The data represent means ± SEM ($n = 3$–5 per condition).

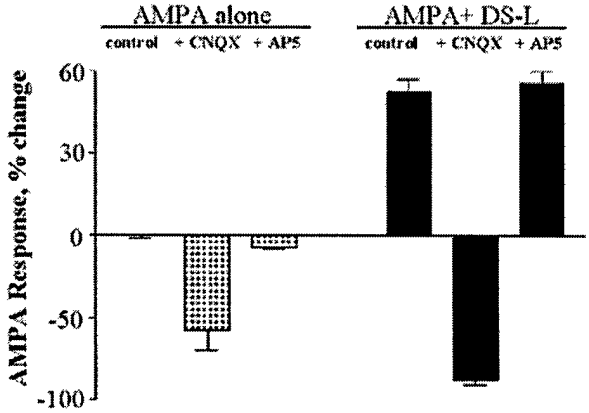

Fig. 8. DS-L modulation of calcium influx is specific for AMPA receptors. Changes in AMPA-induced fluorescent signals in Fluo3AM-loaded neurons are shown without and with the presence of 10 nM DS-L. The 60 μM AMPA-mediated calcium influx and enhancement of this response by DS-L were blocked by 30 μM CNQX, but not by 50 μM AP5. The data represent the mean ± SEM ($n = 7$–13 per condition).

binding and channel properties are due to a direct interaction between the polysaccharide and the receptor. Another possibility is that dextran sulfate indirectly influences AMPA receptors by interacting with or altering interactions between polysaccharides and polysaccharide carrier proteins of the synaptic environment and the surrounding extracellular matrix. We believe this is unlikely based on the fact that dextran sulfate altered AMPA receptor binding in a solubilized system where organized matrices were disrupted completely. Dextran sulfate also altered the functional properties of isolated AMPA receptors that were reconstituted in pure lipid bilayers, thus in the absence of organized matrices.

The polysaccharide modulation exhibited sulfate- and size-dependencies with respect to all AMPA receptor properties monitored in the present study. Ligand binding, channel kinetics, and calcium influx through AMPA receptors were effectively modulated by a large dextran sulfate species, whereas little effect was produced by smaller dextran sulfate or sulfate-free dextran. Such findings may be related to the fact that the biological activity of glycosaminoglycans is based on specific sugar residues, size of the polysaccharides, and the number of sulfates they possess (see Rouslahti, 1988, 1989). Increasing the length of the polymer chain adds increasing numbers of negatively charged sulfates, giving the larger dextran sulfate more charge and possibly stronger interactions with the AMPA receptor. It is known that polysaccharides, through a high degree of specificity, induce protein-protein or protein-carbohydrate interactions that may alter receptor structure and function (Lam et al., 1998; Hilgenberg et al., 1999; Capila and Linhardt, 2002). Also of interest in this context is that AMPA receptors can adopt a range of conformational states that influence functional properties of the AMPA channel (see Jin et al., 2003). Thus, it is possible that the highly charged, 500-kDa dextran sulfate promotes intermolecular interactions that modulate receptor function.

Clustering of neurotransmitter receptors, indeed, has been found to modulate the channel and binding functionality (Takagi et al., 1992; Chen et al., 2001). Receptor clustering has been implicated in synaptic transmission (Xia et al., 1999; Ango et al., 2002) and synapse formation (O'Brien et al., 2002; Cottrell et al., 2000), and polysaccharides and proteoglycans are known to regulate receptor clustering (Zhou et al., 1997; Moransard et al., 2003). Interestingly, polysaccharide modulation has been shown to facilitate clustered AMPA channel responses, exhibiting a remarkable degree of cooperativity (Hall et al., 1996). Thus, the large dextran sulfate in the present study may affect AMPA receptor properties by facilitating both the physical and functional clustering of the receptors. Synaptic polysaccharides, then, may modulate the basal activity of the synapse by promoting cooperative activation of AMPA receptors. Further understanding of polysaccharide-receptor interactions at the molecular level may provide insight into the regulation of activity-dependent events such as synaptogenesis and synaptic plasticity.

ACKNOWLEDGMENT

We thank Mr. B. Kawasaki for excellent technical assistance.

REFERENCES

Ango F, Robbe D, Tu JC, Xiao B, Worley PF, Pin JP, Bockaery J, Fagni L. 2002. Homer-dependent cell surface expression of metabotropic glutamate receptor type 5 neurons. Mol Cell Neurosci 20:323–329.

Arai AC, Kessler M, Rogers G, Lynch G. 2000. Effects of the potent Ampakine CX614 on hippocampal recombinant AMPA receptors: interactions with cyclothiazide and GYKI 52466. Mol Pharmacol 58:802–813.

Bahr BA, Vodyanoy V, Hall RA, Suppiramaniam V, Kessler M, Sumikawa K, Lynch G. 1992. Functional reconstitution of α-amino-3-hydroxy-5-methylisoxazole-4 -propionate (AMPA) receptors from rat brain. J Neurochem 59:1979–1982.

Bahr BA, Hoffman KB, Kessler M, Hennegriff M, Park GY, Yamamoto RS, Kawasaki BT, Vanderklish PW, Hall RA, Lynch G. 1996. Distinct distributions of α-amino-3-hydroxy-5-methyl-4-isoxazolepropionate (AMPA) receptor subunits and a related 53,000 M_R antigen (*GR53*) in brain tissue. Neuroscience 74:707–721.

Bahr BA, Staubli U, Xiao P, Chun D, Ji Z, Esteban ET, Lynch G. 1997. Arg-gly-asp-ser-selective adhesion and the stabilization of long-term potentiation: pharmacological studies and the characterization of a candidate matrix receptor. J Neurosci 17:1320–1329.

Bahr BA, Solomon Y, Suppiramaniam V. 1999. Structural chemistries underlying synaptic signaling and regulation. J Mol Biol Biotech 1:35–48.

Bahr BA, Bendiske J, Brown QB, Munirathinam S, Caba E, Rudin M, Urwyler S, Sauter A, Rogers G. 2002. Survival signaling and selective neuroprotection through glutamatergic transmission. Exp Neurol 174: 37–47.

Brakebusch C, Seidenbecher CI, Asztely F, Rauch U, Matthies H, Meyer H, Krug M, Bockers TM, Zhou X, Kreutz MR, Montag D, Gundelfinger ED, Fassler R. 2002. Brevican-deficient mice display impaired hippocampal CA1 long-term potentiation but show no obvious deficits in learning and memory. Mol Cell Biol 22:7417–7427.

Capila I, Linhardt RJ. 2002. Heparin-protein interactions. Angew Chem Int Ed Engl 41:391–412.

Chen L, Wang H, Vicini S, Olsen RW. 2001. The gamma-aminobutyric acid type A (GABAA) receptor associated protein (GABARAP) promotes GABAA receptor clustering and modulates the channel kinetics. Proc Natl Acad Sci USA 97:11557–11562.

Correia SS, Duarte CB, Faro CJ, Pires EV, Carvalho AL. 2003. Protein kinase C gamma associates directly with the GluR4 α-amino-3-hydroxy-5-methyl-4-isoxazole propionate receptor subunit. Effect on receptor phosphorylation. J Biol Chem 278:6307–6313.

Cottrell JR, Dube GR, Egles C, Liu G. 2000. Distribution, density, and clustering of functional glutamate receptors before and after synaptogenesis in hippocampal neurons. J Neurophysiol 84:1573–1587.

Hall RA, Kessler M, Lynch G. 1992. Evidence that high- and low-affinity DL-α-amino-3-hydroxy-5-methylisoxazole-4-propionic acid (AMPA) binding sites reflect membrane-dependent states of a single receptor. J Neurochem 59:1997–2004.

Hall RA, Vodyanoy V, Quan A, Sinnarajah S, Suppiramaniam V, Kessler M, Bahr BA. 1996. Effects of heparin on the properties of solubilized and reconstituted rat brain AMPA receptors. Neurosci Lett 217:179–183.

Hennegriff M, Arai A, Kessler M, Vanderklish P, Mutneja MS, Rogers G, Neve RL, Lynch G. 1997. Stable expression of recombinant AMPA receptor subunits: Binding affinities and effects of allosteric modulators. J Neurochem 68:2424–2434.

Hilgenberg LG, Hoover CL, Smith MA. 1999. Evidence of an agrin receptor in cortical neurons. J Neurosci 19:7384–7393.

Hoffman KB. 1998. The relationship between adhesion molecules and neuronal plasticity. Cell Mol Neurobiol 18:461–475.

Hoffman KB, Kessler M, Lynch G. 1997. Sialic acid residues indirectly modulate the binding properties of AMPA-type glutamate receptors. Brain Res 753:309–314.

Jin R, Banke TG, Mayer ML, Traynelis SF, Gouaux E. 2003. Structural basis for partial agonist action at ionotropic glutamate receptors. Nature Neuroscience 6:803–808.

Kaksonen M, Pavlov I, Voikar V, Lauri SE, Hienola A, Riekki R, Lakso M, Taira T, Rauvala H. 2002. Syndecan-3-deficient mice exhibit enhanced LTP and impaired hippocampus-dependent memory. Mol Cell Neurosci 21:158–172.

Kessler M, Mutaneja MS, Rogers G, Lynch G. 1998. Regional preferences of AMPA receptor modulators determined through agonist binding autoradiography. Brain Res 783:121–126.

König N, Poluch S, Estabel J, Durand M, Drian MJ, Exbrayat JM. 2001. Synaptic and non-synaptic AMPA receptors permeable to calcium. Jpn J Pharmacol 86:1–17.

Kramar EA, Bernard JA, Gall CM, Lynch G. 2002. α3 integrin receptors contribute to the consolidation of long-term potentiation. Neuroscience 110:29–39.

Lam K, Rao VS, Qasba PK. 1998. Molecular modeling studies on binding of bFGF to heparin and its receptor FGFR1. J Biomol Struct Dyn 15:1009–1027.

Lander C, Zhang H, Hockfield S. 1998. Neurons produce a neuronal cell surface-associated chondroitin sulfate proteoglycan. J Neurosci 18:174–183.

Launey T, Ivanov A, Ferrand N, Gueritaud JP. 1998. Developing rat brainstem motoneurons in organotypic culture express calcium permeable AMPA-gated receptors. Brain Res 781:148–158.

Lauri SE, Kaukinen S, Kinnunen T, Ylinen A, Imai S, Kaila K, Taira T, Rauvala H. 1999. Regulatory role and molecular interactions of a cell-surface heparan sulfate proteoglycan (N-syndecan) in hippocampal long-term potentiation. J Neurosci 19:1226–1235.

Lauterborn JC, Lynch G, Vanderklish P, Arai A, Gall CM. 2000. Positive modulation of AMPA receptors increases neurotrophin expression by hippocampal and cortical neurons. J Neurosci 20:8–21

Lin SS, Levitan IB. 1991. Concanavalin A: a tool to investigate neuronal plasticity. Trends Neurosci 14:273–277.

Lüthi A, Laurent JP, Figurov A, Muller D, Schachner M. 1994. Hippocampal long-term potentiation and neural cell adhesion molecules L1 and NCAM. Nature 372:777–779.

Mahanty NK, Sah P. 1998. Calcium-permeable AMPA receptors mediate long-term potentiation in interneurons in the amygdala. Nature 394:683–687.

McKinney RA, Capogna M, Durr R, Gahwiler BH. 1999. Miniature synaptic events maintain dendritic spines via AMPA receptor activation. Nat Neurosci 2:44–49.

Moransard M, Borges LS, Willmann R, Marangi PA, Brenner HR, Ferns MJ, Fuhrer C. 2003. Agrin regulates rapsyn interaction with surface acetylcholine receptors, and this underlies cytoskeletal anchoring and clustering. J Biol Chem 278:7350–7359.

Muller D, Wang C, Skibo G, Toni H, Cremer H, Calaora V, Rougon G, Kiss JZ. 1996. PSA-NCAM is required for activity-induced synaptic plasticity. Neuron 17:413–422.

Nagarajan N, Quast C, Boxall AR, Shahid M, Rosenmund C. 2001. Mechanism and impact of allosteric AMPA receptor modulation by the Ampakine CX546. Neuropharmacology 41:650–663.

O'Brien R, Xu D, Mi R, Tang X, Hopf C, Worley P. 2002. Synaptically targeted narp plays an essential role in the aggregation of AMPA receptors at excitatory synapses in cultured spinal neurons. J Neurosci 22:4487–4498.

Pellegrini-Giampietro DE, Bennett MV, Zukin RS. 1992. Are Ca(2+)-permeable kainate/AMPA receptors more abundant in immature brain? Neurosci Lett 144:65–69.

Riedel G, Platt B, Micheau J. 2003. Glutamate receptor function in learning and memory. Behav Brain Res 140:1–47.

Rønn LC, Hartz BP, Bock E. 1998. The neural cell adhesion molecule (NCAM) in development and plasticity of the nervous system. Exp Gerontol 33:853–864.

Rønn LC, Bock E, Linnemann D, Jahnsen H. 1995. NCAM-antibodies modulate induction of long-term potentiation in rat hippocampal CA1. Brain Res 677:145–151.

Rouslhati E. 1988. Structure and biology of proteoglycans. Annu Rev Cell Biol 4:229–255.

Rouslhati E. 1989. Proteoglycans in cell regulation. J Biol Chem 264: 13369–13372.

Shapiro M. 2001. Plasticity, hippocampal place cells, and cognitive maps. Arch Neurol 58:874–881.

Sinnarajah S, Suppiramaniam V, Kumar KP, Hall RA, Bahr BA, Vodyanoy V. 1999. Heparin modulates the single channel kinetics of reconstituted AMPA receptors from rat brain. Synapse 31:203–209.

Staubli U, Chun D, Lynch G. 1998. Time-dependent reversal of long-term potentiation by an integrin antagonist. J Neurosci 18:3460–3469.

Staubli U, Izrael Z, Xu F. 1996. Remembrance of odors past: enhancement by central facilitation of AMPA receptors. Behav Neurosci 110:1067–1073

Staubli U, Rogers G, Lynch G. 1994. Facilitation of glutamate receptors enhances memory. Proc Natl Acad Sci USA 91:777–781.

Suppiramaniam V, Bahr BA, Sinnarajah S, Owens K, Rogers G, Yilma S, Vodyanoy V. 2001. Member of the Ampakine class of memory enhancers prolongs the single channel open time of reconstituted AMPA receptors. Synapse 40:154–158.

Takagi T, Pribilla I, Kirsch J, Betz H. 1992. Coexpression of the receptor-associated protein gephyrin changes the ligand binding affinities of α2 glycine receptors. FEBS Lett 303:178–180.

Vodyanoy V, Bahr BA, Suppiramaniam V, Hall RA, Baudry M, Lynch G. 1993. Single channel recordings of reconstituted AMPA receptors reveal low and high conductance states. Neurosci Lett 150:80–84.

Wong LA, Mayer ML. 1993. Differential modulation by cyclothiazide and concanavalin A of desensitization at native α-amino-3-hydroxy-5-methyl-isoxazolepropionic acid- and kainate-preferring glutamate receptors. Mol Pharmacol 44:504–510.

Xia J, Zhang X, Staudinger J, Huganir RL. 1999. Clustering of AMPA receptors by the synaptic PDZ domain-containing protein PICK1. Neuron 22:179–187.

Zhou H, Muramatsu T, Halfter W, Tsim KW, Peng HB. 1997. A role of midkine in the development of the neuromuscular junction. Mol Cell Neurosci 10:56–70.

ACADEMIC PRESS

Available online at www.sciencedirect.com

SCIENCE DIRECT®

Neurobiology of Disease 14 (2003) 513–523

Neurobiology of Disease

www.elsevier.com/locate/ynbdi

Death mechanisms in status epilepticus-generated neurons and effects of additional seizures on their survival

Christine T. Ekdahl,[a,*] Changlian Zhu,[b,c] Sara Bonde,[a] Ben A. Bahr,[d] Klas Blomgren,[b,e] and Olle Lindvall[a]

[a] *Section of Restorative Neurology, Wallenberg Neuroscience Center, BMC A11, SE-221 84, Lund, Sweden*
[b] *Department of Physiology, Box 432, SE-405 30, Göteborg, Sweden*
[c] *Department of Pediatrics, The Third Affiliated Hospital, Zhengzhou University, P.R. China*
[d] *Department of Pharmaceutical Sciences and the Neurosciences Program, University of Connecticut, Storrs, CT 06269-2092, USA*
[e] *Department of Paediatrics, The Queen Silvia Children's Hospital, SE-41685, Göteborg, Sweden*

Received 26 March 2003; revised 10 August 2003; accepted 26 August 2003

Abstract

Status epilepticus (SE) increases neurogenesis in the subgranular zone (SGZ) of the adult dentate gyrus, but many of the newborn cells die, partly through caspase-induced apoptosis. Here we provide immunohistochemical evidence indicating that the caspase-evoked death of the new neurons involves the mitochondrial but not the death-receptor-mediated pathway. Cytochrome c released from mitochondria was found in a subset of progenitor cell progeny, while Fas ligand and tumor necrosis factor 1 receptor-associated domain as well as the mitochondria-related, caspase-independent apoptosis-inducing factor were not detected. We also show that additional seizures, induced at different stages during neuronal differentiation of progenitor cell progeny following SE, neither potentiate cell death mechanisms in the SGZ nor compromise the survival of the new cells. Thus, we found similar expression of cytochrome c, active caspase-3, caspase-cleaved PARP, and TUNEL/Hoechst-positive DNA fragmentation, as well as numbers of new cells in the SGZ in rats exposed to additional seizures at days 6 and 7 or days 33 and 34 following SE as in control animals only subjected to SE. We propose that the degree of survival of newly generated neurons is determined primarily by the initial SE insult and the ensuing pathology in the tissue environment, whereas spontaneous seizures play a minor role.
© 2003 Elsevier Inc. All rights reserved.

Keywords: Neurogenesis; Apoptosis; Seizures; Status epilepticus; Dentate gyrus; Bromodeoxyuridine; Cytochrome c; Caspase-3; TUNEL; Poly(ADP-ribose)polymerase

Introduction

In the adult brain, the generation of new neurons continues from neural stem cells or progenitor cells located in the subgranular zone (SGZ) of the dentate gyrus (DG) and the subventricular zone (SVZ) lining the lateral ventricle (Gage et al., 1998). Brain insults such as epileptic seizures and cerebral ischemia, which are associated with neuronal death, trigger a strong proliferative response in both the SGZ and the SVZ (Bengzon et al., 1997; Parent et al., 1997, 2002a; Liu et al., 1998; Nakagawa et al., 2000; Arvidsson et al., 2002). This finding has raised the possibility that insult-generated new neurons might be able to replace the injured and dying neurons. Recent experimental evidence indicates that such neuronal self-repair can occur in the adult brain both after selective photolytic lesions (Magavi et al., 2000) and ischemic insults leading to more extensive damage (Arvidsson et al., 2002; Nakatomi et al., 2002; Parent et al., 2002b).

Neurogenesis comprises at least four distinct steps: proliferation, migration, differentiation, and survival (Gage et al., 1998). Poor survival is a general problem with the newly proliferated cells following both epileptic (Ekdahl et al.,

* Corresponding author. Lund University, Section of Restorative Neurology, Wallenberg Neuroscience Center, BMC A11, Sölvegatan 17, SE-221 84 Lund, Sweden. Fax: +46-222-0560.
E-mail address: christine.ekdahl@neurol.lu.se (C.T. Ekdahl).

0969-9961/$ – see front matter © 2003 Elsevier Inc. All rights reserved.
doi:10.1016/j.nbd.2003.08.022

2001) and ischemic insults (Arvidsson et al., 2002), which minimizes the possible impact of neurogenesis on functional recovery in the damaged areas. Not least from a clinical perspective, it is highly warranted to explore the mechanisms of death of the new neurons and identify the triggering and aggravating factors. At the time of maximum cell proliferation 1 week following status epilepticus (SE) (Parent et al., 1997), progenitor cell progeny in the SGZ show DNA fragmentation and active caspase-cleaved poly-(ADP-ribose)polymerase (PARP) expression (Ekdahl et al., 2001, 2002). Caspases are key players in several forms of programmed cell death (Cohen, 1997), and inhibition of caspases leads to increased survival of both proliferating cells and new neurons generated in the SGZ after SE (Ekdahl et al., 2001, 2002). Markers for two other cysteine protease families involved in programmed cell death, the calpains and the cathepsins, were not detected in the newly formed cells (Ekdahl et al., 2001, 2002). Taken together, these observations indicate that caspase-mediated apoptotic death compromises the survival of SE-generated DG neurons. In agreement, the number of newly formed cells following SE was increased after administration of the DNA synthesis inhibitor cycloheximide (Covolan et al., 2000).

The severity of SE and, in particular, the proportion of generalized clonic seizures influences the survival step during neurogenesis (Mohapel et al., 2001). Hypothetically, the death of the newborn cells after SE may be due to recurring spontaneous seizure episodes or to neuropathological changes in the surrounding tissue environment. In humans, SE is often followed by spontaneous seizures (Maytal et al., 1989; Hauser et al., 1990; Verity et al., 1993), and animal models of SE have shown that spontaneous seizures can start to occur 1–2 weeks following the initial epileptic insult (Bertram and Cornett, 1993; Nissinen et al., 2000; Gorter et al., 2001). The onset of spontaneous seizures coincides with the time of maximum seizure-induced proliferation (Parent et al., 1997) and caspase-mediated cell death in the SGZ (Ekdahl et al., 2002). The previous finding that one single seizure can cause apoptosis in the SGZ (Bengzon et al., 1997) and the temporal pattern of spontaneous seizures support the idea that such seizures could trigger the death of the newly proliferated cells.

In this study, rats were subjected to electrical SE and exposed to additional seizures at either of two time points, days 6 and 7 or days 33 and 34, thereafter. The objectives were two-fold: first, to elucidate in more detail, using various immunohistochemical markers, the cell death pathways operating in the new neurons; and second, to determine whether the new neurons are particularly susceptible to seizure-induced damage either early after their generation or at a time when they have adopted a more mature phenotype. For this purpose, we assessed changes in the expression of the various cell death markers as well as quantified the number of surviving, new neurons.

Materials and methods

Animals and surgery

Seventy-two adult male Sprague-Dawley rats (B&K Universal, Stockholm, Sweden), weighting 270–340 g at the time of surgery, were used. Rats were housed separately under 12-h light/12-h dark conditions with ad libitum access to water and food. Experimental procedures followed guidelines set by the Malmoe-Lund Ethical Committee for the use and care of laboratory animals (M239/99) and were carried out in accordance with the European Communities Council Directive of 24 November 1986 (86/609/EEC). All rats were anesthetized with sodium pentobarbital (65 mg/kg i.p.) and implanted with a twisted insulated stainless-steel stimulating/recording electrode (Plastics One, Roanoke, VA, USA) unilaterally into the right ventral hippocampal CA1–CA3 region (coordinates: 4.8 mm caudal and 5.2 mm lateral to bregma, 6.3 mm ventral from dura, toothbar at −3.3 mm; Paxinos and Watson, 1997).

Induction of status epilepticus

Ten days following surgery, all rats except 15 nonstimulated controls were subjected to electrically induced, self-sustained SE (Mohapel et al., 2001; Ekdahl et al., 2002). The rats received suprathreshold stimulations consisting of 10-s trains of 1-ms biphasic square wave pulses at a frequency of 50 Hz. The stimulations were interrupted every 10 min for 1 min to allow for electroencephalogram (EEG) recording and measurement of afterdischarges (MacLab; AD Systems, Hastings, UK). Rats exhibiting more than 10 min of continuous generalized clonic seizures received only 60 min of stimulation, whereas the other rats had 90 min of stimulation. The stimulation period was extended in rats exhibiting mostly partial seizures to induce a more severe insult, resembling that in animals with generalized clonic seizures (see results section below). After cessation of stimulations, all rats exhibited self-sustained, continuous ictal EEG activity, which was associated with varying severity of motor behavioral seizures, categorized into distinct SE profiles. The milder profiles consisted of hyperactive motor behavior, or partial seizures, scored as grade 1 and 2 in the classical kindling motor behavior scale (Racine, 1972), and the more severe SE profile comprised generalized clonic seizures rated as grade 3 to 5 (Mohapel et al., 2001). Behavioral convulsions and ictal EEG activity were arrested with pentobarbital (65 mg/kg i.p.) at 2 h after stimulation offset. EEG was recorded for 2 to 4 min every other morning from day 2 and onward to measure spontaneous spiking activity.

Induction of additional seizures

Twenty-five rats were subjected to two sessions of stimulations with the same parameters as during the initial SE

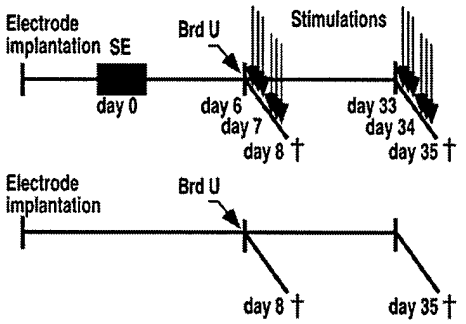

Fig. 1. Experimental design and group assignment. All rats (n = 72) were implanted with an electrode in the CA1/CA3 region of the right ventral hippocampus, and 10 days later, except for 15 nonstimulated controls, they were subjected to electrically induced status epilepticus. At day 6 after the insult all rats (excluding six rats used for retroviral transduction) received BrdU injections and were perfused either 2 days or 4 weeks later. Additional stimulations were applied on days 6 and 7 (n = 14) or day 33 and 34 (n = 11).

insult, interrupted every 4–10 min for 1 min of EEG registration. Each session ended when the rats had exhibited three generalized clonic grade 3–5 seizures. To ascertain that the animals did not develop SE, they were only included in the experiments if the spontaneous seizures ceased within 10 min after the stimulation period was over. The short-term survival group (n = 14) received additional stimulations 2 h after the last BrdU injection at day 6 and at day 7. The long-term survival group (n = 11) had their additional stimulations at days 33 and 34 (Fig. 1).

Bromodeoxyuridine (BrdU) administration

Six days after SE, all animals (excluding six rats, which were injected with a retroviral vector, see below) were given a series of four injections (every 2 h during a 6-h period) of the thymidine analogue BrdU (50 mg/kg i.p., Sigma, Sweden) dissolved in potassium phosphate-buffered saline (KPBS) for labeling of mitotic cells (Dolbeare, 1995). Rats were perfused either 2 days (n = 40) or 28 days (n = 26) later (Fig. 1).

Retroviral injections

At 1 week after SE, six rats were anesthetized with halothane and injected with a green fluorescent protein (GFP)-carrying retroviral vector (1 μl 1 $\times$ 10^9 transducing U/ml), produced as previously described (Ory et al., 1996), into the dorsal DG (coordinates: AP −3.6 mm, ML 2.0 mm, DV −2.8 mm) using a glass micropipette attached through a polyethylene tube to a Hamilton syringe. The rats were perfused either 2 days or 4 weeks later (n = 4 and n = 2, respectively).

Tissue fixation and sectioning

Rats received an overdose of anesthesia and were transcardially perfused with 50 ml of saline followed by 250 ml of ice-cold formaldehyde solution [4% paraformaldehyde (PFA) in 0.1 M PBS, pH 7.4]. Brains were removed, postfixed overnight in the same medium, and then placed in 20% sucrose/0.1 M phosphate buffer for at least 24 h, after which coronal sections (30 μm) through the dorsal hippocampus were cut on a freezing microtome and stored in cryoprotecting solution. For cytochrome c, active caspase-3, apoptosis inducing factor (AIF), BrdU/cytochrome c, and BrdU/active caspase-3 stainings, brains were put in PFA for at most 12 h after perfusion, before dehydration with graded ethanol and xylene. The brains were then paraffin-embedded and cut into 5-μm-thick coronal sections.

Primary antibodies

The following primary antibodies were used for immunohistochemical stainings: caspase activity was examined with a rabbit anti-rat caspase-cleaved poly(ADP-ribose) polymerase (cPARP) antibody (1:50; Cell Signaling Technology, Beverly, MA, USA; Au-Yeung et al., 2001; Erhardt et al., 2001; Han et al., 2001) and a biotinylated rabbit anti-active caspase-3 antibody (1:50; Pharmingen, San Diego, CA, USA; Zhu et al., 2000; Blomgren et al., 2001). Calpain activity was detected with a rabbit affinity-purified antibody against calpain-mediated fodrin breakdown product (FBDP) (1:50; Bahr et al., 1995, 2002; Bednarski et al., 1995). The death receptor pathway was examined with a mouse anti-Fas ligand antibody (1:50; Upstate Biotechnology, NY, USA; Henshall et al., 2001b) and a rabbit anti-tumor necrosis factor receptor 1-associated death domain (TRADD) antibody (1:100; Santa Cruz Biotechnology, Santa Cruz, CA; Wang et al., 2000). The goat anti-AIF antibody (1:100, 2 μg/ml; sc-9416, Santa Cruz Biotechnology; Zhang et al., 2002; Ferrand-Drake et al., 2003; Zhu et al., 2003) was used for detecting a mitochondrial-related non-caspase-mediated pathway. The mitochondria-related caspase-mediated pathway was evaluated with a mouse anti-cytochrome c antibody (1:500, 2 μg/ml; clone 7H8.2C12, Pharmingen; Zhang et al., 2002; Ferrand-Drake et al., 2003; Zhu et al., 2003). Newly formed cells were detected with a rat anti-BrdU antibody (1:100; Oxford Biotechnology Ltd., Oxfordshire, UK). The neuronal or glial fate of the newly formed cells were examined with double-labeling of BrdU with a mouse antibody against the neuronal marker neuron-specific nuclear protein (NeuN) (1:100; Chemicon, Temecula, CA, USA), or antibodies against activated microglia, i.e., mouse anti-ED1 antibody (1:200; Serotec, Oslo, Norway), and the astrocytic marker S100beta, a rabbit antibody (1:10,000; Swant, Bellinzona, Switzerland). The morphology of the newly formed cells transfected with a GFP-carrying retroviral vector were stud-

ied with a rabbit-anti-GFP antibody (1:20,000; Abcam, Cambridge, UK).

Single-label immunohistochemistry

Free-floating sections were mounted in KPBS onto microscope slides and dried before preincubation in 5% normal serum for 1.5 h. Subsequently, the sections were incubated overnight with rabbit anti-rat caspase-cPARP, rabbit affinity-purified antibody against calpain-mediated FBDP, or mouse anti-Fas ligand antibody in 3% bovine serum albumin (BSA) (only for the cPARP staining) and 0.25% Triton X-100 at +4°C overnight. Biotinylated goat anti-rabbit or horse anti-mouse antibody (1:50; Vector Laboratories, Burlingame, CA, USA) was applied for 1.5 h, followed by quenching for 12 min in 3% hydrogen peroxide before incubation with avidin-biotin-peroxidase complex (Elite ABC kit, Vector Laboratories) for 1.5 h and treatment with diaminobenzidine (0.5 mg/ml) and hydrogen peroxide. Rinsing in KPBS was applied between each step for all three stainings. For the TRADD staining, sections were free-floating and put in 3% hydrogen peroxide and 10% methanol for 30 min, preincubated with normal serum in 0.25% Triton X, before a rabbit anti-TRADD antibody was added overnight in +4°C, followed by biotin goat anti-rabbit antibody, incubation in avidin-biotin-peroxidase complex and treatment with diaminobenzidine. Paraffin sections for active caspase-3, cytochrome c, AIF staining were deparaffinized with xylene and rehydrated in graded ethanol concentrations. After washing in PBS, antigen retrieval was performed by heating the sections in +80°C 10 mM sodium citrate buffer for 30 min (for active caspase-3) or by boiling in the same buffer for 10 min (cytochrome c and AIF stainings). For active caspase-3 staining, sections were treated with proteinase K 10 μg/ml in PBS, for 10 min at room temperature (RT), rinsed with PBS, and incubated with biotinylated rabbit anti-active caspase-3 antibody in 1% BSA in Tris-buffered saline with 0.1% Triton X-100 (TBST) at +4°C overnight. For the cytochrome c and AIF staining, nonspecific binding was blocked for 30 min with 5% horse serum in PBS. Sections were incubated for 1 h at RT with goat anti-AIF antibody in 1% BSA in TBS or mouse anti-cytochrome c antibody in TBS containing 1% BSA or in PBS with 0.2% Triton X-100, followed by a biotinylated horse anti-goat antibody (1:200, 3 μg/ml; Vector Laboratories) or biotinylated horse anti-mouse antibody (1:200, 2 μg/ml; Vector Laboratories) for 60 min. Endogenous peroxidase activity was blocked with 3% H_2O_2 for 5 min. Visualization was performed using avidin-biotin-peroxidase complex and 0.5 mg/ml 3,3′-diaminobenzidine (DAB) enhanced with 15 mg/ml ammonium nickel sulfate, 2 mg/ml beta-D-glucose, 0.4 mg/ml ammonium chloride, and 0.01 mg/ml beta-glucose oxidase (Sigma). Negative controls, where the primary antibody was omitted, were completely blank. Also, preabsorbtion with a peptide for AIF, provided by the manufacturer, or a 20-fold surplus of purified bovine heart cytochrome c (Sigma) completely abolished those stainings.

Terminal deoxynucleotidyl transferase-mediated fluorescein-dUTP nick end-labeling (TUNEL)/Hoechst staining

In situ detection of single- and double-stranded DNA breaks was performed by TUNEL. Free-floating sections were mounted in KPBS onto glass microscope slides and dried. The sections were pretreated with 4% PFA for 20 min, methanol for 30 min, proteinase K (10 μg/ml KPBS) for 6 min, 4% PFA for 5 min, and ice-cold 0.1% Triton X-100 in 0.1% sodium citrate for 2 min with KPBS rinses between each step. Subsequently, each section was incubated in the dark at +37°C for 60 min in terminal deoxynucleotidyl transferase (TdT) buffer containing 17 μl of TdT enzyme solution and 150 μl of TUNEL label solution with fluorescein-conjugated dUTP (Boehringer Mannheim, Germany). Sections were counterstained with Hoechst 33342 (10 μg/ml; Molecular Probes, The Netherlands) for 10 min in the dark. Slides were coverslipped with glycerol-based mounting medium.

Double-label immunohistochemistry

For BrdU double labeling, free-floating sections were denatured in 1 M HCl for 30 min at +65°C. The sections were then preincubated with normal serum in 0.25% Triton X-100 for 1 h. Subsequently, the sections were incubated overnight in +4°C with rat anti-BrdU antibody and mouse anti-NeuN antibody, mouse anti-EDI antibody, or rabbit anti-S100beta primary antibody. This step was followed by rinsing and incubation in the dark for 2 h with Cy3-conjugated donkey anti-rat antibody (1:400; Jackson ImmunoResearch, West Grove, PA, USA) and biotiny lated horse anti-mouse or goat anti-rabbit antibody (1:200; Vector Laboratories). After rinsing, sections were incubated in streptavidin-conjugated Alexa Fluor 488 (1:200; Molecular Probes) in the dark for 2 h, mounted on glass slides, and finally coverslipped with glycerol-based mounting medium. For GFP/NeuN double labeling, rabbit-anti-GFP antibody was used followed by biotinylated goat anti-rabbit and streptavidin-conjugated Alexa Fluor 488, and NeuN was visualized with Cy3-conjugated horse anti-mouse (1:200; Jackson ImmunoResearch). Paraffin-embedded sections for BrdU/cytochrome c or active caspase-3 staining were deparaffinized with xylene and rehydrated in graded ethanol concentrations. After washing in PBS, antigen retrieval was performed by heating the sections in +80°C 10 mM sodium citrate buffer (pH 6.0) for 30 min, followed by rinsing with PBS, preincubation in 4% BSA in TBST for 30 min and incubation with rat-anti-BrdU in 1% BSA in TBST at +4°C overnight. The sections were then rinsed, incubated in the dark for 2 h with Cy3-conjugated donkey anti-rat antibody (1:400), rinsed, preincubated in normal serum in PBS for 30

Table 1
Characteristics of seizures induced by additional hippocampal stimulations at different time points after status epilepticus[a]

	Additional stimulations days 6 and 7	Additional stimulations days 33 and 34
First day		
Electrical stimulation (min)	12.9 ± 3.3[b]	8.1 ± 1.8[b]
Partial seizures (grade 1–2) (min)	10.9 ± 1.3	9.8 ± 2.0
Generalized seizures (grade 3–5) (min)	1.8 ± 0.3	2.5 ± 0.9
Second day		
Electrical stimulation (min)	0.9 ± 0.2	3.6 ± 1.0
Partial seizures (grade 1–2) (min)	9.2 ± 1.6	12.3 ± 2.5
Generalized seizures (grade 3–5) (min)	1.4 ± 0.1	1.4 ± 0.1

[a] Mean ± SEM.
[b] Significantly longer stimulation period at days 6 and 33, compared to days 7 and 34, respectively.

min, and incubated with mouse anti-cytochrome c antibody in PBS for 1 h or rabbit anti-active caspase-3 antibody in normal serum in PBS for 2 h at RT followed by fluorescein-conjugated horse anti-mouse (1:200; Vector Laboratories) for 1 h or Alexa Fluor 488 goat anti-rabbit (1:200; Vector Laboratories) for 2 h in the dark.

Cell quantification

All analyses were performed by an observer blind to the treatment conditions. Immunostainings were examined with an Olympus AX-70 light microscope. The number of positive cells was counted in the GCL and within two cell diameters below this region in the SGZ (referred to as GCL/SGZ) as well as in the dentate hilus. FBDP was also assessed in the CA1 and CA3 regions. To reduce counting bias, only central cell profiles (Coggeshall and Lekan, 1996) exceeding 3 μm were included. Furthermore, the TUNEL-positive cells had to exhibit pycnotic morphology and condensed nuclei with the Hoechst stain to be included in the analyses. With each staining, the number of labeled cells in three coronal sections from each rat, located between 3.3 mm and 4.3 mm posterior to bregma (encompassing the dorsal hippocampal region), was counted and expressed as average number of cells per section. For all stainings, the counts are reported as mean number of cells per section. Colocalization of BrdU-positive cells with either NeuN, ED1, or S100beta was assessed using a confocal scanning light microscope (Bio-Rad MRC1024UV, UK) with Kr/Ar 488 and 568 nm excitation filter. A double-stained cell was defined as having the strongest intensity of both stainings within the same or directly neighboring 1-μm-thick optical section through the cell in a consecutive *Z*-series of at least four sections, with an overlap of the stainings in at least three sections. In each rat, 50 BrdU-positive cells were analyzed for either NeuN, ED1, or S100beta double labeling in the SGZ/GCL and dentate hilus. Colocalization of BrdU/ cytochrome c and BrdU/active caspase-3 staining was assessed in 5-μm-thick sections in epifluorescence.

Statistical analysis

All comparisons were performed using one-way analysis of variance (ANOVA) followed by post hoc Bonferroni test. Data are presented as means ± SEM, and differences are considered significant at $P < 0.05$.

Results

Seizure parameters

Thirty-nine rats developed partial and 12 rats generalized SE, and were randomly selected for additional stimulations at either days 6 and 7 or days 33 and 34, or only connected to the stimulator at these time points. There were no significant differences between the groups with respect to the percentage of time exhibiting generalized or partial convulsive behavior during the induction of SE (SE alone: 81% partial and 13% generalized seizures; SE + additional seizures: 82% partial and 12% generalized seizures). The duration of the additional stimulations did not differ between the day 6/7 and day 33/34 stimulation groups, but decreased significantly between the first and second day of stimulation at both time points (Table 1). Also the duration of partial (grade 1–2) or generalized (grade 3–5) behavioral seizures in response to additional stimulations was similar in the two groups (Table 1). Behavioral and EEG seizure activity stopped within 10 min after the end of the stimulation period. The mean frequency of spontaneous spiking was recorded during the 1-week or 5-week survival time following SE and did not differ between groups (short-term survival group: SE 0.25 ± 0.04 Hz vs. SE + add stim. 0.29 ± 0.04 Hz; long-term survival group: SE 0.20 ± 0.04 Hz vs. SE + add stim. 0.17 ± 0.04 Hz). Spontaneous behavioral seizures were occasionally observed in all groups.

Newly proliferated cells in the subgranular zone express markers of the mitochondrial but not the death-receptor pathway following status epilepticus

Eight days following SE, several cell death markers were detected in the DG. Cytosolic cytochrome c expression was observed in small, single cells in the SGZ/GCL, and in big, multipolar cells located both in the SGZ/GCL and dentate hilus (Fig. 2A). Staining for active caspase-3 showed a heterogenous morphology of positive cells, which included small cells, either single or in cluster formation, in the SGZ/GCL, as well as big, multipolar cells located in the SGZ/GCL and the dentate hilus (Fig. 2C). The number of small cells expressing active caspase-3 was several-fold higher compared to those containing cytochrome c (data not shown). Caspase-cleaved PARP expression was found exclusively in single or clustered small cells in the SGZ/GCL (Fig. 2E) (Ekdahl et al., 2002). Cytosolic and nuclear AIF expression was detected in multipolar cells in the SGZ/GCL and the dentate hilus (Fig. 2G). TNFRI-associated TRADD was observed throughout the DG, but only in glial cells (Fig. 2H). Thus, double labeling of TRADD with the astrocytic marker GFAP showed almost 100% overlap (data not shown). We did not detect any expression of the TNF superfamily ligand Fas or calpain-mediated FBDP in the SGZ/GCL (Fig. 2I and J). Small, pycnotic TUNEL/Hoechst-labeled cells were found in the SGZ/GCL and to a much lesser extent in the hilus.

We then explored whether the small cytochrome c- and active caspase-3-positive cells, located singly or in clusters in the SGZ/GCL, had been formed after SE. Eight days after the epileptic insult, almost 10% of the BrdU-labeled cells in the SGZ were double-labeled with cytochrome c. Single-labeled cytochrome c-positive cells were scarce (Fig. 3A–C). More than 80% of the BrdU-positive cells also expressed active caspase-3. Some cells single-labeled with active caspase-3 surrounded the double-labeled cells in the SGZ/GCL (Fig. 3D–G).

Survival of new neurons in the subgranular zone is unaffected by additional seizures following status epilepticus

In the animals that did not receive additional stimulations following SE, there was an 8-fold increase of the number of small single or cluster-forming, BrdU-labeled, newly proliferated cells in the SGZ/GCL at day 8, i.e., 2 days after BrdU injections (Fig. 4). Over the subsequent 4 weeks, the number of cells decreased by about 80%. Similarly, in the dentate hilus, the BrdU-positive cells had increased 5-fold at day 8, but at day 35 we observed a marked loss (around 60%) of the proliferated cells. However, there was still a significant increase of the number of BrdU-positive cells at day 35 compared to nonstimulated controls. When animals with partial and generalized SE were analyzed separately, we observed a similar loss of BrdU-positive cells from day 8 to day 35 in the SGZ/GCL and dentate hilus, with no significant difference between groups (data not shown). We have previously observed (Mohapel et al., 2001) a marked difference in the survival of the new neurons between animals exhibiting partial and clonic SE, evoked by 60 min of electrical stimulation. Our present finding suggests that prolonging the stimulation period from 60 to 90 min in rats exhibiting partial SE leads to a loss of the new cells comparable to that observed after generalized SE with 60 min stimulation.

Two groups of SE animals were electrically stimulated until they had exhibited three generalized seizures on both days 6 and 7 or on days 33 and 34, and were killed on days 8 and 35, respectively. We observed no significant differences between animals with and without additional stimulations in the number of BrdU-positive cells in SGZ/GCL or dentate hilus at either time point (Fig. 4). Confocal microscopical analysis revealed that in both treatment groups, the number of BrdU/NeuN-double labeled cells at day 35 exceeded 90% in the SGZ/GCL (SE: 93.8 ± 1.7% vs. SE + add. stim: 94.7 ± 1.2%), and 50% in the dentate hilus (SE: 57.9 ± 5.2% vs. SE + add. stim: 56.2 ± 6.9%). Double stainings for activated microglia (ED1) and astrocytes (S100beta) showed that only a minor fraction of the newly formed cells in the SGZ/GCL adopted a glial phenotype following SE (BrdU/ED1 and BrdU/S100beta were both less than 1%). These percentages, as well as the total number of ED1- and S100beta-positive cells in the SGZ, did not change significantly following additional stimulations either in the short-term or long-term survival group (data not shown).

We wanted to evaluate the phenotype of SE-generated cells at the time of additional stimulations. Due to the difficulties in assessing the morphology with BrdU and NeuN staining, we also used labeling with a GFP-retroviral vector. At the early time point (9 days following SE and 2 days after viral injection), the cells were located in clusters in the SGZ, with short dendrites and small cell bodies (Fig. 5A). After 4-week survival, i.e., 5 weeks following SE, the GFP/NeuN-positive cells had developed an extensive dendritic tree and the same shape of cell body as mature granule cells (Fig. 5B).

Expression of cell death markers in the subgranular zone is unaffected by additional seizures following status epilepticus

The induction of additional seizures at day 6 and day 7 following SE did not change the pattern or the number of cells expressing cytochrome c, TUNEL/Hoechst, AIF, and TRADD in the SGZ/GCL at day 8 (Fig. 6). Because the vast majority of SE-induced newly proliferated BrdU-positive cells were double-labeled with active caspase-3 already without additional stimulations, which we also previously have observed with caspase-cleaved PARP (Ekdahl et al., 2002), we did not quantify the number of cells expressing these cell death markers after the seizures at day 6 and day

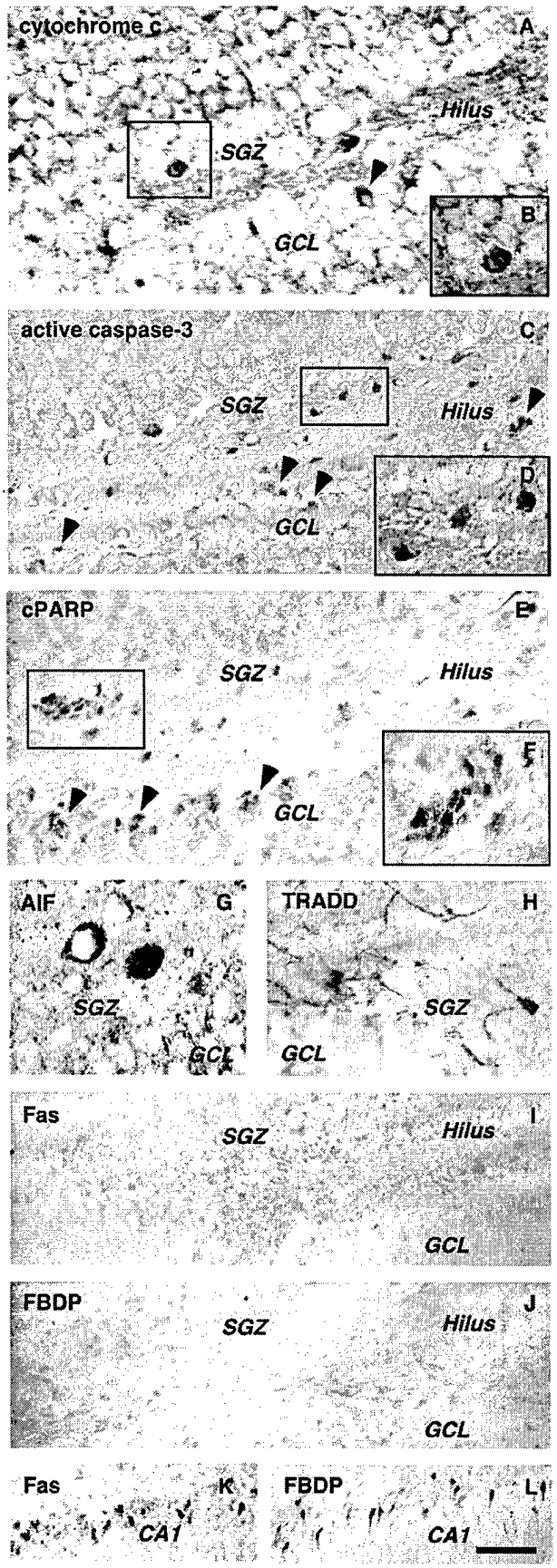

7. Additional seizures resulted in an induction of Fas ligand expression in the CA1 pyramidal neurons (Fig. 2K). We also observed calpain-mediated FBDP expression in the CA1 region (Fig, 2L) in 50% of the rats at 8 days following SE, and after the additional seizures the number of animals with FBDP expression increased to 86%. However, due to large variations within the groups, the increase in the number of FBDP-positive cells was not statistically significant (SE: 15.0 ± 11.0 vs. SE + add. stim: 32.6 ± 16.1 cells).

At day 35 following SE, only a few TUNEL/Hoechst-positive cells remained in the SGZ/GCL and caspase-cleaved PARP expression was no longer observed. Additional seizures at days 33 and 34 did not change the number of the remaining TUNEL/Hoechst-positive cells (3.4 ± 0.6 vs. 2.4 ± 0.3 cells in the SGZ, 0.7 ± 0.2 vs. 0.8 ± 0.2 cells in the hilus, with or without additional stimulation, respectively). Also, no FBDP-positive cells could be detected in the CA1 region at this time point, and additional seizures failed to induce any expression.

Discussion

A large proportion of the new neurons formed in the adult brain after SE (Ekdahl et al., 2001) and stroke (Arvidsson et al., 2002) die within the first weeks after the insult. The cell loss in the dentate SGZ occurs at least partly through activation of caspases. Here we provide evidence that the caspase-evoked death of the newborn neurons involves the mitochondrial but probably not the death-receptor pathway. Protein expression of mitochondria-related cytochrome c was observed in a subset of progenitor cell progeny in the SGZ after SE, while the death receptor ligand Fas was only visible in the CA1 region, and the death receptor-associated protein TRADD was exclusively found in astrocytes. The mitochondria-related, caspase-independent AIF pathway was expressed in the nucleus and cytoplasm of large, multipolar cells, most likely interneurons. We also show that additional seizures after the intial SE do not enhance the cell death mechanisms or compromise the survival of the newly formed neurons.

The conclusion that caspase-induced apoptotic death contributes to the loss of newly generated neurons after SE

Fig. 2. Several cell death markers are expressed in the subgranular zone at 8 days following status epilepticus. Cytochrome c (A), active caspase-3 (C), and caspase-cleaved PARP (E) were expressed in small single cells or clusters (arrowheads). In contrast, AIF was expressed in multipolar cells, presumably interneurons (G), and TRADD in glial cells (H). Fas ligand and calpain-mediated FBDP were only detected in the CA1 region (K and L), and not in the subgranular zone (I and J). The insets are higher magnification of cytochrome c- (B), active caspase-3- (D), and cleaved PARP-positive cells (F) marked by the squares in A, C, and E, respectively. SGZ, subgranular zone; GCL, granule cell layer; Hilus; dentate hilus. Scale bar, 16 μm (A and D), 10 μm (B); 20 μm (C and F), 40 μm (E, I, and J), 13 μm (G and H); 40 μm (K), and 57.2 μm (L).

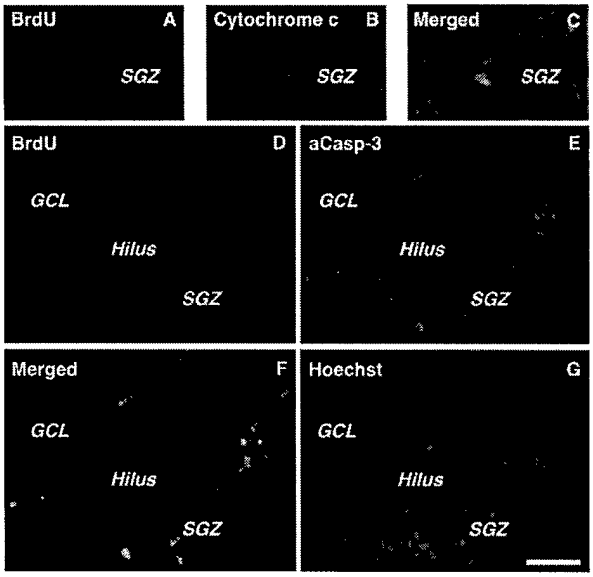

Fig. 3. BrdU-positive cells express cytochrome c and active caspase-3 in the subgranular zone at 8 days following status epilepticus. Images of 5-μm-thick sections illustrate labeling for BrdU (red; A and D), cytochrome C (green; B), and active caspase-3 (green; E). C and F are merged pictures of A and B, and D and E, respectively. (G) Hoechst-positive nuclear staining of the DG seen in D–F. SGZ, subgranular zone; GCL, granule cell layer; Hilus, dentate hilus. Scale bar, 10 μm (A–C) and 35 μm (D–G).

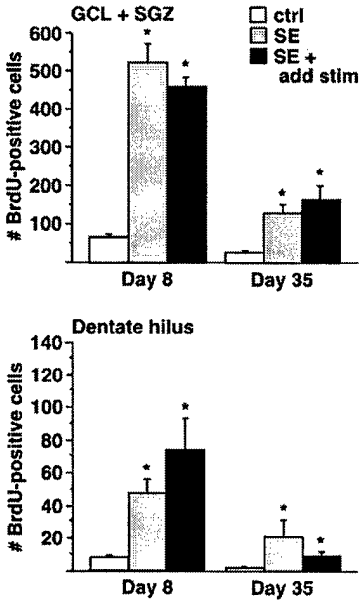

Fig. 4. Additional seizures following status epilepticus do not change the number of BrdU-positive cells in the subgranular zone or the dentate hilus. Animals exhibited three generalized seizures on both day 6 and day 7 or on day 33 and day 34 following status epilepticus, and were perfused on days 8 and 35, respectively. Data are given as number of positive cells per section. Bars represent mean ± SEM. $*P < 0.05$, ANOVA followed by post hoc Bonferroni test.

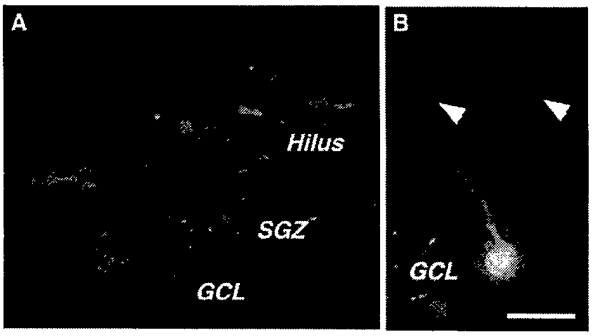

Fig. 5. Status epilepticus-generated cells develop a more mature neuronal phenotype during a 4-week survival period. Animals were injected with a green fluorescent protein (GFP)-carrying retroviral vector at 1 week following status epilepticus. Two days later, most of the newly formed GFP-positive cells (green) lay in clusters in the subgranular zone (SGZ) and possessed short dendritic processes (A). After 4 weeks of survival (35 days following status epilepticus), the vast majority of the GFP-positive cells expressed the neuronal marker NeuN (red) (B) and had developed long dendritic trees (B; arrow heads). GCL, granule cell layer; Hilus, dentate hilus. Scale bar, 21 μm (A) and 16 μm (B).

is based on two main lines of evidence: first, epileptic seizures and SE lead to apoptosis in the SGZ (Sloviter et al., 1996; Bengzon et al., 1997; Ekdahl et al., 2001), including the new neurons (Ekdahl et al., 2001), and caspase inhibitor infusions rescue part of these neurons (Ekdahl et al., 2001, 2002); and second, many of the newly formed neurons in the SGZ and GCL express active caspase-cleaved PARP protein (Ekdahl et al., 2002). Here we have explored two possible ways of activating caspases in the new neurons formed after SE, the mitochondrial and the death-receptor pathway, respectively. Western blots on hippocampal tissue have indicated that both pathways are active following SE (Henshall et al., 2001a,b,c, 2002). The mitochondrial pathway involves translocation of cytochrome c from mitochondria to the cytoplasm, which initiates the caspase cascade (Hengartner, 2000). We observed increased cytochrome c staining in BrdU-labeled newly proliferated cells in the SGZ/GCL. The number of BrdU-positive cells expressing cytochrome c in the SGZ/GCL was clearly lower than that of BrdU/active caspase-3 and BrdU/cleaved PARP double-labeled cells. The high percentage of BrdU/active caspase-3-positive cells (more than 80%) is in line with previous data showing caspase-cleaved PARP expression in almost 70% of the newly formed cells at 8 days following SE (Ekdahl et al., 2002). Previous double staining for TUNEL/cleaved PARP at the same time point has shown that only a small proportion of the cleaved PARP-positive cells is TUNEL labeled (Ekdahl et al., 2002). Taken together these findings provide further support for the hypothesis that active caspase-3 and cleavage of PARP protein can be associated with other processes besides the initiation of apoptotic cell death (Chan and Mattson, 1999).

The mitochondria can also release AIF, which induces caspase-independent large-scale DNA fragmentation and apoptosis (Susin et al., 1999). Arguing against a role of this

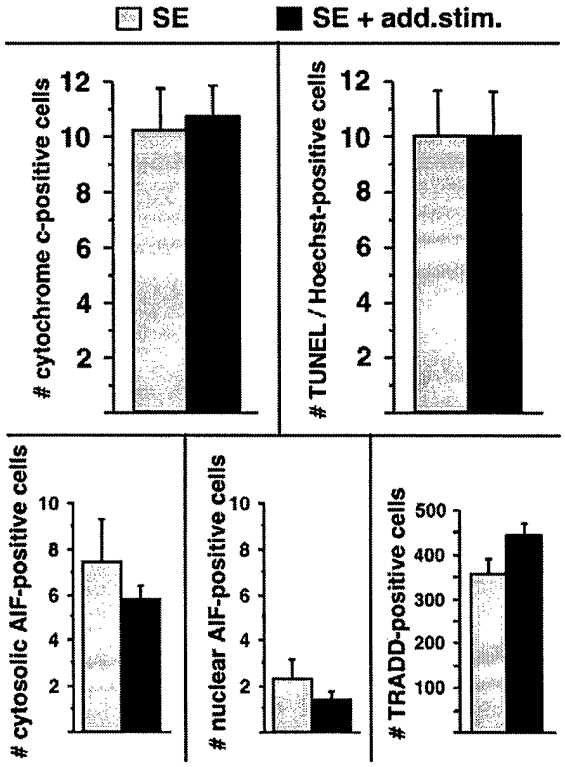

Fig. 6. Additional seizures following status epilepticus do not affect the expression of cell death markers in the subgranular zone. Animals received three generalized seizures on both day 6 and day 7 or on day 33 and day 34 following status epilepticus, and were perfused on days 8 and 35, respectively. Data are given as number of positive cells in the SGZ/GCL per 5-μm-thick sections for cytochrome c and AIF, and 30-μm-thick sections for TUNEL/Hoechst and TRADD. Bars represent mean ± SEM. $^*P < 0.05$.

factor, AIF was detected neither in the nucleus nor in the cytosol of the small SGZ cells. Also, we did not obtain any evidence indicating that the caspase activation in the new cells involves death-inducing receptors such as the Fas receptor and TNF receptor 1. Binding of death-receptor ligands like Fas triggers receptor clustering and formation of a death-inducing signaling complex, which activates caspases. TRADD is an adaptor protein in a complex with TNF receptor 1 (Hengartner, 2000; Allan and Rothwell, 2001). There was no expression of the Fas ligand in the SGZ, and TRADD could only be detected in glial cells. Our data therefore support that progenitor cell progeny die preferentially through a mitochondria-related, caspase-mediated pathway, because of lack of death receptor expression or function in the newborn cells.

Following SE in patients, there is a 30–80% risk of developing recurring seizures (Maytal et al., 1989; Hauser et al., 1990; Verity et al., 1993), and in animals the occurrence of spontaneous seizures ranges from 45% to 100% depending on the SE model (Nissinen et al., 2000; Gorter et al., 2001). Whether there is a relationship between the degree of neuronal degeneration and the amount of spontaneous seizures is controversial (Bertram and Cornett, 1993; Mello et al., 1993; Nissinen et al., 2000; Gorter et al., 2001; Pitkanen, 2002). Gorter et al. (2001) reported that rats with more spontaneous seizures also exhibited more severe neuronal degeneration following electrically induced SE in the hippocampus. In contrast, Pitkanen et al. (2002) found no such correlation after electrically induced SE in the amygdala. Antiepileptic drugs administered after kainic acid- or pilocarpine-induced SE have either prevented both the development of spontaneous seizures and neuronal degeneration, or only the degeneration (Loscher, 2002). Here we wanted to explore the role of spontaneous seizures for the death of the newly formed DG cells. It has been shown that the latency period between the SE and the first spontaneous seizure differs between individual rats and different SE models (Nissinen et al., 2000). Following electrically induced SE in the hippocampus, the latency period has been estimated to be 1 week (Gorter et al., 2001). This time interval coincides with the occurrence of cell proliferation in the SGZ as well as caspase-mediated death of the newly formed cells (Parent et al., 1997; Ekdahl et al., 2002). In an attempt to mimic the first spontaneous seizures following SE, which often are secondarily generalized (Mello et al., 1993; Gorter et al., 2001), we stimulated rats at days 6 and 7 until they developed generalized clonic seizures. Normally, the early spontaneous seizures have a frequency of about 0.1–2 per day (Nissinen et al., 2000; Gorter et al., 2001) and the animals were therefore subjected to three generalized clonic seizures each day. There are two main reasons why a survival period of 2 days after the BrdU injections (24-h survival after the last seizure in a 2-day stimulation session) was chosen. First, additional seizures may induce a new increase in proliferation and therefore confound the number of BrdU-positive cells generated by the initial SE insult. Because seizure-induced proliferation starts after 3 days (Parent et al., 1997), perfusing the rats at 24 h minimizes the risk of including such a second wave of new BrdU-positive cells in the counting. Second, cell death in the SGZ can be observed as early as 2 h after seizures (Bengzon et al., 1997), and part of the newly formed cells produced after SE undergo cell death already during the first 24 h after birth (Ekdahl et al., 2001, 2002). Death of newly formed cells caused by the additional stimulations is therefore likely to be detectable at 24 h. However, six additional seizures did not change either the expression of cell death markers or the number of surviving, newly proliferated cells in the SGZ at 1 week following SE. In contrast, more rats expressed calpain-produced FBDP in the CA1 pyramidal layer, indicating that the cell death mechanisms had been aggravated in this region. Also, at 5 weeks following SE, additional seizures did not affect the low level of cell death in the SGZ. No upregulation of FBDP was observed in CA1 at this time point. Taken together, our data indicate that spontaneous seizures do not compromise the survival of SE-generated neurons either when they are newborn or at a time point when they have developed a more mature phe-

notype. Furthermore, two recent studies have also shown that the frequency of spontaneous seizures after SE does not correlate with the degree of death of mature hippocampal neurons (Pitkanen et al., 2002; Gorter et al., 2003).

In summary, our findings indicate that a mitochondrial caspase-mediated death pathway operates in the SE-generated progenitor cell progeny in the SGZ to the same extent with and without additional seizures. Compared to mature hippocampal neurons, the new neurons do not seem to be particularly susceptible to seizure-induced cell death. In a parallel study (Mohapel et al., 2001), we have found that the survival of the newly formed cells is influenced to a large extent by the severity of the initial SE insult. Considering the present data, it is therefore conceivable that whether a new neuron, generated after SE, will die or not, is determined primarily by the degree of insult-induced neuropathological changes in the tissue environment whereas spontaneous seizures play only a minor role.

Acknowledgments

Supported by grants from the Swedish Research Council, the Hardebo, Lundbeck, Åhlén, Wilhelm and Martina Lundgren, Magnus Bergvall and P Westling Foundations, the Göteborg Medical Society, the Swedish Society of Medicine, and the Swedish Society for Medical Research. We thank Monica Lundahl and Kristian Nilsson for technical assistance, Professor Henrik Hagberg for valuable comments on the manuscript, and Cecilia Lundberg for providing the retroviral vector and technical support.

References

Allan, S.M., Rothwell, N.J., 2001. Cytokines and acute neurodegeneration. Nat. Rev. Neurosci. 2, 734–744.

Arvidsson, A., Collin, T., Kirik, D., Kokaia, Z., Lindvall, O., 2002. Neuronal replacement from endogenous precursors in the adult brain after stroke. Nat. Med. 9, 963–970.

Au-Yeung, K.K., Zhu, D.Y., O.K., Siow, Y.L., 2001. Inhibition of stress-activated protein kinase in the ischemic/reperfused heart: role of magnesium tanshinoate B in preventing apoptosis. Biochem. Pharmacol. 62, 483–493.

Bahr, B.A., Bendiske, J., Brown, Q.B., Munirathinam, S., Caba, E., Rudin, M., Urwyler, S., Sauter, A., Rogers, G., 2002. Survival signaling and selective neuroprotection through glutamatergic transmission. Exp. Neurol. 174, 37–47.

Bahr, B.A., Tiriveedhi, S., Park, G.Y., Lynch, G., 1995. Induction of calpain-mediated spectrin fragments by pathogenic treatments in long-term hippocampal slices. J. Pharmacol. Exp. Ther. 273, 902–908.

Bednarski, E., Vanderklish, P., Gall, C., Saido, T.C., Bahr, B.A., Lynch, G., 1995. Translational suppression of calpain I reduces NMDA-induced spectrin proteolysis and pathophysiology in cultured hippocampal slices. Brain Res. 694, 147–157.

Bengzon, J., Kokaia, Z., Elmer, E., Nanobashvili, A., Kokaia, M., Lindvall, O., 1997. Apoptosis and proliferation of dentate gyrus neurons after single and intermittent limbic seizures. Proc. Natl. Acad. Sci. USA 94, 10432–10437.

Bertram, E.H., Cornett, J., 1993. The ontogeny of seizures in a rat model of limbic epilepsy: evidence for a kindling process in the development of chronic spontaneous seizures. Brain Res. 625, 295–300.

Blomgren, K., Zhu, C., Wang, X., Karlsson, J.O., Leverin, A.L., Bahr, B.A., Mallard, C., Hagberg, H., 2001. Synergistic activation of caspase-3 by m-calpain after neonatal hypoxia-ischemia: a mechanism of "pathological apoptosis"? J. Biol. Chem. 276, 10191–10198.

Chan, S.L., Mattson, M.P., 1999. Caspase and calpain substrates: roles in synaptic plasticity and cell death. J. Neurosci. Res. 58, 167–190.

Coggeshall, R.E., Lekan, H.A., 1996. Methods for determining numbers of cells and synapses: a case for more uniform standards of review [published erratum appears in J. Comp. Neurol. 1996 May 20;369(1): 162] [see comments]. J. Comp. Neurol. 364, 6–15.

Cohen, G.M., 1997. Caspases: the executioners of apoptosis. Biochem. J. 326, 1–16.

Covolan, L., Ribeiro, L.T., Longo, B.M., Mello, L.E., 2000. Cell damage and neurogenesis in the dentate granule cell layer of adult rats after pilocarpine- or kainate-induced status epilepticus. Hippocampus 10, 169–180.

Dolbeare, F., 1995. Bromodeoxyuridine: a diagnostic tool in biology and medicine, Part 1: historical perspectives, histochemical methods and cell kinetics. Histochem. J. 27, 339–369.

Ekdahl, C.T., Mohapel, P., Elmer, E., Lindvall, O., 2001. Caspase inhibitors increase short-term survival of progenitor-cell progeny in the adult rat dentate gyrus following status epilepticus. Eur. J. Neurosci. 14, 937–945.

Ekdahl, C.T., Mohapel, P., Weber, E., Bahr, B., Blomgren, K., Lindvall, O., 2002. Caspase-mediated death of newly formed neurons in the adult rat dentate gyrus following status epilepticus. Eur. J. Neurosci. 16, 1463–1471.

Erhardt, J.A., Ohlstein, E.H., Toomey, J.R., Gabriel, M.A., Willette, R.N., Yue, T.L., Barone, F.C., Parsons, A.A., 2001. Activation of caspase-3/caspase-3-like activity in rat cardiomyocytes by an RGD peptide, but not the GPIIb/IIIa antagonist lotrafiban. Thromb. Res. 103, 143–148.

Ferrand-Drake, M., Zhu, C., Gido, G., Hansen, A.J., Karlsson, J.O., Bahr, B.A., Zamzami, N., Kroemer, G., Chan, P.H., Wieloch, T., Blomgren, K., 2003. Cyclosporin A prevents calpain activation despite increased intracellular calcium concentrations, as well as translocation of apoptosis-inducing factor, cytochrome c and caspase-3 activation in neurons exposed to transient hypoglycemia. J. Neurochem. 85, 1431–1442.

Gage, F.H., Kempermann, G., Palmer, T.D., Peterson, D.A., Ray, J., 1998. Multipotent progenitor cells in the adult dentate gyrus. J. Neurobiol. 36, 249–266.

Gorter, J.A., Goncalves Pereira, P.M., van Vliet, E.A., Aronica, E., Lopes da Silva, F.H., Lucassen, P.J., 2003. Neuronal cell death in a rat model for mesial temporal lobe epilepsy is induced by the initial status epilepticus and not by later repeated spontaneous seizures. Epilepsia 44, 647–658.

Gorter, J.A., van Vliet, E.A., Aronica, E., Lopes da Silva, F.H., 2001. Progression of spontaneous seizures after status epilepticus is associated with mossy fibre sprouting and extensive bilateral loss of hilar parvalbumin and somatostatin-immunoreactive neurons. Eur. J. Neurosci. 13, 657–669.

Han, H., Wang, H., Long, H., Nattel, S., Wang, Z., 2001. Oxidative preconditioning and apoptosis in L-cells. Roles of protein kinase B and mitogen-activated protein kinases. J. Biol. Chem. 276, 26357–26364.

Hauser, W.A., Rich, S.S., Annegers, J.F., Anderson, V.E., 1990. Seizure recurrence after a 1st unprovoked seizure: an extended follow-up. Neurology 40, 1163–1170.

Hengartner, M.O., 2000. The biochemistry of apoptosis. Nature 407, 770–776.

Henshall, D.C., Araki, T., Schindler, C.K., Lan, J.Q., Tiekoter, K.L., Taki, W., Simon, R.P., 2002. Activation of Bcl-2-associated death protein and counter-response of Akt within cell populations during seizure-induced neuronal death. J. Neurosci. 22, 8458–8465.

Henshall, D.C., Bonislawski, D.P., Skradski, S.L., Araki, T., Lan, J.Q., Schindler, C.K., Meller, R., Simon, R.P., 2001a. Formation of the

Apaf-1/cytochrome c complex precedes activation of caspase-9 during seizure-induced neuronal death. Cell Death Differ. 8, 1169–1181.

Henshall, D.C., Bonislawski, D.P., Skradski, S.L., Lan, J.Q., Meller, R., Simon, R.P., 2001b. Cleavage of bid may amplify caspase-8-induced neuronal death following focally evoked limbic seizures. Neurobiol. Dis. 8, 568–580.

Henshall, D.C., Skradski, S.L., Bonislawski, D.P., Lan, J.Q., Simon, R.P., 2001c. Caspase-2 activation is redundant during seizure-induced neuronal death. J. Neurochem. 77, 886–895.

Liu, J., Solway, K., Messing, R.O., Sharp, F.R., 1998. Increased neurogenesis in the dentate gyrus after transient global ischemia in gerbils. J. Neurosci. 18, 7768–7778.

Loscher, W., 2002. Animal models of epilepsy for the development of antiepileptogenic and disease-modifying drugs. A comparison of the pharmacology of kindling and post-status epilepticus models of temporal lobe epilepsy. Epilepsy Res. 50, 105–123.

Magavi, S.S., Leavitt, B.R., Macklis, J.D., 2000. Induction of neurogenesis in the neocortex of adult mice. Nature 405, 951–955.

Maytal, J., Shinnar, S., Moshe, S.L., Alvarez, L.A., 1989. Low morbidity and mortality of status epilepticus in children. Pediatrics 83, 323–331.

Mello, L.E., Cavalheiro, E.A., Tan, A.M., Kupfer, W.R., Pretorius, J.K., Babb, T.L., Finch, D.M., 1993. Circuit mechanisms of seizures in the pilocarpine model of chronic epilepsy: cell loss and mossy fiber sprouting. Epilepsia 34, 985–995.

Mohapel, P., Ekdahl, C.T., Lindvall, O., 2001. Differential increases in hippocampal neurogenesis and cell death following status epilepticus. Soc. Neurosci. Abstr. 27, 2015.

Nakagawa, E., Aimi, Y., Yasuhara, O., Tooyama, I., Shimada, M., McGeer, P.L., Kimura, H., 2000. Enhancement of progenitor cell division in the dentate gyrus triggered by initial limbic seizures in rat models of epilepsy. Epilepsia 41, 10–18.

Nakatomi, H., Kuriu, T., Okabe, S., Yamamoto, S., Hatano, O., Kawahara, N., Tamura, A., Kirino, T., Nakafuku, M., 2002. Regeneration of hippocampal pyramidal neurons after ischemic brain injury by recruitment of endogenous neural progenitors. Cell 110, 429–441.

Nissinen, J., Halonen, T., Koivisto, E., Pitkanen, A., 2000. A new model of chronic temporal lobe epilepsy induced by electrical stimulation of the amygdala in rat. Epilepsy Res. 38, 177–205.

Ory, D.S., Neugeboren, B.A., Mulligan, R.C., 1996. A stable human-derived packaging cell line for production of high titer retrovirus/vesicular stomatitis virus G pseudotypes. Proc. Natl. Acad. Sci. USA 93, 11400–11406.

Parent, J.M., Valentin, V.V., Lowenstein, D.H., 2002a. Prolonged seizures increase proliferating neuroblasts in the adult rat subventricular zone-olfactory bulb pathway. J. Neurosci. 22, 3174–3188.

Parent, J.M., Vexler, Z.S., Gong, C., Derugin, N., Ferriero, D.M., 2002b. Rat forebrain neurogenesis and striatal neuron replacement after focal stroke. Ann. Neurol. 52, 802–813.

Parent, J.M., Yu, T.W., Leibowitz, R.T., Geschwind, D.H., Sloviter, R.S., Lowenstein, D.H., 1997. Dentate granule cell neurogenesis is increased by seizures and contributes to aberrant network reorganization in the adult rat hippocampus. J. Neurosci. 17, 3727–3738.

Paxinos, G., Watson, C., 1997. The Rat Brain in Stereotaxic Coordinates. Academic Press, Inc, San Diego, CA, USA.

Pitkanen, A., 2002. Efficacy of current antiepileptics to prevent neurodegeneration in epilepsy models. Epilepsy Res. 50, 141–160.

Pitkanen, A., Nissinen, J., Nairismagi, J., Lukasiuk, K., Grohn, O.H., Miettinen, R., Kauppinen, R., 2002. Progression of neuronal damage after status epilepticus and during spontaneous seizures in a rat model of temporal lobe epilepsy. Prog. Brain Res. 135, 67–83.

Racine, R.J., 1972. Modification of seizure activity by electrical stimulation. II. Motor seizure. Electroencephalogr. Clin. Neurophysiol. 32, 281–294.

Sloviter, R.S., Dean, E., Sollas, A.L., Goodman, J.H., 1996. Apoptosis and necrosis induced in different hippocampal neuron populations by repetitive perforant path stimulation in the rat. J. Comp. Neurol. 366, 516–533.

Susin, S.A., Lorenzo, H.K., Zamzami, N., Marzo, I., Snow, B.E., Brothers, G.M., Mangion, J., Jacotot, E., Costantini, P., Loeffler, M., Larochette, N., Goodlett, D.R., Aebersold, R., Siderovski, D.P., Penninger, J.M., Kroemer, G., 1999. Molecular characterization of mitochondrial apoptosis-inducing factor. Nature 397, 441–446.

Verity, C.M., Ross, E.M., Golding, J., 1993. Outcome of childhood status epilepticus and lengthy febrile convulsions: findings of national cohort study. BMJ 307, 225–228.

Wang, Y., Wu, T.R., Cai, S., Welte, T., Chin, Y.E., 2000. Stat1 as a component of tumor necrosis factor alpha receptor 1-TRADD signaling complex to inhibit NF-kappaB activation. Mol. Cell. Biol. 20, 4505–4512.

Zhang, X., Chen, J., Graham, S.H., Du, L., Kochanek, P.M., Draviam, R., Guo, F., Nathaniel, P.D., Szabo, C., Watkins, S.C., Clark, R.S., 2002. Intranuclear localization of apoptosis-inducing factor (AIF) and large scale DNA fragmentation after traumatic brain injury in rats and in neuronal cultures exposed to peroxynitrite. J. Neurochem. 82, 181–191.

Zhu, C., Qui, L., Wang, X., Hallin, U., Cande, C., Kroemer, G., Hagberg, H., Blomgren, K., 2003. Involvement of apoptosis-inducing factor in neuronal death after hypoxia-ischemia in the neonatal rat brain. J. Neurochem. 86, 306–317.

Zhu, C., Wang, X., Hagberg, H., Blomgren, K., 2000. Correlation between caspase-3 activation and three different markers of DNA damage in neonatal cerebral hypoxia-ischemia. J. Neurochem. 75, 819–829.